

# **BASG Thermomechanical Pump Helium II Transfer Tests**

G. L. Mills, D. A. Newell and A. R. Urbach

CONTRACT NAS2-11979  
March 1990

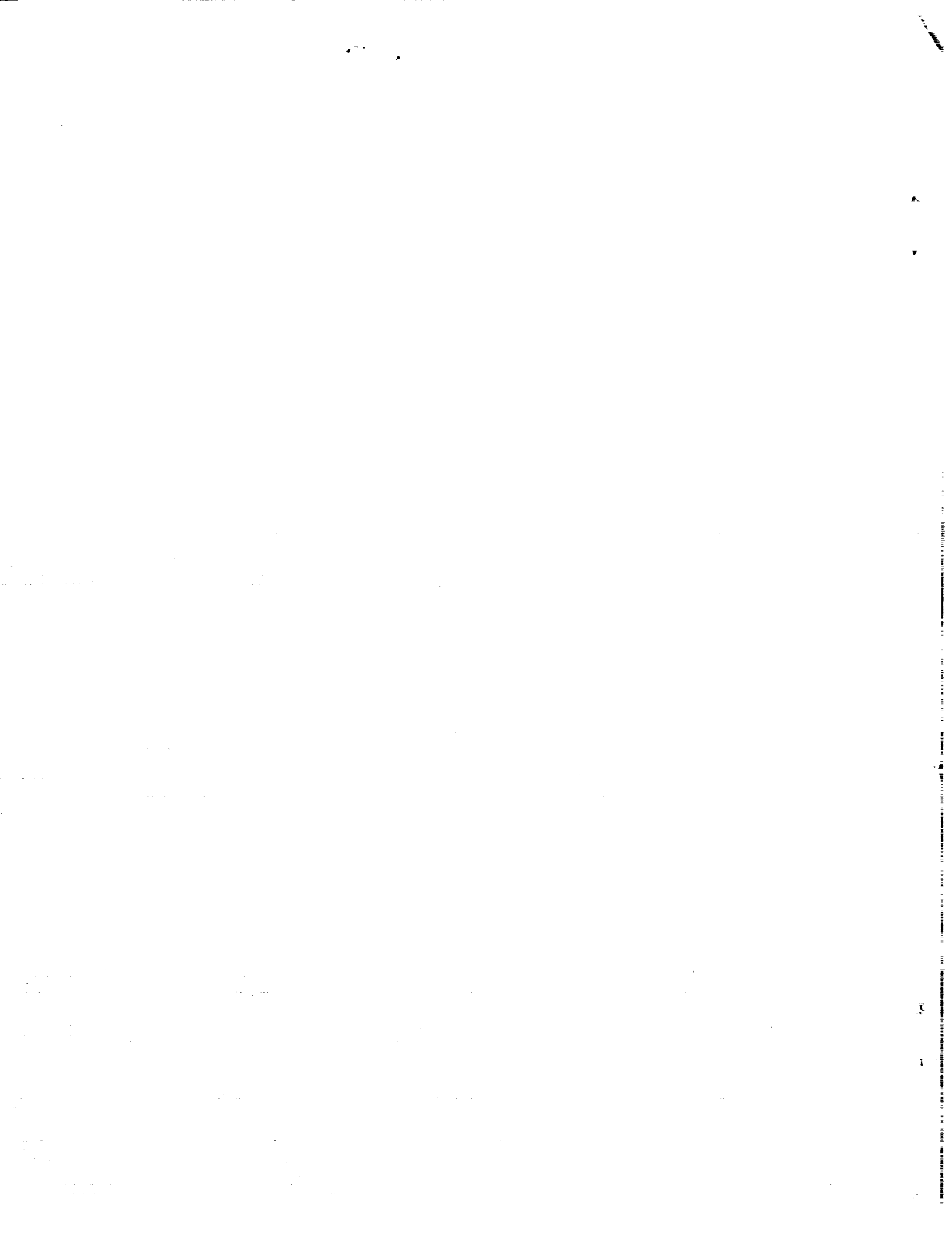


National Aeronautics and  
Space Administration

(NASA-CR-177541) BASG THERMOMECHANICAL PUMP  
HELIUM II TRANSFER TESTS (Ball Aerospace  
Systems Div.) 72 p CSDL 228

N90-21097

Unclas  
G3/18 0272345



NASA Contractor Report 177541

# **BASG Thermomechanical Pump Helium II Transfer Tests**

G. L. Mills  
D. A. Newell  
A. R. Urbach

Ball Aerospace  
Systems Group  
P.O. Box 1062  
Boulder, Colorado

Prepared for  
Ames Research Center  
CONTRACT NAS2-11979  
March 1990



National Aeronautics and  
Space Administration

**Ames Research Center**  
Moffett Field, California 94035-1000

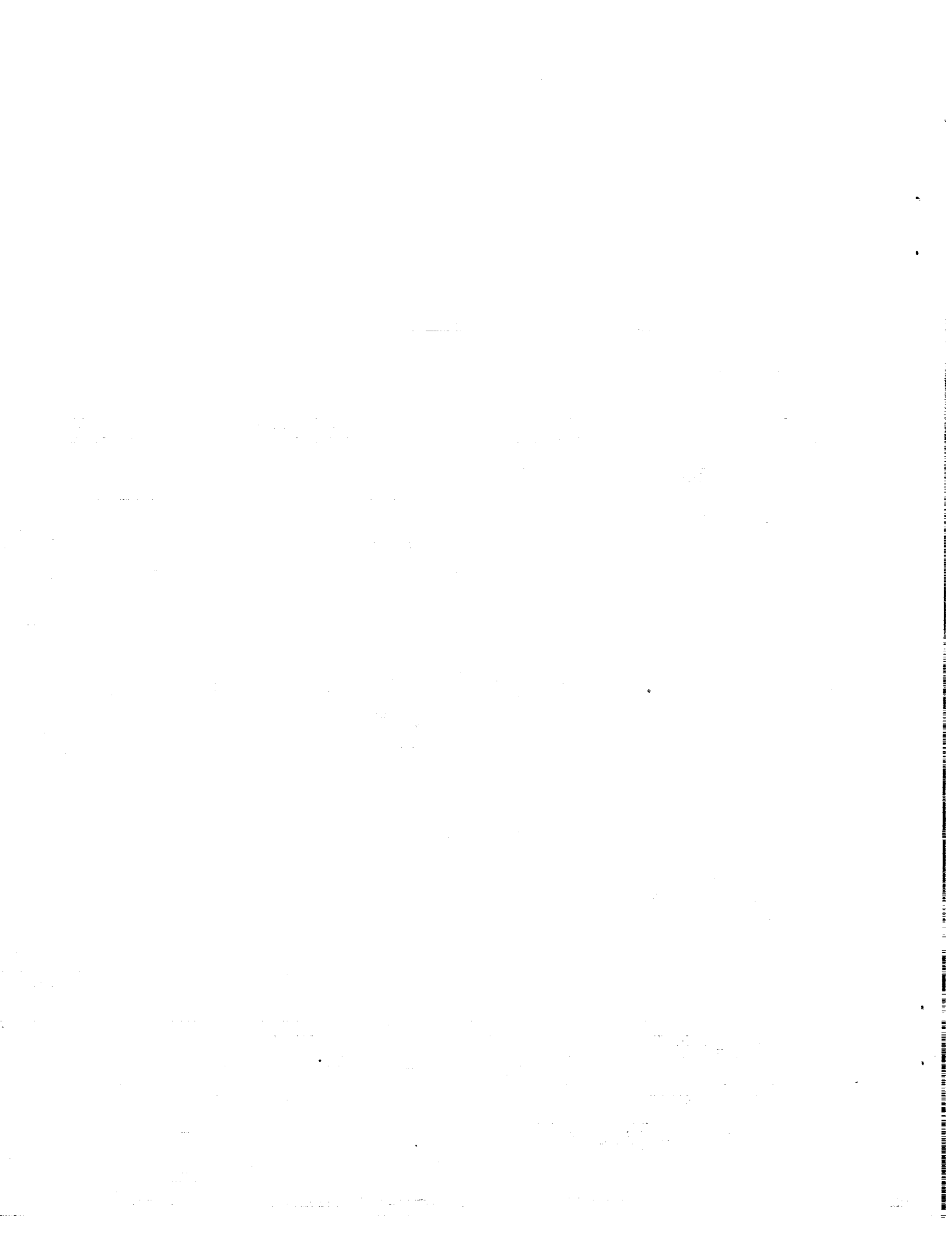


## TABLE OF CONTENTS

<u>Section</u>	<u>Title</u>	<u>Page</u>
	EXECUTIVE SUMMARY .....	1
1	INTRODUCTION .....	1-1
2	DISCUSSION OF TESTS PERFORMED DURING 1986 .....	2-1
	2.1 TEST APPARATUS DESCRIPTION .....	2-1
	2.2 ESTIMATED DATA ACCURACY AND LIMITATIONS .....	2-4
	2.3 CHRONOLOGICAL SUMMARY OF TESTS PERFORMED IN 1986 .....	2-4
	2.4 TEST PROCEDURES AND RESULTS .....	2-6
3	DISCUSSION OF TESTS PERFORMED DURING 1989 .....	3-1
	3.1 TEST APPARATUS DESCRIPTION .....	3-1
	3.2 CALIBRATION PROCEDURE .....	3-6
	3.2.1 Calibration Test .....	3-6
	3.2.2 GRT Calibration .....	3-6
	3.2.3 Cold Pressure Sensor Calibrations .....	3-7
	3.2.4 Estimated Data Accuracy and Limitations .....	3-7
	3.3 CHRONOLOGICAL SUMMARY OF TESTS PERFORMED IN 1989 .....	3-9
	3.4 TEST PROCEDURES AND RESULTS .....	3-9
	3.4.1 Flow Tests .....	3-10
	3.4.2 No flow Tests .....	3-32
4	COMPARISON TO FLOW MODEL .....	4-1
5	STUDY OVERALL CONCLUSIONS .....	5-1
	REFERENCES .....	5-3

## ILLUSTRATIONS

<u>Figure</u>		
1	Simplified Flow Schematic of the 1986 Helium Transfer Experiment .....	2
2	Simplified Flow Schematic of the 1989 Helium Transfer Experiment .....	2
3	Summary of the 1986 flow runs.....	3
4	Summary of the 1989 flow runs .....	3
5	Summary of the no flow data.....	5

TABLE OF CONTENTS (Continued)

Figure

6	Summary of the no flow data.....	5
7	Detailed Flow Schematic of the 1986 Helium Transfer Experiment .....	2-2
8	Scanning electron microscope photograph of the porous plug interior .....	2-3
9	The porous plug assembly used in path B.....	2-5
10	The pressure measured and calculated for one of the 1986 no flow experiments.....	2-7
11	The liquid volume and flow rate during the first 1986 transfer experiment.....	2-7
12	Temperature profiles along path A during run 1 of the 1986 tests .....	2-9
13	Temperature profiles along path A during run 2 of the 1986 tests .....	2-9
14	Pressure in tanks during 1986 fill of an initially warm (run 2 along path B).....	2-10
15	Detailed Flow Schematic of the apparatus used in the 1989 helium transfer tests.....	3-2
16	Overall view of the apparatus used in the 1989 helium transfer tests .....	3-3
17	The small tank and the first part of the transfer line used in the 1989 helium transfer tests.....	3-3
18	The porous plug assembly used on path A in the 1989 helium transfer tests.....	3-4
19	The porous plug heaters used in the 1989 helium transfer tests.....	3-4
20	Heater power during 1989 run 1 along path A.....	3-11
21	Flow rate out of the small tank during 1989 run 1 along path A.....	3-11
22	Liquid volume during 1989 run 1 along path A.....	3-12
23	Pressures during 1989 run 1 along path A.....	3-12
24	Supply dewar temperature and the first two temperatures along path A during 1989 run 1.....	3-13

TABLE OF CONTENTS (Continued)

Figure

25	Final three temperatures along path A and the receiver dewar temperature during 1989 run 1.....	3-13
26	Pressure profile during 1989 run 1 along path A.....	3-14
27	Temperature profile during 1989 run 1 along path A.....	3-14
28	Heater power during 1989 run 2 along path A.....	3-15
29	Flow rate out of the small tank during 1989 run 2 along path A.....	3-15
30	Liquid volume during 1989 run 2 along path A.....	3-16
31	Pressures during 1989 run 2 along path A.....	3-16
32	Supply dewar temperature and the first two temperatures along path A during 1989 run 2.....	3-17
33	Final three temperatures along path A and the receiver dewar temperature during 1989 run 2.....	3-17
34	Pressure profile during 1989 run 2 along path A.....	3-18
35	Temperature profile during 1989 run 2 along path A.....	3-18
36	Heater power during 1989 run 3 along path A.....	3-19
37	Flow rate out of the small tank during 1989 run 3 along path A.....	3-19
38	Liquid volume during 1989 run 3 along path A.....	3-20
39	Pressures during 1989 run 3 along path A.....	3-20
40	Supply dewar temperature and the first two temperatures along path A during 1989 run 3.....	3-21
41	Final three temperatures along path A and the receiver dewar temperature during 1989 run 3.....	3-21
42	Pressure profile during 1989 run 3 along path A.....	3-22
43	Temperature profile during 1989 run 3 along path A.....	3-22
44	Heater power during 1989 run 4 along path A.....	3-24
45	Flow rate out of the small tank during 1989 run 4 along path A.....	3-24
46	Liquid volume during 1989 run 4 along path A.....	3-25

TABLE OF CONTENTS (Continued)

Figure

47	Pressures during 1989 run 4 along path A.....	3-25
48	Supply dewar temperature and the first two temperatures along path A during 1989 run 4.....	3-26
49	Final three temperatures along path A and the receiver dewar temperature during 1989 run 4.....	3-26
50	Pressure profile during 1989 run 4 along path A.....	3-27
51	Temperature profile during 1989 run 4 along path A.....	3-27
52	Heater power during 1989 run 5 along path A.....	3-28
53	Flow rate out of the small tank during 1989 run 5 along path A.....	3-28
54	Liquid volume during 1989 run 5 along path A.....	3-29
55	Pressures during 1989 run 5 along path A.....	3-29
56	Supply dewar temperature and the first two temperatures along path A during 1989 run 5.....	3-30
57	Final three temperatures along path A and the receiver dewar temperature during 1989 run 5.....	3-30
58	Pressure profile during 1989 run 5 along path A.....	3-31
59	Temperature profile during 1989 run 5 along path A.....	3-31
60	Heater power during 1989 no flow run 1 along path A.....	3-33
61	Flow rate out of the small tank during 1989 no flow run 1 along path A.....	3-33
62	Liquid volume during 1989 no flow run 1 along path A.....	3-34
63	Pressures during 1989 no flow run 1 along path A.....	3-34
64	Supply dewar temperature and the first two temperatures along path A during 1989 no flow run 1.....	3-35
65	Final three temperatures along path A and the receiver dewar temperature during 1989 no flow run 1.....	3-35
66	Pressure profile during 1989 no flow run 1 along path A.....	3-36
67	Temperature profile during 1989 no flow run 1 along path A..	3-36
68	Heater power during 1989 no flow run 2 along path A.....	3-37



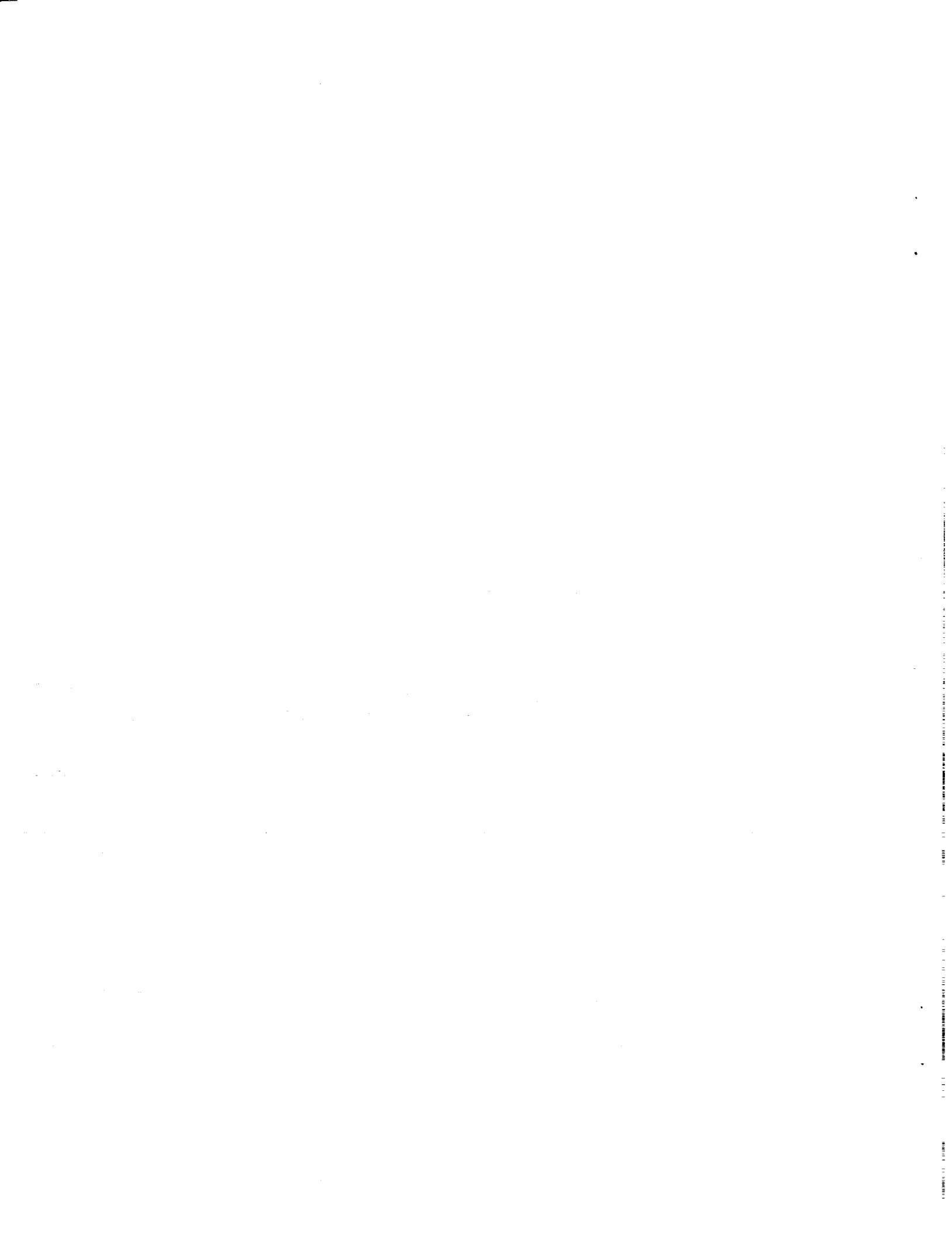
TABLE OF CONTENTS (Continued)

Figure

69	Flow rate out of the small tank during 1989 no flow run 2 along path A.....	3-37
70	Liquid volume during 1989 no flow run 2 along path A.....	3-38
71	Pressures during 1989 no flow run 2 along path A.....	3-38
72	Supply dewar temperature and the first two temperatures along path A during 1989 no flow run 2.....	3-39
73	Final three temperatures along path A and the receiver dewar temperature during 1989 no flow run 2.....	3-39
74	Pressure profile during 1989 no flow run 2 along path A....	3-40
75	Temperature profile during 1989 no flow run 2 along path A.	3-40
76	Experiment and computer generated pressure profiles for 1989 run 5, 9.0 minutes, along path A.....	4-2
77	Experiment and computer model generated pressure profiles for 1989 run 4, 10.0 minutes, along path A.....	4-3
78	Experiment and computer model generated pressure profiles for 1989 run 3, 7.0 minutes, along path A.....	4-4

Table

1	PRESSURE AND TEMPERATURE SENSORS USED IN THE 1989 TESTS ...	3-5
---	---	-----



## EXECUTIVE SUMMARY

The purpose of the effort described in this report was to perform experiments and calculations related to using a thermomechanical pump in the space-based resupply of the Space Infrared Telescope Facility (SIRTF) with Helium II. The need for this effort was identified in the original SIRTF Instrument Changeout and Cryogen Replacement (STICCR) study.

Thermomechanical (fountain effect) pumps have long been suggested as a means for pumping large quantities of Helium II.<sup>1</sup> More recently, the unique properties of Helium II have made it useful for cooling space instruments. Several space science missions, including SIRTF, are now being planned which would benefit greatly from on-orbit resupply of Helium II.<sup>2</sup> The use of a thermomechanical pump in accomplishing this resupply has been examined at a system level.<sup>3</sup> The characterization of thermomechanical and centrifugal pumps as components has also been investigated.<sup>4,5,6</sup>

We performed a series of experiments to demonstrate that large volumes of Helium II can be transferred with a thermomechanical pump at high flow rates and at high efficiency from one dewar to another through valves and lines that are similar to the plumbing arrangement that would be necessary to accomplish such a transfer on-orbit. In addition, temperature, pressure, and flow rate data taken during the tests were used to verify and refine a computer model we have developed.<sup>6,7</sup>

The test apparatus was cooled, filled, and successfully operated twice. The first test (September 1986) was only partially successful. The thermomechanical pumps transferred Helium II from one dewar to another and back, and a warm tank was cooled and filled using a thermomechanical pump. However, the flow rate was much lower than expected, 90 liters/hour, instead of the goal of 300 liters/hour. There were also numerous problems with the instrumentation and data acquisition system. After the first series of tests, modifications were made to the test apparatus, instrumentation, and data acquisition system. In June 1989 a second series of tests was successfully performed. Flow rates of up to 550 liters/hour were achieved and accurate temperature, pressure, and flow rate data were obtained.

### TEST RESULTS OVERVIEW

The following paragraphs present a summary of both the 1986 and 1989 transfer test results. Figures 1 and 2 present the 1986 and 1989 system schemes of the test apparatus. The no-flow runs are with valves closed downstream of the porous plug stopping all flow.

#### Summary of Flow Tests

In Figures 3 and 4, the flow data from the 1986 and 1989 test runs are plotted based on flow rate, power input, and supply dewar pressure. The 1989 flow rates are a strong function of the supply dewar pressure (or temperature) and heat input near the porous plug. This is consistent with the theory of thermomechanical pumps given in references 1 and 3. It also appears that the flow rate is not affected by flow restrictions downstream of the porous plug or heat input far downstream of the plug. The 1986 flow rates are not a function of supply dewar pressure or heat input. This is probably due to the plug used in the 1986 tests being very undersized, such that it could not pass more than 80 to 90 liters/hour, and the flow rate accuracy being approximately 20 liters/hour. Also the range of supply dewar pressure was very limited in the 1986 data.

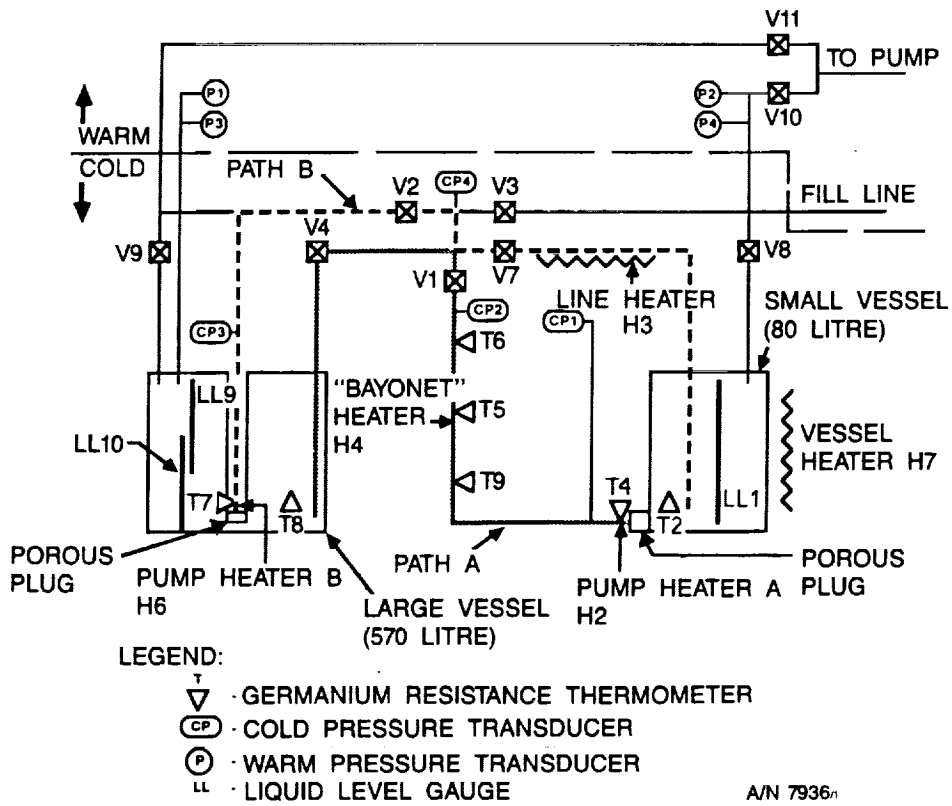


Figure 1. Simplified Flow Schematic of the 1986 Helium Transfer Experiment.

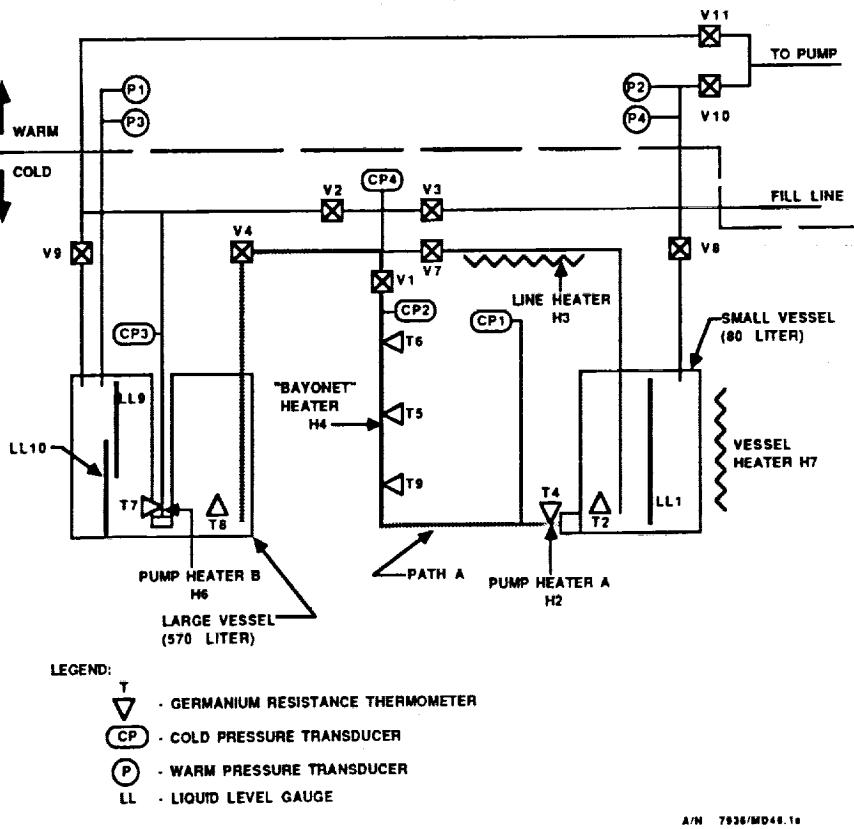


Figure 2. Simplified Flow Schematic of the 1989 Helium Transfer Experiment.

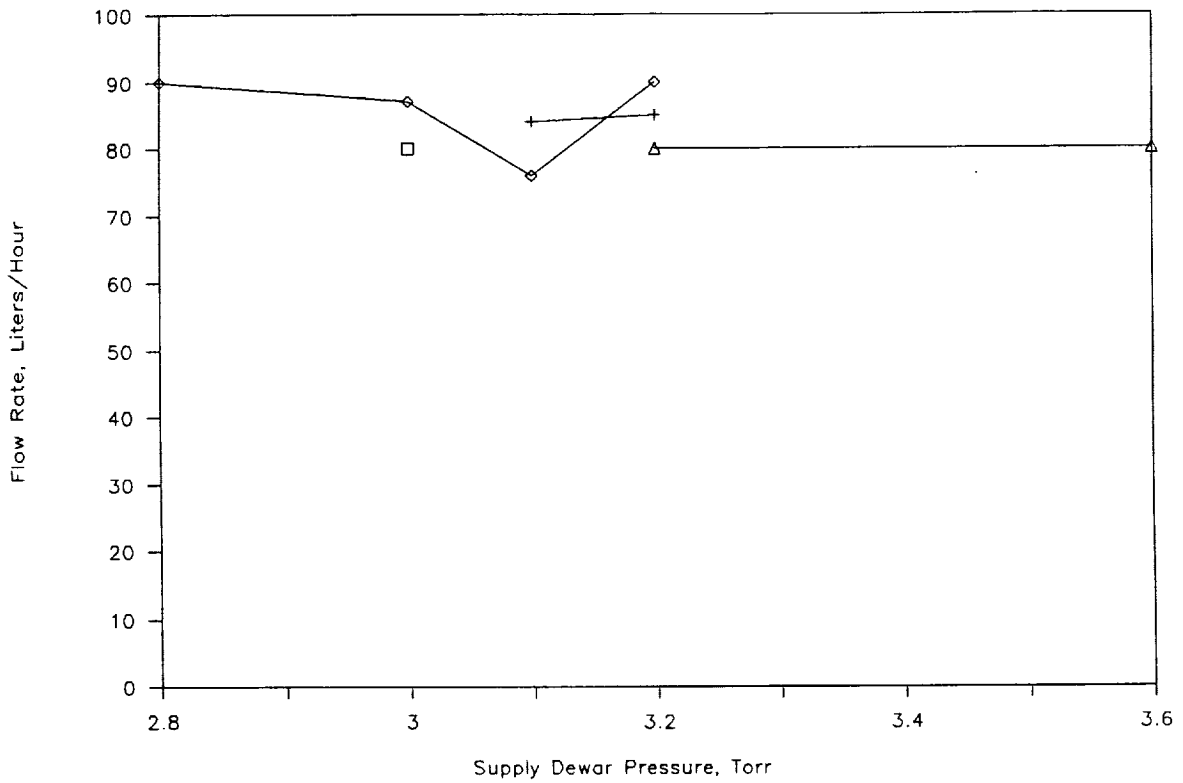


Figure 3. Summary of the 1986 flow runs. A heat input at the porous plug of 3.0 watts is the □ symbol, 4.0 watts is the + symbol, 6.0 watts is the ◇ symbol and 12.0 watts is the △ symbol.

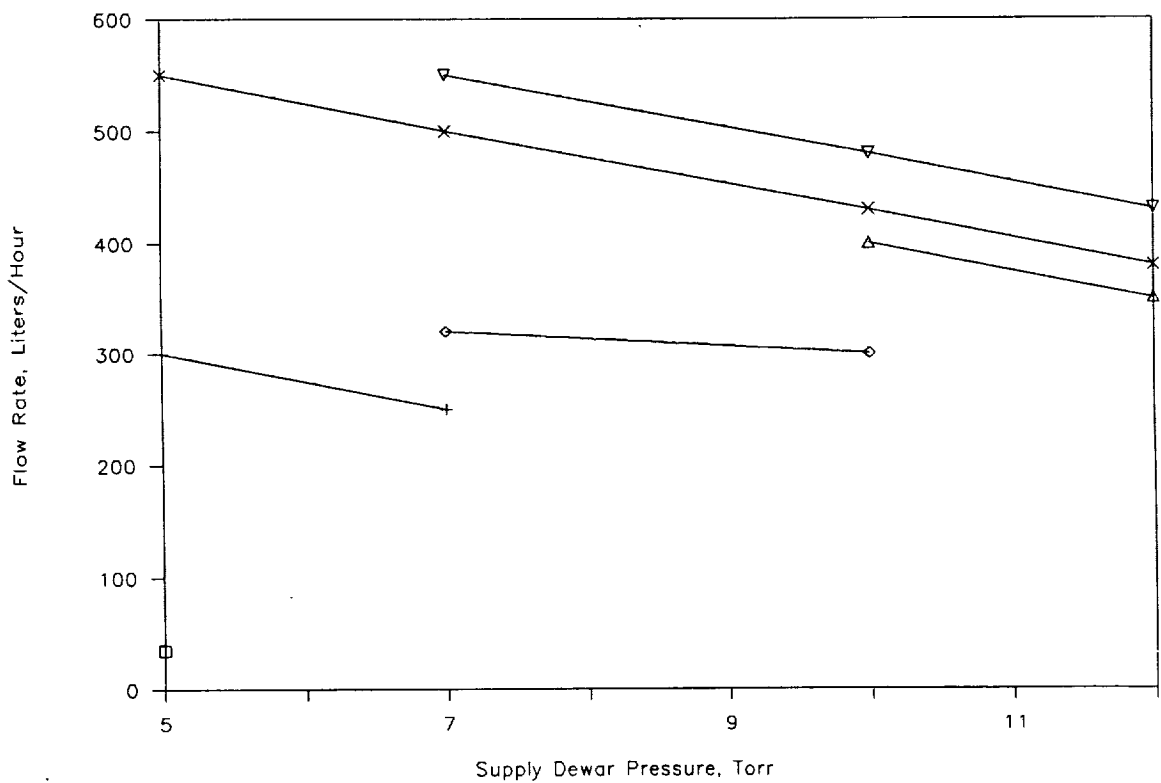


Figure 4. Summary of the 1989 flow runs. Zero heat input at the porous plug is the □ symbol, 6.0 watts is the + symbol, 12.0 watts is the ◇ symbol, 18.0 watts is the △ symbol, 20.0 watts is the x symbol and 24.0 watts is the ▽ symbol.

The Reynolds number of the Helium II flow through the transfer line was approximately 240,000 at the 90 liters/hour achieved in the 1986 tests and 1.5 million at the 550 liters/hour achieved in the 1989 tests.

#### Summary of No-flow Tests

In **Figures 5** and **6** the data from the 1986 and 1989 tests is plotted based on the supply dewar temperature, downstream temperature, and resulting downstream pressure. Note that **Figure 5** shows the apparent thermal conductance of the porous plugs since, in the no-flow condition, the only place that the added heat could go is across the porous plug, to the lower temperature supply dewar. The 1986 plug shows a much lower apparent conductance than the 1989 plug, which is to be expected given its greater thickness and smaller area.

The 1989 data in **Figure 5** shows that as the power is increased, the temperature difference across the plug increases, but not linearly as would be expected if the apparent conductance was just due to the thermal conductance of the ceramic material. Part of this apparent conductance is probably due to normal component flowing back through the porous plug. This apparent conductance would cause a loss of efficiency in a porous plug pump operated at high differential pressures and temperatures. The pressure developed by the porous plug is a strong function of the supply dewar temperature and the downstream temperature. This data is consistent with the data of reference 8 and the theory of reference 9.

#### Summary of Cooldown Test

In the 1986 test, the ability of a thermomechanical pump to cool and fill an initially warm tank was demonstrated. The receiving tank was drained of all Helium II and was warmed to 60 K. The thermomechanical pump was able to cool and fill the receiving tank. The Helium II appeared to start coming through the porous plug as soon as the vent on the receiving tank was closed and the pressure in the receiving tank rose above that in the supply tank. The vent valve on the receiving tank had to be regulated to keep the pressure in the receiving tank from becoming very high as the Helium II liquid entered the warm tank and boiled.

#### Summary of Fill Tests

In both the 1986 and 1989 tests, we demonstrated that a thermomechanical pump can completely fill a receiving dewar that is not vented. This was expected, due to the high conductivity of Helium II and its strong tendency to be in equilibrium with its vapor, and the high thermal efficiency of thermomechanical pumps. If the heat input is not too great, all the heat causes flow through the plug with little heating of the liquid.

#### COMPUTER MODEL

Concurrently with the development of the experimental hardware, Ball has developed a computer program, Superflow, which models Helium II flow for one-dimensional, steady-state cases. We used this model interactively with the test hardware to predict the experiment results and to guide the hardware design. The results of the experiment were used to further refine the model. Currently, the model is generating flow rates and pressures within 10 percent of the experimental values when the experimental conditions are used as boundary conditions.

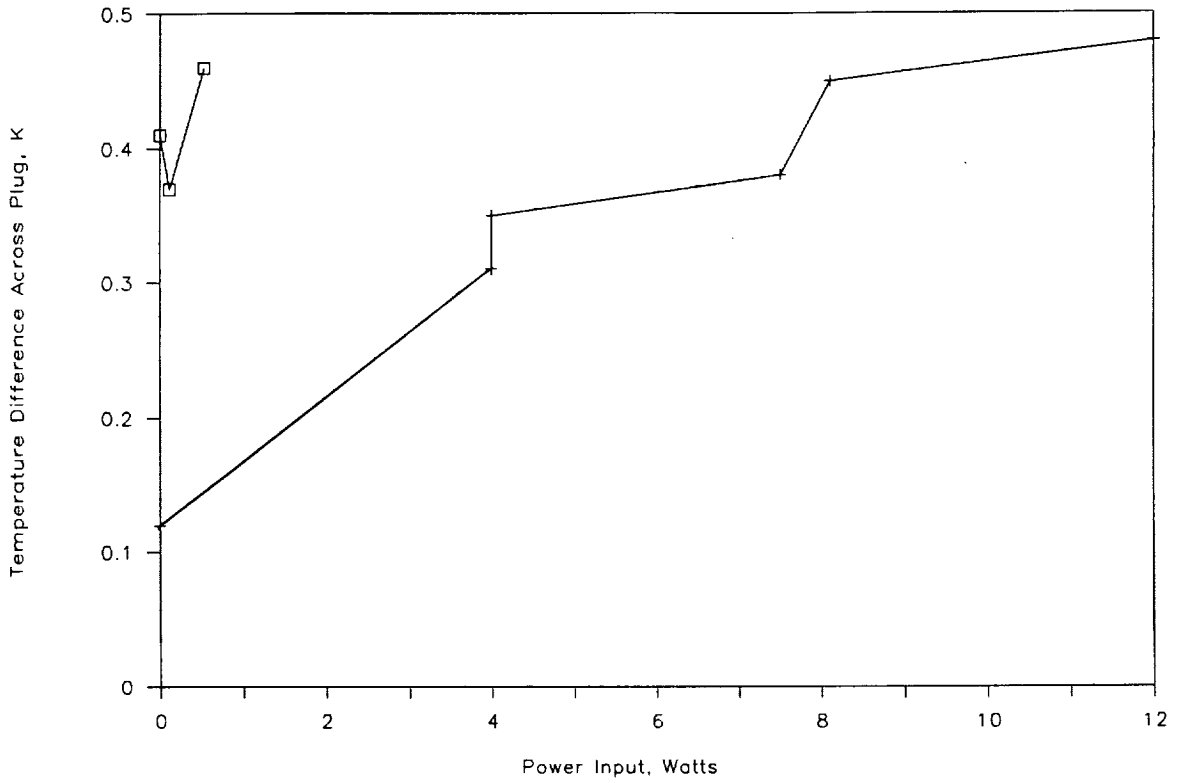


Figure 5. Summary of the no flow data. The data from the 1986 tests is the □ symbol and the data from the 1989 tests is the + symbol.

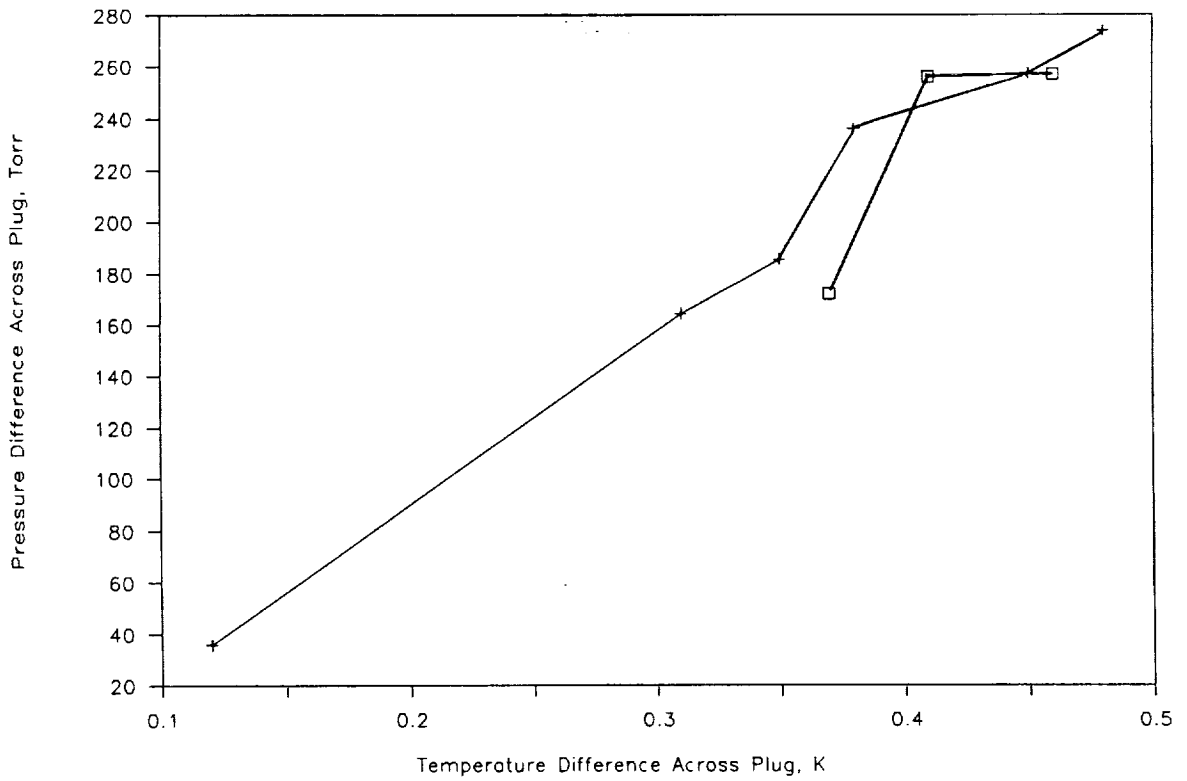


Figure 6. Summary of the no flow data. The data from the 1986 tests is the □ symbol and the data from the 1989 tests is the + symbol.

## CONCLUSIONS REACHED REGARDING PUMP PERFORMANCE

1. Thermomechanical pumps can rapidly transfer large quantities of Helium II from one dewar to another through a long transfer line with significant flow restrictions and heat input. We achieved flow rates of 550 liters/hour through a transfer line that was 6.1 meters long and contained two valves.
2. Thermomechanical pumps are an efficient and reliable means for transferring Helium II.
3. Thermomechanical pumps can be used to cool and fill an initially warm tank. We cooled and filled a dewar tank that was initially at 60 K using only a thermomechanical pump.
4. The Ball model, Superflow 2.0, accurately predicts the flow rate and pressure profile for the various cases tested once the proper plug characteristics and friction factors for valves and corrugated tubing are entered into it.



## Section 1 INTRODUCTION

This report presents the test results achieved at Ball Aerospace while performing Helium II tests to evaluate the system effects of using a thermomechanical pump. NASA-Ames Research Center (ARC) funded Ball under Contract Number NAS2-11979 to conduct tests and calculations relating to thermomechanical pump technology as used in space-based superfluid helium resupply systems. This effort is in support of the Space Infrared Telescope Facility (SIRTF).

SIRTF is a long-life, space-based telescope for infrared astronomy from  $2\ \mu\text{m}$  to  $700\ \mu\text{m}$  currently under investigation by NASA-ARC. It will be cooled to below 2 K by superfluid helium. The lifetime of the mission will be limited by the lifetime of the liquid helium supply. To maximize the scientific return for the total overall cost of the SIRTF mission, it will be necessary to periodically replenish the liquid helium cryogen life or find some means to develop and guarantee an ultra-long-life dewar.

Specific tasks identified by the Statement of Work were:

- Experiment Preparation. The contractor shall determine by computer simulation the maximum transfer rate that can be achieved with a practical modification of the contractor's existing equipment. The contractor shall modify the equipment to achieve this flow rate with a goal being 300 liters/hour. The contractor shall precalibrate the liquid level sensors and cryogenic pressure transducers in a small superfluid helium system. The contractor shall assemble and leak check the system, and achieve a high vacuum in the guard vacuum space.
- Steady State Flow Experiments. The contractor shall measure the pressure, temperature, and heat flow in a transfer line as a function of mass flow rate, along the transfer line. The range of these parameters shall span the range from zero flow to the maximum flow rate that can be practically achieved with the apparatus. These measurements shall be compared to previous simulations of the transfer process. The effects of coupler and transfer line heat leak shall be simulated with heaters.
- Transient Behavior. The contractor shall perform a cooldown of the transfer line and the receiver tank. During the cooldown, the contractor shall monitor the pressure, temperature, heat and mass flow histories of the tanks and of the transfer line, and shall compare these results to previous calculations, if any, of the process.
- Pump Performance. The contractor shall measure the pressure head vs. mass flow as a function of heat input of the two thermomechanical pumps, relate performance to heater design and location, and compare the results to calculations and simulations of the pump performance. The contractor shall perform transfers under conditions predicted by computer simulations to create the fastest and most efficient transfers, and compare the results to the simulations.
- Deliverable Items. The contractor shall deliver a report containing a summary of the experimental data and theoretical calculation simulations. The report shall also contain a summary of the accuracy of the data and any significant deviations between theory and the experiment. The contractor shall also deliver detailed experimental data upon the request of the customer.



## Section 2 DISCUSSION OF TESTS PERFORMED DURING 1986

The following paragraphs document the test apparatus configuration; some of the receiving and bench tests performed to calibrate the porous plugs; and the transfer test results.

### 2.1 TEST APPARATUS DESCRIPTION

A flow schematic of the test apparatus is shown in Figure 7. The large vessel has a volume of 570 liters. It is surrounded by three vapor-cooled shields, multilayer insulation, and an outer shell. The large vessel is annular with a 45.7 cm diameter instrument cavity in the middle. The small vessel is an 80-liter welded stainless steel cylinder with dished heads. It is located in the large vessel instrument cavity, but is thermally isolated from the large vessel by fiberglass supports, 20 layers of multilayer insulation, and vacuum.

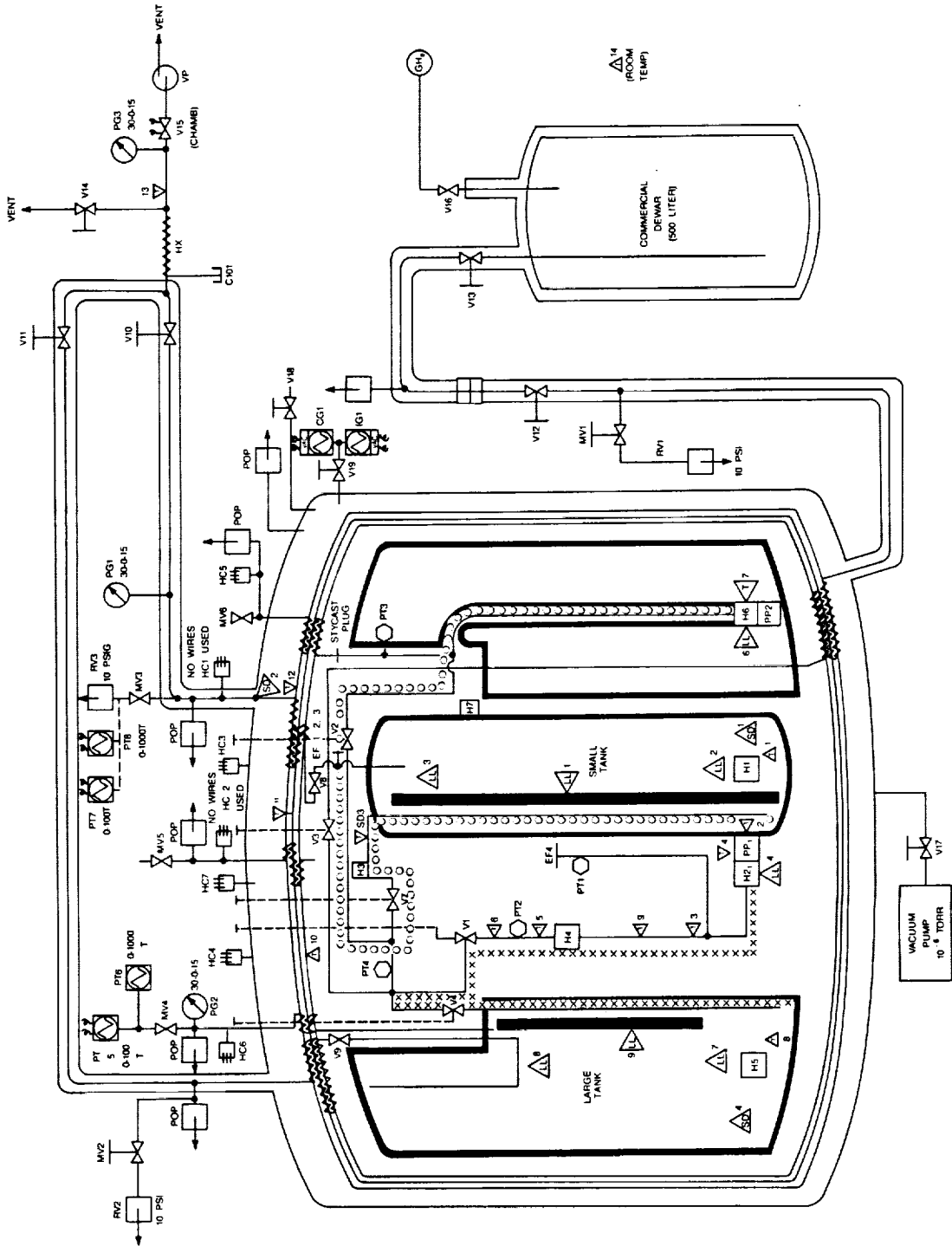
The plumbing and valve arrangement and the two thermomechanical pumps allowed Helium II to be pumped from either the small vessel to the large vessel (path A) or from the large vessel to the small vessel (path B). The path A transfer line was 609 cm long, 447 cm of which was corrugated stainless steel flexible tubing that had a minimum ID of 1.25 cm and a maximum ID of 1.88 cm. The balance of the transfer line was rigid stainless steel tubing with an ID of 1.0 cm. The path A transfer path had an electric heater wrapped around a section 7.0 cm long, 145 cm downstream of the porous plug. Path A also had two globe-style bellows valves: one (V1) with a 0.3 cm diameter orifice 430 cm downstream of the porous plug, and the other (V4) with a 1.5 cm orifice 540 cm downstream of the porous plug.

A germanium resistance thermometer was placed on each side of the porous plug, at three locations downstream of the porous plug (at 81, 151 and 421 cm), and in the large vessel which acted as a receiver dewar. Three Siemens KPY-12 pressure transducers were placed downstream of the porous plug: one to measure the pressure at the plug on 0.2 cm diameter tube that branched off the plug and ran vertically to the top of the small tank, one 428 cm from the plug, and one 502 cm from the plug.

Transfer path B was 350 cm long, was almost entirely corrugated tubing like that used in path A, and included globe valves downstream of the plug. A section of path B, 92 cm long downstream of the plug, was wrapped with heater wire. There was a GRT mounted on the downstream side of the plug and a pressure transducer downstream of the plug.

The vent lines from the large and small vessels were routed through high-conductance valves and a heater hose to a vacuum pumping system with a capacity of 700 liters/second down to one torr.

The porous plugs used as the thermomechanical pumps in both flow paths were made of a porous ceramic similar in composition to mullite ceramic. Bubble tests of these plugs showed them to have a maximum surface pore diameter of 0.5 micron. By weighing the plugs dry and then saturated with water, we determined that the plugs had a 41 percent void volume. Several plugs from the same batch were broken with a hammer across the thickness, and scanning electron microscope (SEM) photographs were taken of the plug microstructure. Figure 8, as well as other photographs not shown, show that the microstructure is quite rough, with many void dimensions much larger than 0.5 microns. SEM photographs of the surface of the plugs indicated fewer voids on the surface than



NOTE T119 = GR1  
T1014 = PLATINUM

- △ — SILICON DIODE
- ⊖ — VACUUM PUMP
- HX — HEAT EXCHANGER
- ⊗ — VACUUM XOUZER
- PP — POROUS PLUG
- H — ELECTRIC HEATER
- — RELIEF DEVICE
- ⊘ — VALVE
- — HERMETIC CONNECTOR
- ⊖ — COLD PRESSURE XOUZER
- ⊖ — LIQUID LEVEL SENSOR
- ⊖ — TEMPERATURE SENSOR
- ⊖ — PRESSURE TRANSDUCER
- ⊖ — PRESSURE GAUGE
- XXX — PATH 'A'
- — PATH 'B'

Figure 7. Detailed Flow Schematic of the 1986 Helium Transfer Experiment

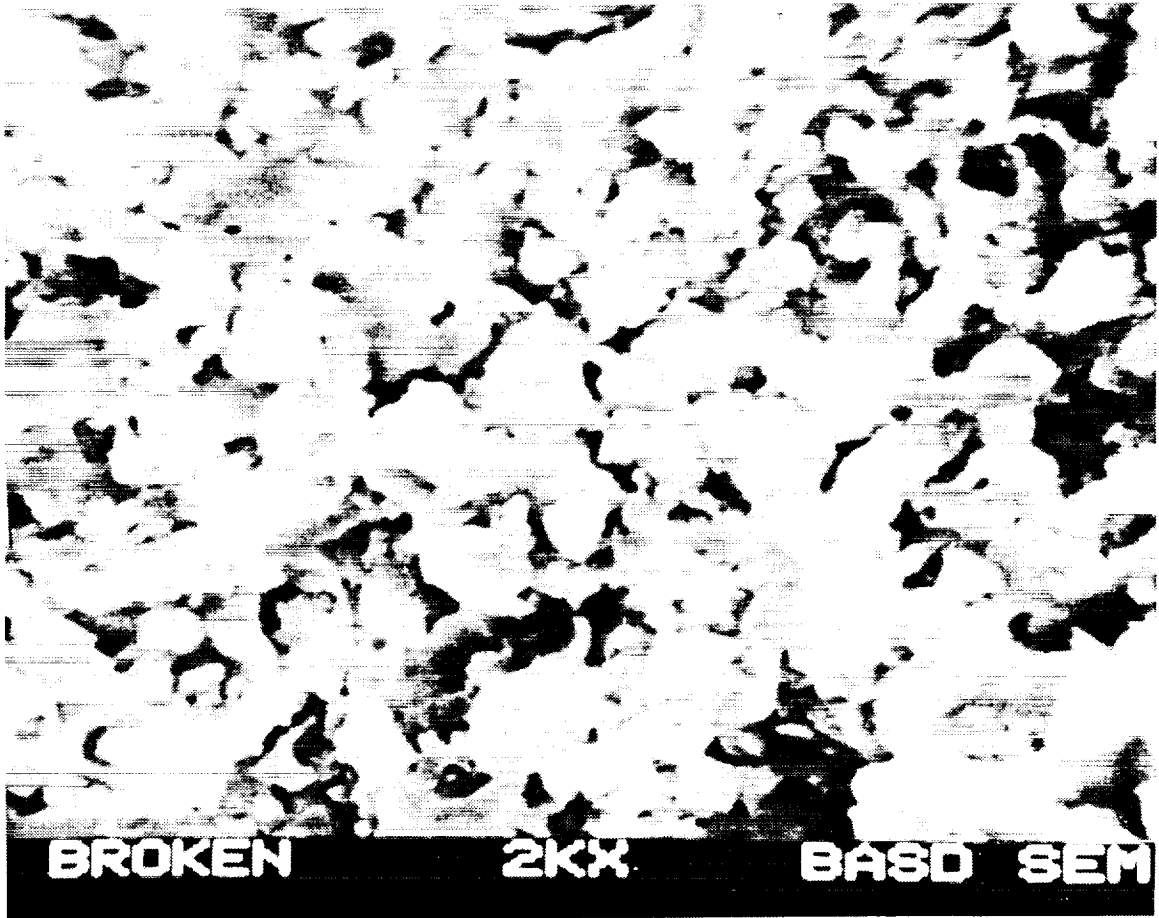


Figure 8. Scanning electron microscope photograph of the porous plug interior.

inside the plug. The plug manufacturer, Coors Ceramics, has reported a "skin effect" such as this in other applications.

The porous plug used in path A was 1.27 cm thick and 3.81 cm in diameter. It was bonded into a stainless steel retainer and a GRT was bonded to each side with Stycast epoxy as shown in Figure 9. The resulting exposed surface area was 9.7 cm<sup>2</sup>. The retainer was sealed between the heater housing and a flange on the side of the small vessel using bolts and indium wire. The heater was mounted approximately 0.5 cm from the surface of the plug.

The porous plug used in path B was 1.27 cm thick and 2.54 cm in diameter. It was bonded into a stainless steel retainer and a GRT was bonded to one side as shown in Figure 9. The resulting exposed surface area was 4.10 cm<sup>2</sup>. The retainer was sealed to the heater housing using indium wire. The heater housing was welded onto the end of the vacuum-jacketed transfer line which hung inside the large vessel.

The heaters used in both flow paths were precision wire wound resistors which had very low resistance change with temperature. They were mounted in the fluid and sized so that the heat flux stayed substantially below the critical heat flux which would cause boiling, approximately 3 W/cm<sup>2</sup>.

The small vessel was wrapped with phosphor-bronze wire to provide a capability for warming it up. This heater wire was bonded to the small vessel with varnish and was covered with 20 layers of multilayer insulation.

## 2.2 ESTIMATED DATA ACCURACY AND LIMITATIONS

The test apparatus was prepared for the test by pumping a high vacuum (better than 10<sup>-6</sup> torr) on the guard vacuum, and vacuum pumping and helium purging the vessels and all plumbing several times. The two vessels were filled with normal liquid helium and then converted to Helium II by vacuum pumping. The GRTs, which had been calibrated by the manufacturer, were recalibrated by measuring the helium vapor pressure with pressure transducers that have an accuracy of 0.1 torr. The GRTs were repeatable to within 10 mK and were accurate to within 20 mK. The pressure transducers were accurate to within 10 torr; cold pressure transducer 2 (CP2) could read a maximum of 220 torr, while CP1 and CP3 could read a maximum of 260 torr. Cold pressure transducer CP1 was not accurate at pressures less than 10 torr over saturation pressure, since this was the amount of head that the pressure had to overcome.

The flow rate was determined by taking the derivative with respect to time of the small vessel liquid volume. The flow rate data had a noticeable amount of noise on it, which has been traced to the commercial liquid level probe power supplies. Contributing to this problem was the amplifying effect on noise of taking the small difference between two numbers and then multiplying by a large constant.

## 2.3 CHRONOLOGICAL SUMMARY OF TESTS PERFORMED IN 1986

The following is a brief chronological summary of all the tests performed in September 1986. Paths A and B are shown in the simplified test apparatus schematic in Figure 1. The no-flow runs have the valves closed downstream of the porous plug, stopping any flow.

ORIGINAL PAGE  
BLACK AND WHITE PHOTOGRAPH

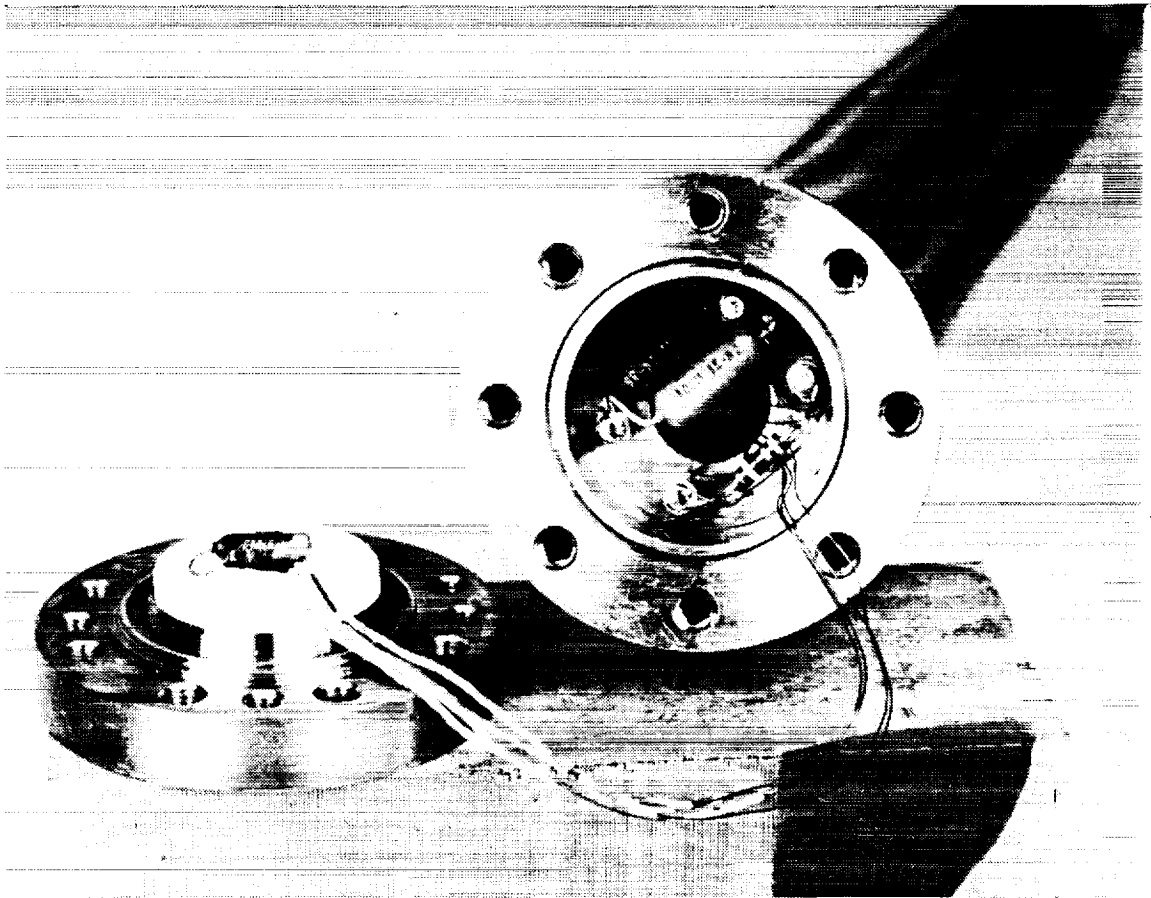


Figure 9. The porous plug assembly used in path B.

9/17/86

No-flow run 1 along path A; 3 W of heater power applied at the porous plug.

Flow run 1 along path A; 3, 6, and 12 W of heater power applied at the porous plug.

No-flow run 1 along path B; 0.8 mW to 1.6 W of heater power applied at the porous plug.

9/18/86

Flow run 1 along path B; 0.9 to 4.7 W of heater power applied at the porous plug.

No-flow run 2 along path A; 0 to 1.0 W of heater power applied at the porous plug.

Flow run 2 along path A; 0 to 4.0 W of heater power applied at the porous plug, 2.0 W of heater power applied at the bayonet heater.

9/19/86

Flow run 2 along path B; receiving dewar initially warm (60 K); 0.1 to 1.5 W applied at the porous plug; receiving dewar filled completely.

#### 2.4 TEST PROCEDURES AND RESULTS

The first experiment was to demonstrate the "London pressure"<sup>9</sup> that could be generated by having the thermomechanical pump pressurize a closed line. This was done by closing valves V4, V2, V3, V7, and opening valves V8 and V10. No heat was supplied by the heater, but there was a temperature gradient across the plug, with the downstream side of the plug being warmer because the small tank was being pumped by the vacuum system. **Figure 10** shows the resultant pressure rise with time for the three cold pressure transducers that were connected into the downstream side of the plug. **Figure 10** also shows the pressure on the downstream side of the plug calculated from the temperature on either side of the plug and the "London relation":  $\Delta P = \int \rho s dT$ , where the temperature, T; entropy, S; density, and  $\rho$  are integrated across the plug. The pressure transducer values were adjusted for pressure head effects and the discrepancies between the data and theory are probably due to inaccuracies in the transducer data.

The next experiment was to transfer approximately 40 liters from the small tank to the large tank along path A. This was done by opening valve V4 and allowing helium to flow with no input from the heater. The flow rate began to drop off, and after 12.5 minutes heater H2 was supplied 3 W of power. At a time of 18.0 minutes the H2 power was increased to 6 W, and at 23.5 minutes it was increased to 12 W. At 30 minutes the power to H2 was reduced to zero, and the transfer was allowed to continue for another 14 min.

**Figure 11** shows the liquid volume in both tanks, the total liquid volume, and the flow rate between the two tanks. The liquid volume shown for the small tank is approximately the total volume, while the large tank volume has had an offset factor subtracted from it so that the volume is zero at the start of the flow test for comparison to the small tank.



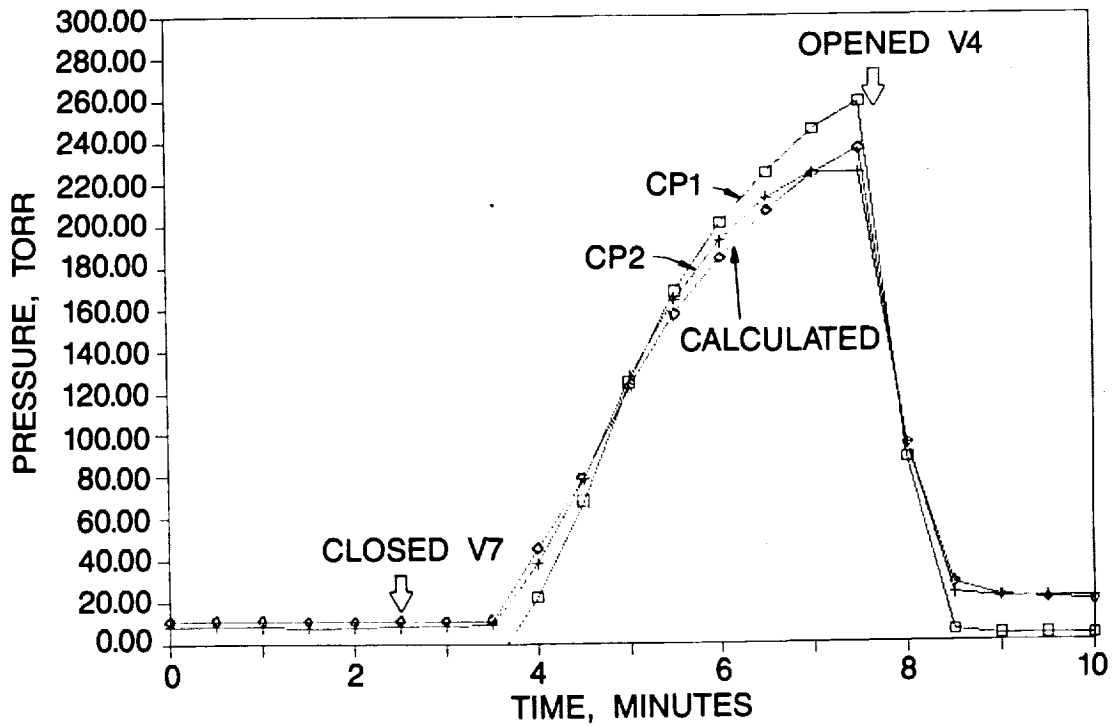


Figure 10. The pressure measured and calculated for one of the 1986 no - flow experiments.

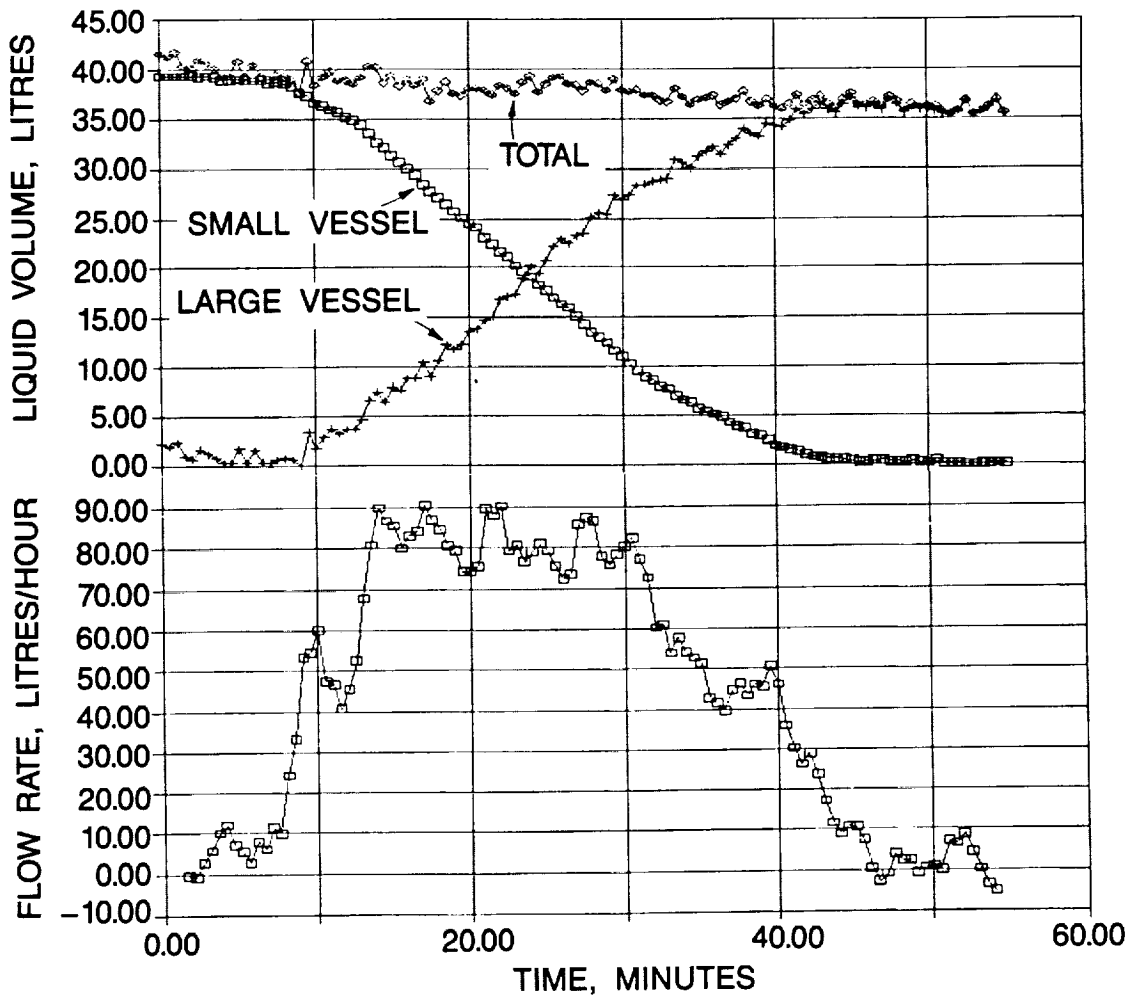


Figure 11. The liquid volume and flow rate during the first 1986 transfer experiment.

It can be seen in Figure 11 that the total liquid volume decreased 3.5 to 0.5 liters during the transfer of 36 liters or a 9.7 ±1.4 percent loss. This compares to a loss of 2.8 liters, which would be expected due to the total electrical heat input and the small tank heat leak. The difference is probably due to the heat leak into the large tank, which is not known. In an ideal transfer, the total helium loss has been calculated to be 1.3 percent at the 1.5 K supply temperature. The experiment was not an ideal transfer in that the power levels over 3 W caused additional helium boiloff, but no additional flow rate. If the transfer had been run with a continuous 3 W input, the resulting helium loss would have been 0.97 liters or 2.4 percent. It appears that the most efficient heater power would have been somewhat less than 3 W.

Figure 12 shows the temperature profile as a function of distance from the supply dewar to the receiver dewar along the transfer line for various heater inputs and flow rates. These profiles show that the flow appears to be restricted by the porous plug at high heater powers.

A similar experiment was performed in which helium was transferred from the small tank to the large tank using path A, but additional heat was added at heater H4 to simulate the heat leak from a bayonet coupling. Figure 13 shows the temperature profile as a function of distance from the supply dewar to the receiver dewar along the transfer line for various heater inputs and flow rates. Note that the flow rates and temperature profiles are similar for the cases where 6 W was applied at H2, where 4 W was applied at H2, and where 2 W was applied at H4.

The final experiment consisted of cooling and filling an initially warm tank. The small tank was heated above 60 K. Valves V7, V8, V9, V10, and V11 were initially opened and the rest of the valves were closed. Valve V2 was opened in an attempt to start the transfer. No transfer started, even when 1.1 W was applied to heater H6. It was noted that the pressure in the receiving (small) tank and line was 3 torr, while the pressure in the supply tank was 16 torr as shown in Figure 14. Valve V10 was then closed and the pressure in the small tank and transfer line increased until it was equal to the pressure in the supply dewar. Within a few minutes, the pressure in the small tank increased and the temperature decreased rapidly, indicating that liquid helium was being transferred. The small tank was then filled at a rate of 30 liters/hour until it was completely full.

It is apparent that a necessary condition for liquid to break through a porous plug is that the pressure on the downstream side of the plug be equal to or greater than the supply side.

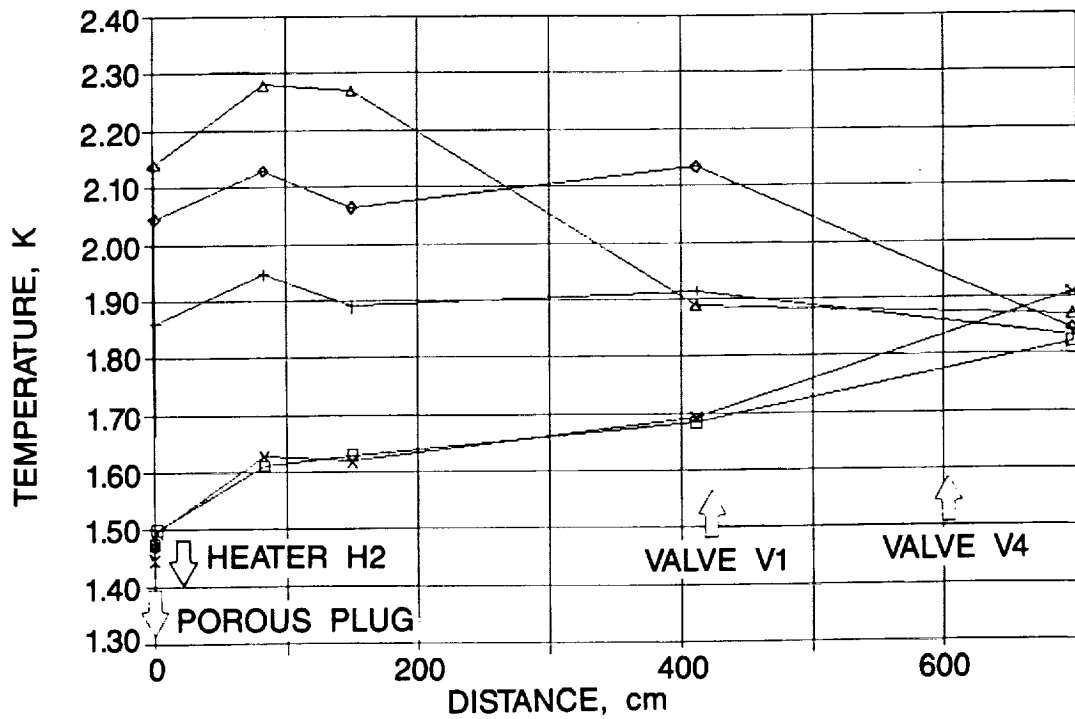


Figure 12. Temperature profiles along path A during run 1 of the 1986 tests. Zero heat input at the porous plug is the  $\square$  and the  $\times$  symbol, 3.0 watts at the porous plug is the  $+$  symbol, 6.0 watts at the porous plug is the  $\diamond$  symbol, and 12.0 watts at the porous plug is the  $\triangle$  symbol.

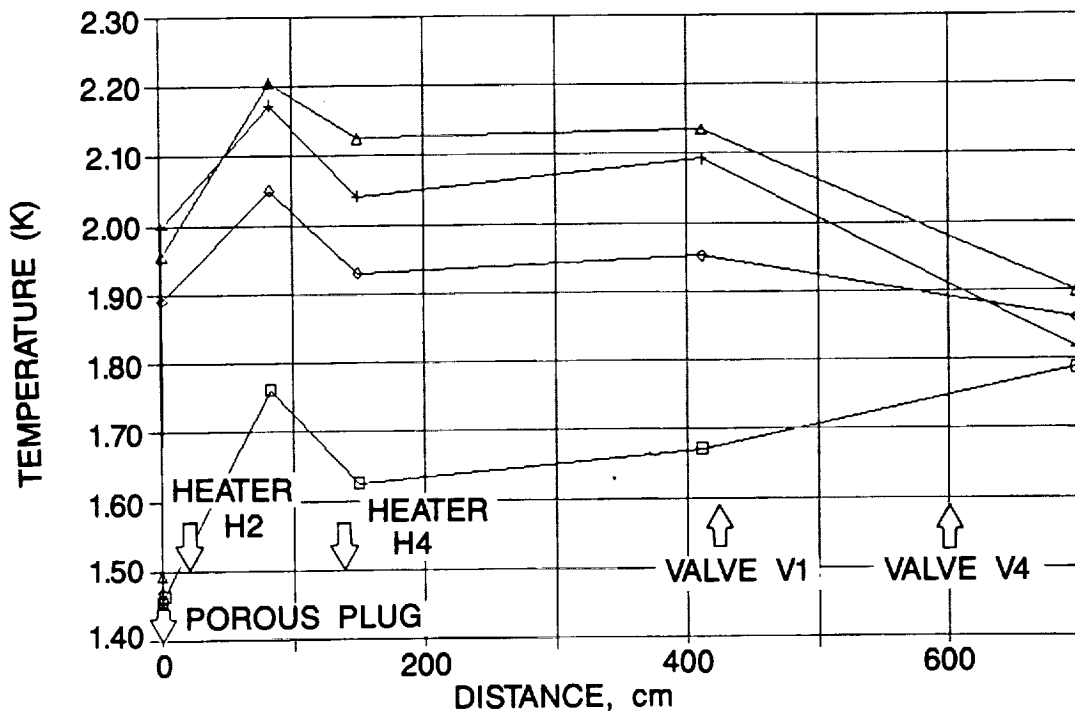


Figure 13. Temperature profiles along path A during run 2 of the 1986 tests. Zero heat input at the porous plug is the  $\square$  symbol, 6.0 watts at the porous plug is the  $+$  symbol, 4.0 watts at the porous plug is the  $\diamond$  symbol, and 4.0 watts at the porous plug and 2.0 watts at the bayonet heater is the  $\triangle$  symbol.

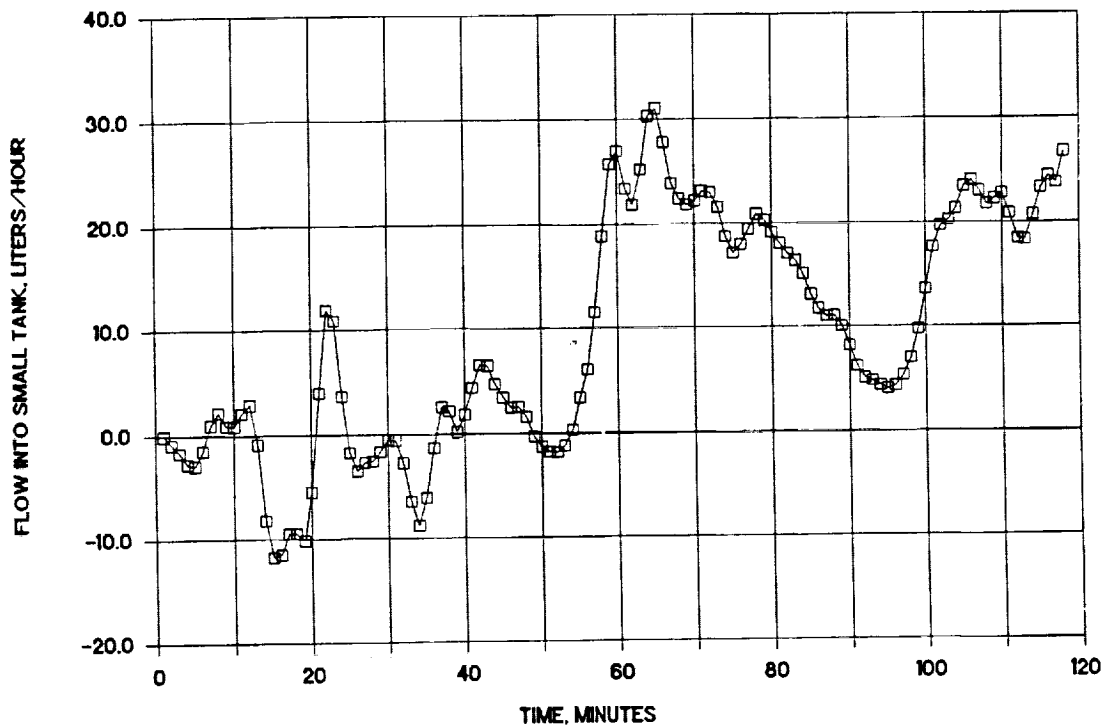
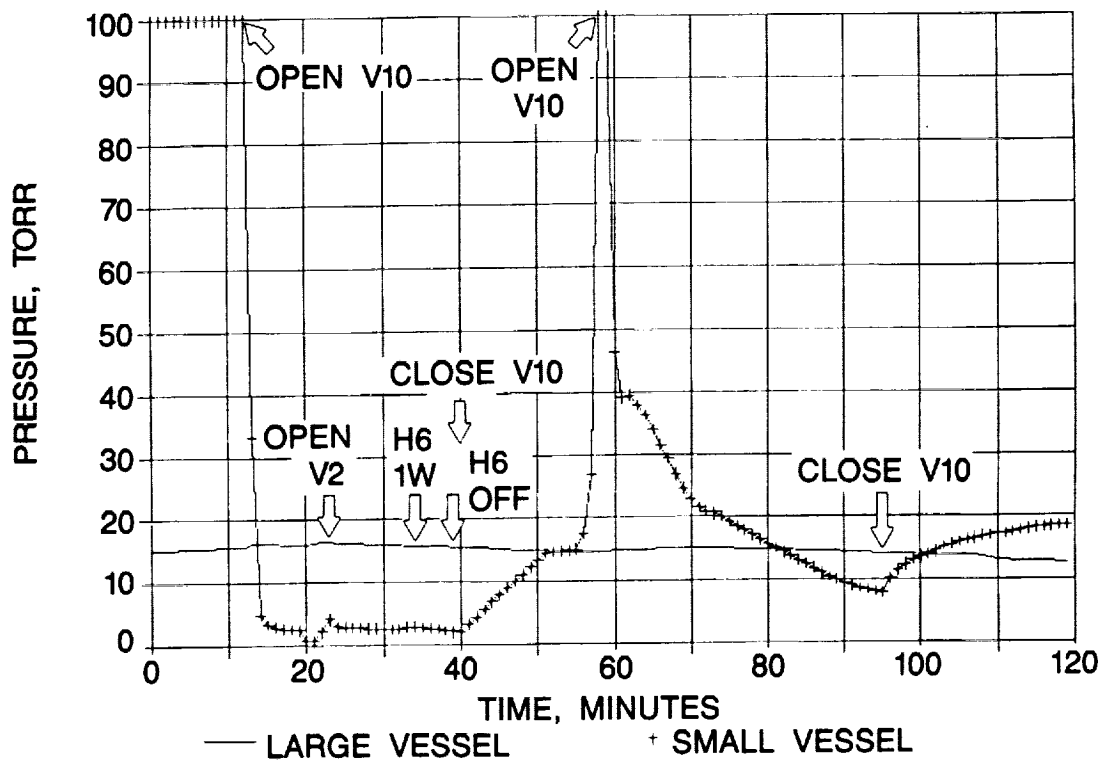


Figure 14. Pressures in tanks and flowrate during 1986 fill of an initially warm (run 2 along path B). The supply dewar pressure is the - symbol and the receiver pressure dewar is the + symbol.

### Section 3 DISCUSSION OF TESTS PERFORMED DURING 1989

The following paragraphs document the test apparatus configuration and test results for the last series of superfluid helium transfer tests.

#### 3.1 TEST APPARATUS DESCRIPTION

The test apparatus which was used in the 1986 test was modified and used again for the 1989 test. These modifications were undertaken to eliminate the problems that occurred during the 1986 test. The plumbing and sensors are shown in Figure 15. As was the case in the 1986 test, a small tank was placed in the instrument cavity of the large dewar, and a transfer line was used to connect the two tanks.

Figure 16 is a photograph of the small tank and the first part of the transfer line before they were installed in the large dewar. Figure 17 shows an external view of the test dewar and the overall test arrangement.

The porous plug in path A was replaced with a porous plug which had a surface area of  $500 \text{ cm}^2$ , 50 times the surface area of the original porous plug. This porous plug was 0.3 cm thick and had four closed-end cylinders 1.9 cm in diameter by 20 cm long. These cylinders were bonded into a stainless steel retainer which was sealed with indium between the heater housing and a flange on the side of the small vessel. A photograph of the assembled porous plug is shown in Figure 18. The heaters, shown in Figure 19, were four 9-inch long, 8-inch thick copper rods wrapped with nichrome wire. These were placed inside a 0.25-inch OD thin-walled brass tube which was filled with epoxy. One of each of the completed heater assemblies were then mounted inside the porous plug cylinders. The porous plug for path B was the same as that used in the 1986 tests. During the 1989 tests, path B was used only to transfer Helium II back to the small tank so that transfers along path A could be run again. No significant data was collected during the path B transfers. During leak tests it was discovered that valve V7 did not close completely. To correct this, valve V9 was placed in series with valve V7. Valve V7 was left open for the entire test and V9 used in its place. Due to problems engaging the actuator on valve V9, the actuator was engaged at the start of the cooldown and left engaged for the entire test.

Germanium resistance thermometers (GRT) were placed on each side of the porous plug, at the bottom of the supply dewar, and at five locations downstream of the porous plug. Three Siemens KPY-12 pressure transducers were placed downstream of the porous plug. One KPY-12 pressure transducer measured the pressure across the plug. The silicon diodes were used to monitor temperatures during the cooldown and warmup of the dewars. Two warm pressure sensors, one 0 to 100 torr and one 0 to 1000 torr, were placed on each dewar and were used to measure the bath pressure when V10 and V11 were closed. The exact location of these sensors is given in Table 1.

To correct the noise problems which occurred during the 1986 tests, each sensor had its own dc power supply and a custom-manufactured amplifier designed to raise the signal from the sensor to a voltage between zero and 10. This voltage was converted into a 12-bit digital signal. The data acquisition system was developed using commercial software and an IBM PC-AT. During data acquisition, the incoming digital signal was sampled once every five seconds. Current temperatures, pressures, liquid

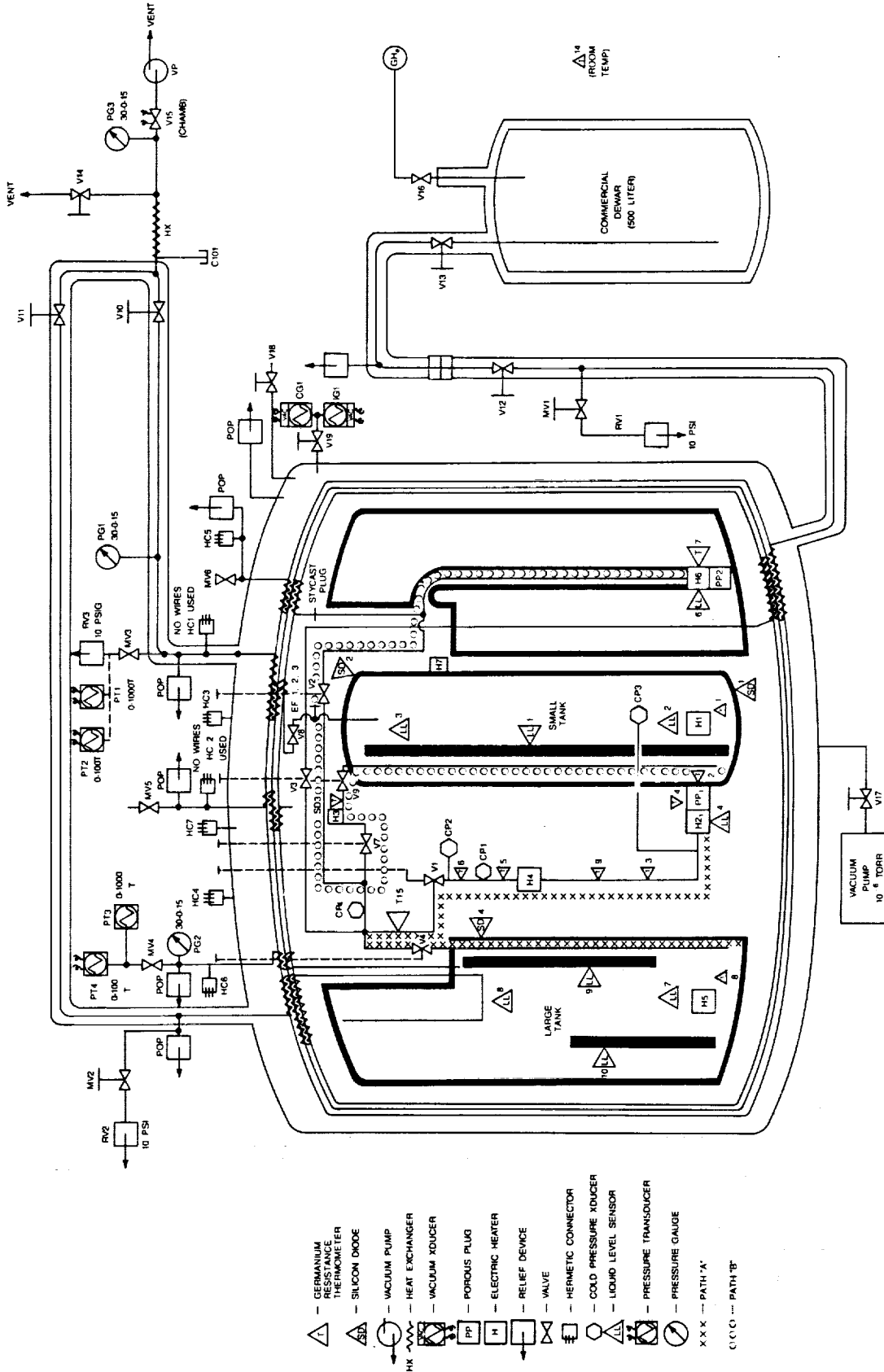


Figure 15. Detailed Flow Schematic of the apparatus used in the 1989 helium transfer tests.

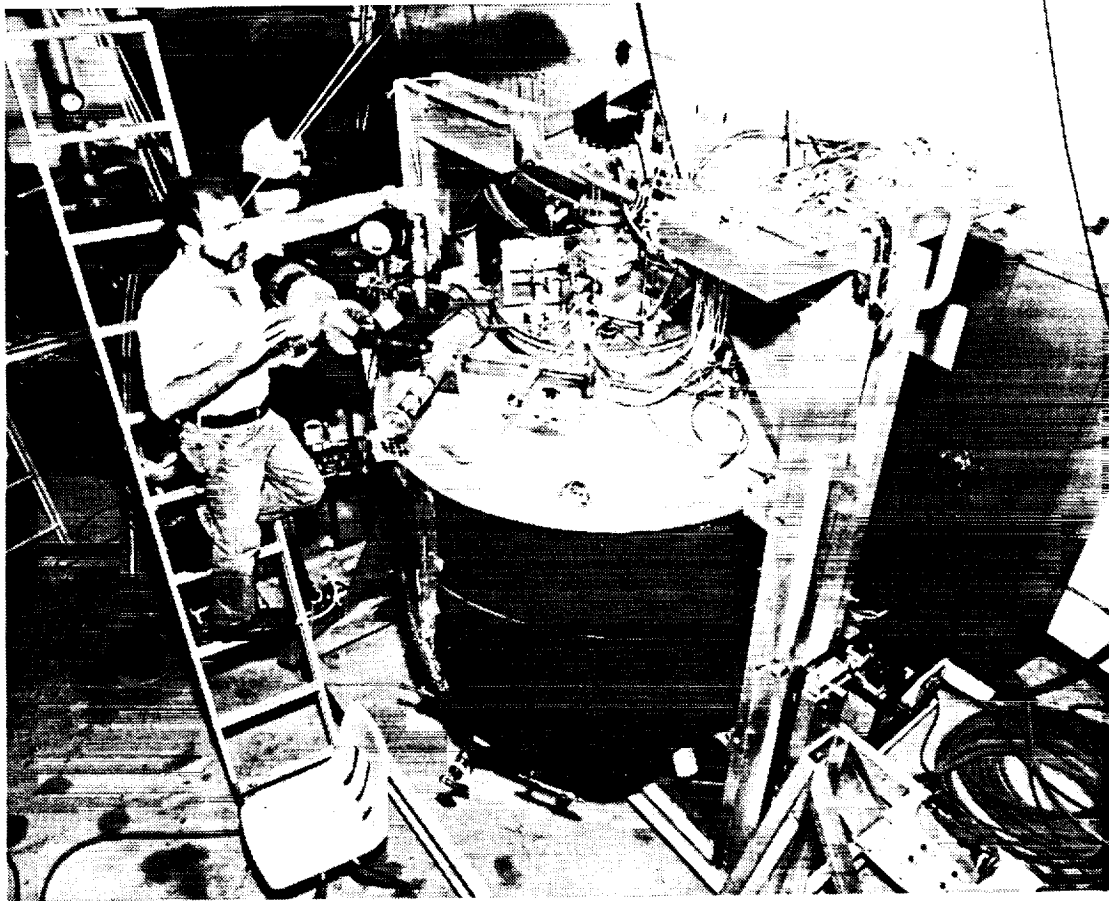


Figure 16. Overall view of the apparatus used in the 1989 helium transfer tests. The test dewar contains both the large and small tanks. The boxes containing the power supplies and amplifiers for the instrumentation are mounted just above the dewar.

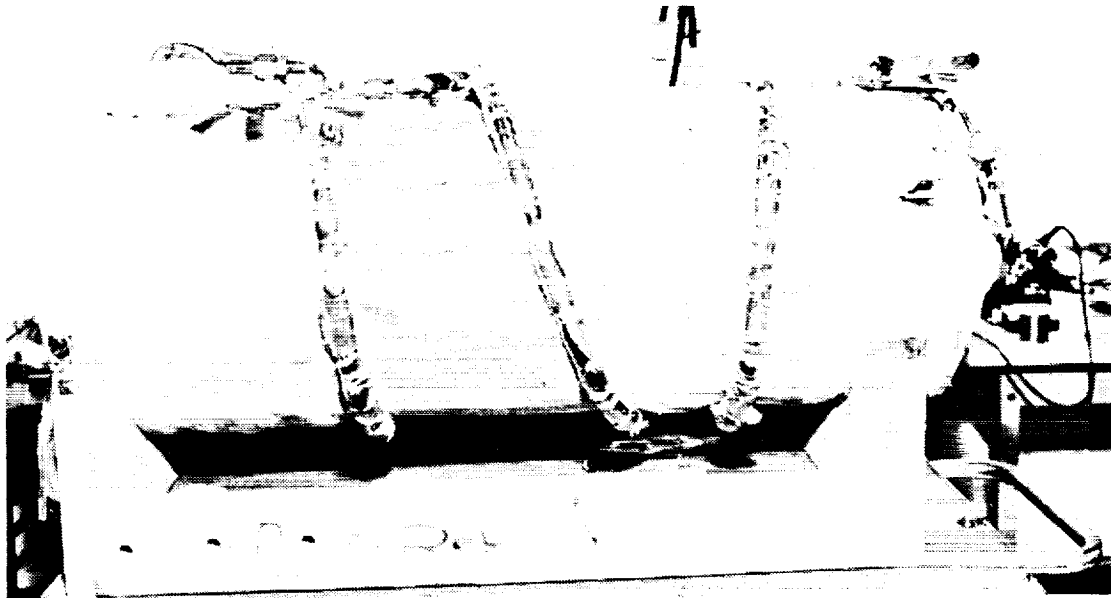
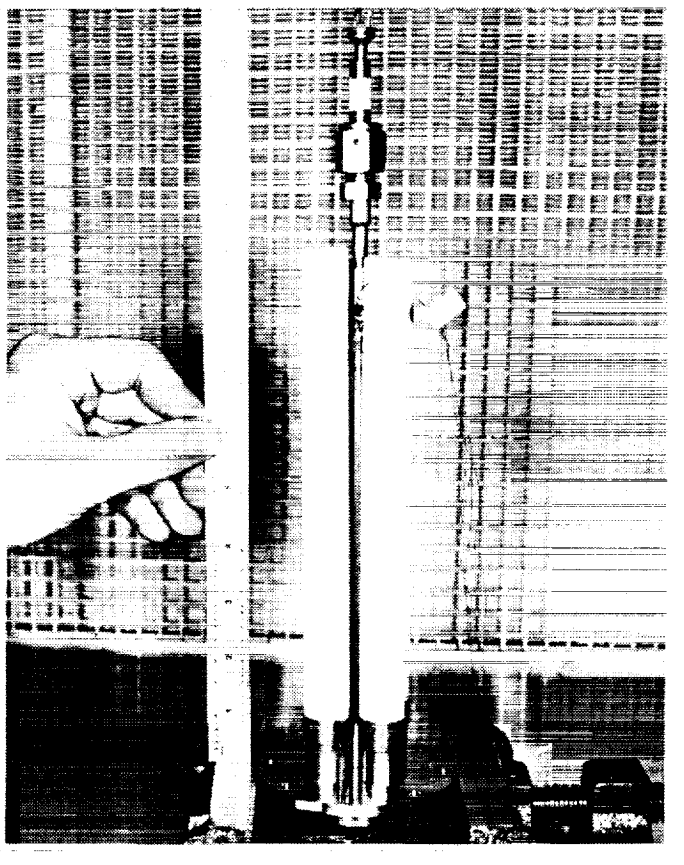


Figure 17. The small tank and the first part of the transfer line used in the 1989 helium transfer tests. The transfer line is wrapped around the small tank, but insulated from it.



ORIGINAL PAGE IS  
OF POOR QUALITY

Figure 18. The porous plug assembly used on path A in the 1989 helium transfer tests. The four plugs are bonded into one retainer. A heater is inserted inside each of the four hollow plug tubes and the assembly is then inserted into the small tank. Cold pressure transducer 3 (CP3) can be seen mounted at the top of the assembly.

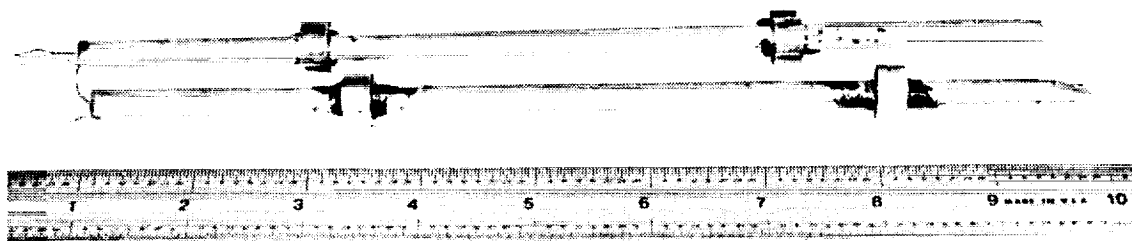


Figure 19. The porous plug heaters used in the 1989 helium transfer tests. The heaters were wired in pairs and one heater was inserted in each porous plug cylinder.



Table 1  
PRESSURE AND TEMPERATURE SENSORS  
USED IN THE 1989 TESTS

<u>SENSOR</u>	<u>LOCATION</u>	<u>REMARKS</u>
CP1	Path A, 151 cm from porous plug	Absolute pressure
CP2	Path A, 428 cm from porous plug	Absolute pressure
CP3	Path A, at porous plug	Differential pressure across porous plug
CP4	Path A, 502 cm from	Absolute pressure
GRT 1	In small tank, 2.0 cm off the bottom	
GRT 2	On supply side of path A porous plug	
GRT 3	On path A transfer line, 29 cm from porous plug	
GRT 4	On downstream side of path A porous plug	
GRT 5	On path A transfer line, 151 cm from porous plug	
GRT 6	On path A transfer line, 421 cm from porous plug	
GRT 7	On downstream side of path B porous plug	Shorted to ground
GRT 8	In large tank	Not connected in 1989 tests, pressure data used
GRT 9	On path A transfer line, 81 cm from porous plug	
GRT 15	On path A transfer line, 505 cm from porous plug	Appears to have had poor thermal connection to transfer line liquid

levels, and flow rates were calculated and displayed on the screen for real-time monitoring of the test. The raw voltage data was also written to a disk file for later evaluation.

### 3.2 CALIBRATION PROCEDURE

#### 3.2.1 Calibration Test

Prior to the final test in 1989, a series of calibration tests was performed. These calibration tests had three main objectives. The first and primary goal was to obtain a set of data which could be used to relate the voltage output of the GRTs and the cold pressure transducers (CPs) to temperature and pressure, respectively. The second objective was to verify the repeatability of these sensors over a number of thermal cycles. The final objective was to identify and eliminate sensors which had low gains, were not repeatable over separate thermal cycles, or had outputs which would be out of the range of the A/D converter in the range of conditions expected during the final helium transfer experiment.

This calibration test was performed in a 7-inch diameter lab dewar with a nitrogen shield. The CPs were connected through a common manifold. On one side was the helium bath and on the other side was Helium 3. This arrangement allowed for calibration of the CPs off the saturation line. Four GRTs were attached to the bottom of a probe which ran the length of the dewar. This ensured that the GRTs were in contact with liquid helium throughout the test.

The electronics were calibrated prior to cooldown using a calibrated decade resistance box. The dewar was filled with liquid helium and the temperature lowered to approximately 1.5 K by pumping on the bath. The pump was then turned off and the bath pressure was allowed to rise past the lambda point. While the bath pressure was rising, the pressure on the Helium 3 side was independently raised and lowered. Once the bath pressure had gone above the lambda point, the pump was reattached and the pressure was again lowered to approximately 4 torr. This thermal cycling was continued until all the liquid helium had evaporated. This complete test procedure was repeated three times and complete data sets taken each time. The data from the first calibration test was extremely noisy due to grounding problems and was not used for calibrations. This was corrected and good data was obtained in the second and third runs.

#### 3.2.2 GRT Calibration

The bath temperature at the time of each data sample was calculated using the pressure measured with a warm pressure sensor. A fifth order logarithmic curve fit equation was calculated relating the pressure and temperatures along the saturation curve. Data for this curve fit was taken from the National Bureau of Standards (NBS) published tables of the vapor pressure for helium.<sup>16</sup> By comparing data from the second and third tests, it was determined that within the accuracy of our setup no change in the GRT's resistance as a function of temperature occurred between cooldowns. Data from the two final runs was combined and a polynomial curve-fit analysis performed. A fifth order polynomial equation was calculated which was then compared with the original data. The largest residual errors in the range of temperatures expected during the test, from 1.4 K to the lambda point, was 5 mK. GRTs 4, 5 and 15 were calibrated during these calibration tests, and these curve-fit equations were used in the analysis of the transfer test data. The fourth GRT which was calibrated during this test

was kept as a backup in case one of the other eight GRTs failed prior to cooldown and needed to be replaced.

The other five GRTs, (GRT1, GRT2, GRT3, GRT6, and GRT9) were calibrated using the in-place calibration data taken during cooldown and warmup. During cooldown of the test dewars, pumping was stopped at 15 predetermined bath pressures and data collected for approximately two minutes. These pressures ranged from 200 torr to 4 torr, with data taken every 5 torr beginning just below the lambda point. This procedure was repeated during the warming of the dewars after all the transfer tests had been completed. Bath temperature was again calculated using the warm pressure sensor and the NBS vapor pressure data. Fifth order curve-fit equations were calculated for these six GRTs which gave temperature as a function of voltage. Again, error analysis was performed comparing the curve-fit equations to the original data, and the largest residual error was 8 mK. The temperatures calculated for these GRTs were compared with the temperatures given by GRT4 and GRT5 using the the calibration equations from the calibration tests. These were within 15 mK of each other.

### 3.2.3 Cold Pressure Sensor Calibrations

During the cooldown for the second calibration test, one of the CPs failed. The line connecting the sensor to the bath was blocked on a second CP, resulting in good data being collected for only two CPs during the second calibration run. Good calibration data was collected on all four of the CPs installed for the third calibration test. CP3 was left in place for both the second and third calibration runs to test for calibration shifts caused by the thermal cycling between cooldowns.

This data showed that the slope of the calibration curve changes only very slightly, but that the zero of the CPs changes significantly between cooldowns, on the order of 6 torr. By comparing the output of the CPs at the same absolute pressure differences but taken at different temperatures, it was determined that very little temperature dependence existed over the temperature range of interest.

Due to the zero shift which occurs during thermal cycles, it was necessary to calibrate the CPs in place after the test setup had been cooled to operating temperatures. This was done using the data collected during the no-flow runs. CP3 measured the pressure difference between the transfer line and the small dewar. Before the start of the no-flow runs, valve V9 was opened to equilibrate the pressures in the small dewar and the transfer line. This data was used to establish the zero point of CP3. Once V9 was closed, the CPs on the transfer line were exposed to the same bath pressure. This pressure was calculated by adding the pressure in the small tank to the pressure measured by CP3. By subtracting the pressure head caused by the column of liquid above the position of each CP, an accurate set of calibration data was obtained and used to calculate the slope and zero for each of the three CPs down the line from the porous plug. As predicted by the calibration tests, the slope that was calculated for these CPs was nearly exactly the same as those found during the calibration tests.

### 3.2.4 Estimated Data Accuracy and Limitations

The absolute best accuracy possible for this test was set by the digital bit conversion of the analog voltages. In the case of the GRTs, this raw voltage data was converted into resistance between zero and 5000 ohms. Given that a 12-bit analog-to-digital conversion was performed, the best resolution possible would be 1 ohm. This represents a best possible temperature resolution of 0.5 mK for a typical GRT. However, additional errors and uncertainty are added because of electrical system noise;

inaccuracy of the curve-fit equations used to convert the voltage output of the sensors to the temperature or pressure; and fluctuations in the sensors themselves, the electronics, and other sources. The accuracy of the curve-fit equations was calculated by comparing values which these equations gave to the original data used to calculate the curve-fits. The noise due to the electronics was estimated by placing a constant resistance across the leads to the sensors and recording the fluctuations in the voltage outputs. Finally, fluctuations in the sensors themselves were estimated by comparing data taken during the series of calibration tests run in 1989. This was kept to a minimum by using those sensors which had proven repeatable.

Taking all these factors into consideration, we have estimated the accuracy of the data. Pressures are accurate to within 1 torr. Temperatures are accurate to within 20 mK when the sensors are in thermal contact with Helium II in the line. Heater power is accurate to within 50 mW. The total liquid volume is accurate to within 4 liters.

The instantaneous flow rates are accurate to within 60 liters/hour, while the average flow rates, calculated from long-term changes in volume, are accurate to within approximately 20 liters/hour. The large amount of noise and uncertainty in the instantaneous flow rates is due to it being derived from the small difference between two liquid level readings only 10 seconds apart and then multiplied by a large factor to get liters per hour. This tends to greatly exaggerate noise due to electrical interference or uneven wetting of the superconducting wire by the Helium II. This data could be smoothed by a variety of methods, such as simply taking longer sample intervals, but all of these methods tend to distort the data with respect to time, which is more subtle and difficult to account for.

Due to a wiring error, the cold pressure transducers could not measure pressures above 280 torr.

Temperature sensor T2 could not measure temperatures below 1.55 K and data from T2 is not shown below this point.

Temperature sensor T7 was shorted to ground across two of its leads and was not usable.

Temperature sensor T15 was sending good data during the initial fill of the test facility with liquid helium. Once this transfer was complete and the roughing pump started, the data from T15 continued to show some temperature dependence, but the voltage output dropped to one-third of the value expected at these temperatures. The electronics, including the power supplies and amplifiers, were checked after the test and eliminated as possible sources of this discrepancy. Two theories have been developed to explain this drop. The first is that the bonding material holding the GRT to the transfer line was cracked during the rapid cooling caused by the start of the transfer of liquid helium, and that solid thermal contact was then lost when the vibrations from the start of the roughing pump shook the GRT loose from the transfer line. The second is that due to its position at the top of the transfer line, this sensor was never in contact with liquid during any of the runs. This problem is still being investigated and a conclusion on the cause and whether the data is recoverable has not been determined. Therefore this data is not shown.

A vacuum pump exhaust flow rate measurement was taken, but an electrical problem caused the measurements to fluctuate back and forth to zero. At the time of this report, this was still being investigated to determine if the non-zero results are

this was still being investigated to determine if the non-zero results are accurate, so this data is also not shown.

### 3.3 CHRONOLOGICAL SUMMARY OF TESTS PERFORMED IN 1989

The following is a brief chronological summary of all the tests performed in June 1989. The no-flow runs are with valves closed downstream of the porous plug, stopping any flow. There was very little instrumentation on path B, and the transfers along path B served primarily to move the Helium II back to the small tank so that a path A transfer could be performed again.

#### 6/20/89

Flow run 1 along path A; 0 and 6.0 W applied at the porous plug.

Flow run 1 along path B; 0.6 to 3.9 W of power applied at the porous plug.

Flow run 2 along path A; 20 W initially applied at the porous plug; later in the run, 18 W applied at the porous plug while 2 W were applied at the bayonet heater.

Flow run 2 along path B; 0.8 W applied at the porous plug.

No-flow run 1 along path A; 4.0 and 7.5 W applied at the porous plug.

Flow run 3 along path A; 24 W applied at the porous plug and 6.0 W at the bayonet heater.

Flow run 3 along path B; 1.0 W applied at the porous plug.

#### 6/21/89

Flow run 4 along path A; 12 W of power applied at the porous plug, 2 W of power applied at the bayonet. Valve V1 initially partially closed and then later fully opened.

Flow run 4 along path B; 1.1 W applied at the porous plug.

No flow run 1 along path A; 4.0, 8.0 and 12.0 W were applied at the porous plug.

Flow run 5 along path A; 20 W of heater power applied at the porous plug; Valve V1 initially partially closed and later fully opened.

Flow run 5 along path B; 1.2 W applied at the porous plug.

### 3.4 TEST PROCEDURES AND RESULTS

Data for this experiment was taken two hours at a time. To avoid having to give times in thousands of seconds since the time data acquisition was started, a start time was defined for each experimental run. This was chosen one or two minutes before the transfer started. All times given in this section are in minutes after this start time.

All data which we know was in error due to amplified sensor outputs which were beyond the capacity of the A/D converter have been eliminated from the graphs in this section.

### 3.4.1 Flow Tests

The results of the first experimental run are shown in Figures 20 through 27. During the first part of this run, no power was supplied to the heater to measure flow rate due to the difference in temperature between the two tanks. The power supplied for the remainder of the flow test, 6 W, was chosen to correspond with power settings used a number of times during the 1986 tests.

In this first run, the valve between the supply tank and the receiver tank (V4) was opened at 0 minutes, but power was not applied to the porous plug heaters for 8.5 minutes. During this time, 5 liters flowed from the supply tank to the receiver at an average flow rate of 35 liters/hour. When 6 W of power was applied at the porous plug, we obtained an average flow rate of 280 liters/hour. Power was turned off at 16.9 minutes and valve V9 opened at 19.2 minutes. During the transfer of Helium II, the vent valve for the supply tank (V10) was kept open and the vent valve for the receiving tank (V11) was closed.

The results of the second experimental run are shown in Figures 28 through 35. The computer model had predicted that 20 W of power input at the porous plug would achieve the maximum flow rate possible with this setup. During the start of this run this power setting was used. During the second half of this run the power input of 20 W was kept constant, but it was split between two locations: at the porous plug and at a location along the transfer line. This was done to simulate the effect of a bayonet coupling heat leak on the transfer.

To begin the second transfer, valve V4 was opened and 20 W of power was applied to the porous plug heater at 2.8 minutes. Approximately 2.5 minutes later, the porous plug heater was reduced to 18 W and 2 W were supplied at the bayonet heater. Both of these heaters were turned off at 14.25 minutes and valve V9 opened at 17 minutes. The average flow rate over the entire run was 470 liters/hour, with instantaneous flow rates of approximately 550 liters/hour at the beginning of the test run and 350 liters/hour at the end of the test run. Adding 2 W of heat at the bayonet instead of at the porous plug did not have a noticeable effect on the flow rate, but it lowered the pressure generated by the porous plug and increased the temperatures downstream of the bayonet heater. There is no event associated with the sudden rise in temperature of T5 and T6 at 4.5 minutes.

During the transfer back to the small dewar after the second test, we were able to fill the small dewar completely full of liquid helium. At the end of the return transfer along path B, the readings from liquid level 1 went to the highest level reached during any of the tests. When this reading was observed, a sudden rise in the small tank pressure was also observed. This is the same result observed during the 1986 test when the small dewar was filled completely.

The results from the third experimental run are shown in Figures 36 through 43. In this transfer, 24 W of power was supplied to the porous plug heater. This was 4 W above the power supply which the computer model had predicted would cause a maximum flow rate to occur. This power was used to test this prediction and to obtain data on an overdriven system. Again during the test power was added at the heater located on the transfer line to simulate a heat leak caused by a bayonet couple.

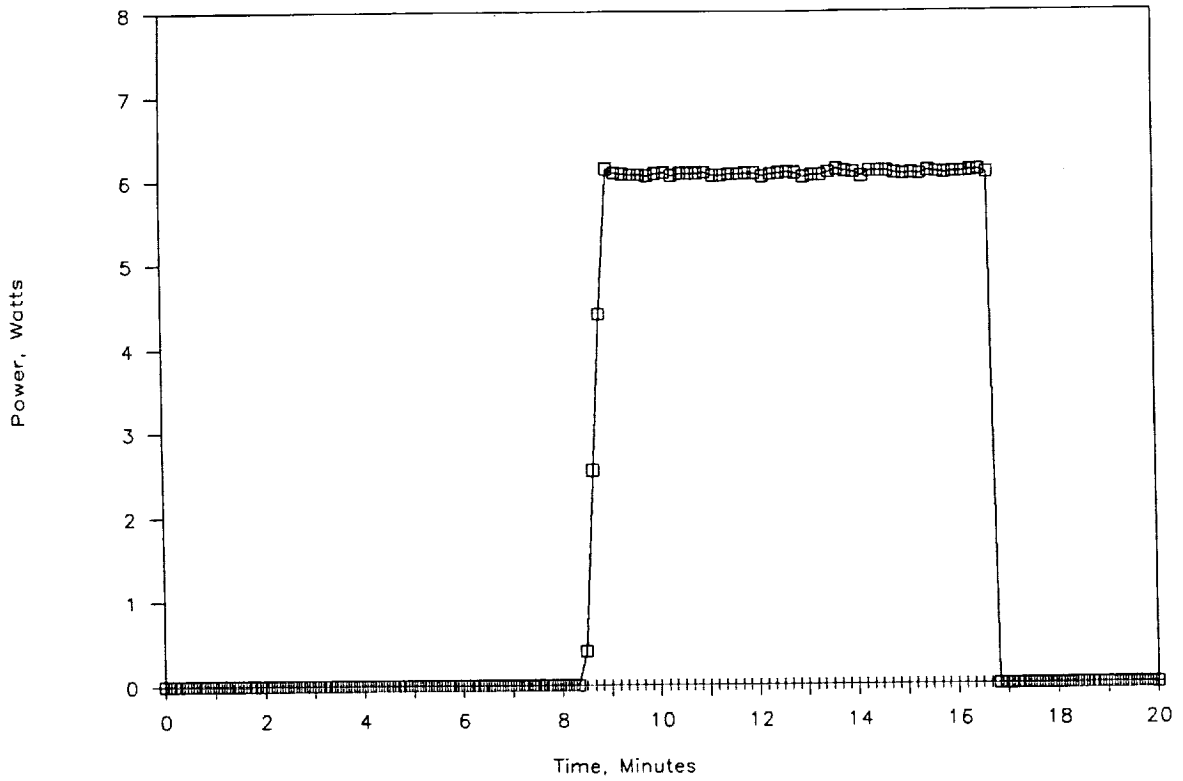


Figure 20. Heater power during 1989 run 1 along path A. The heater power at the porous plug heaters (H2) is the  $\square$  symbol and the heater power at the bayonet heater is the + symbol.

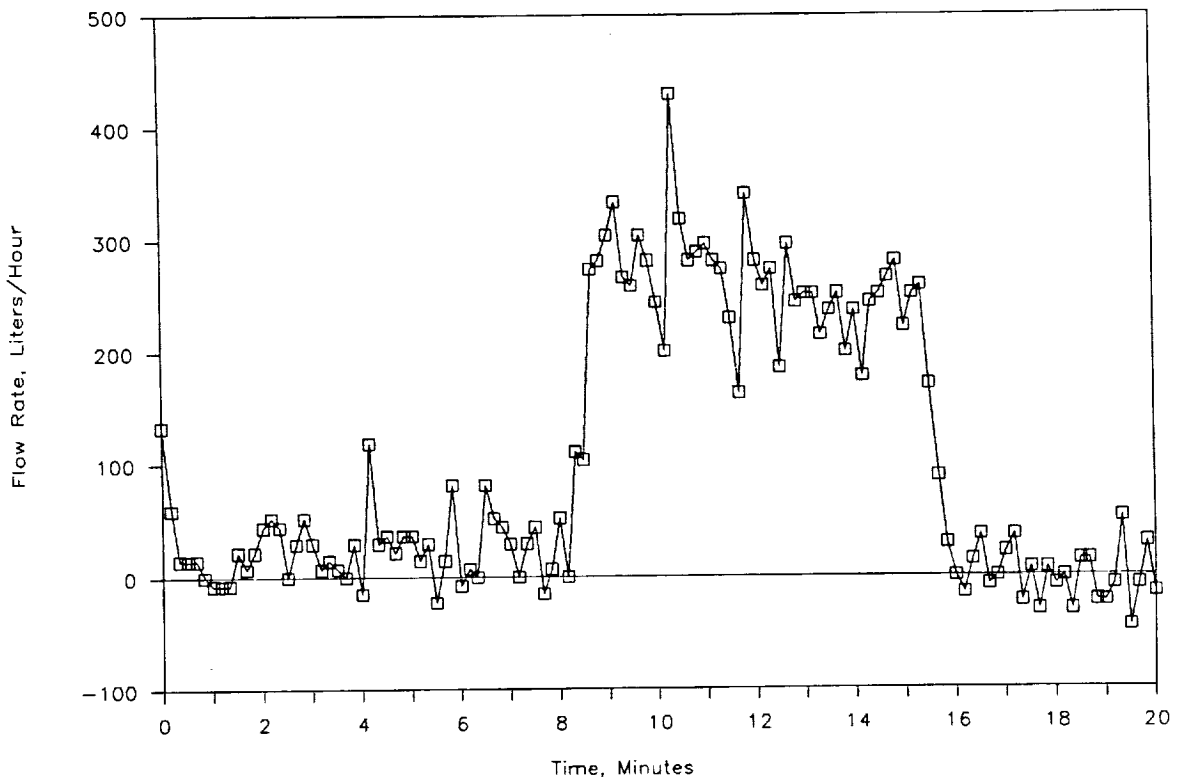


Figure 21. Flow rate out of the small tank during 1989 run 1 along path A.

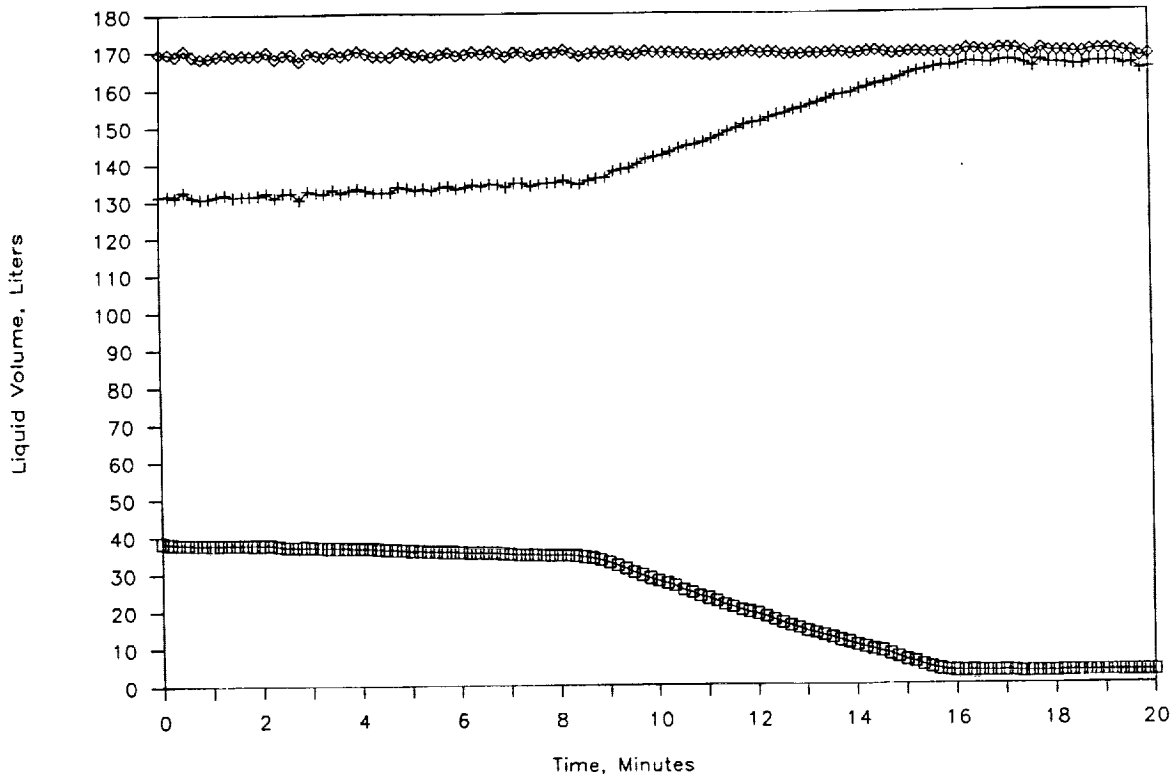


Figure 22. Liquid volume during 1989 run 1 along path A. Liquid volume calculated from LL1 and the small tank geometry is the  $\square$  symbol, liquid volume calculated from LL10 and the large tank geometry is the  $+$  symbol and the sum of the two volumes is the  $\diamond$  symbol.

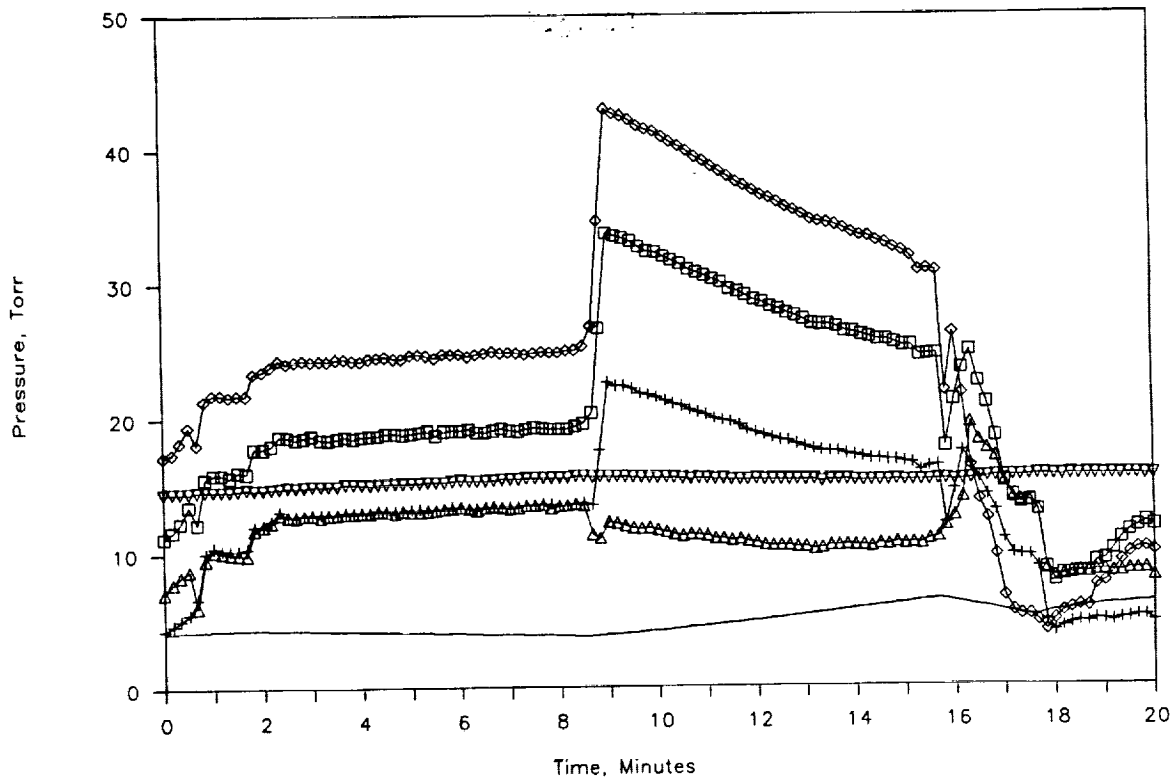


Figure 23. Pressures during 1989 run 1 along path A. The supply dewar is the  $—$  symbol, the receiver dewar is the  $\nabla$  symbol, CP3 (adjusted to show absolute pressure like the other transducers) is the  $\diamond$ , CP1 is the  $\square$  symbol, CP2 is the  $+$  symbol, and CP4 is the  $\triangle$  symbol.



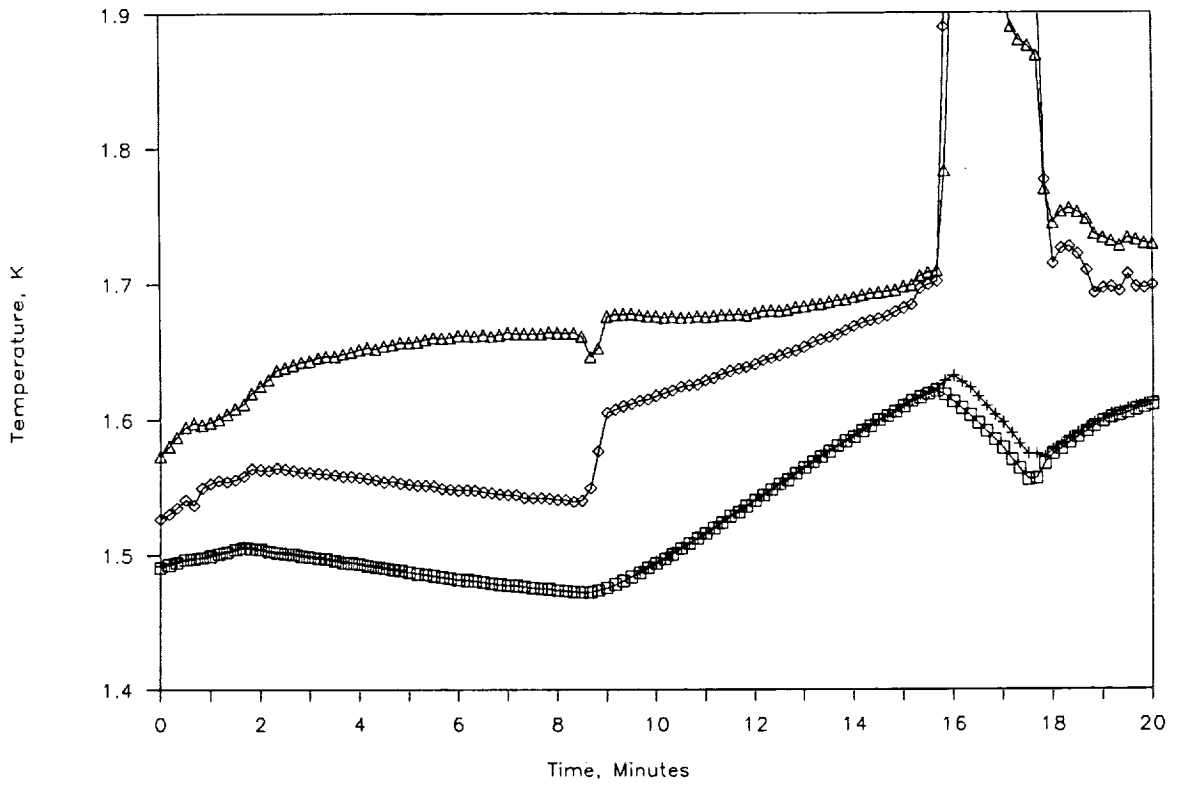


Figure 24. Supply dewar temperature and the first two temperatures along path A during 1989 run 1. T1, the supply dewar, is the  $\square$  symbol, T2 is the + symbol, T4 is the  $\diamond$ , and T3 is the  $\triangle$  symbol.

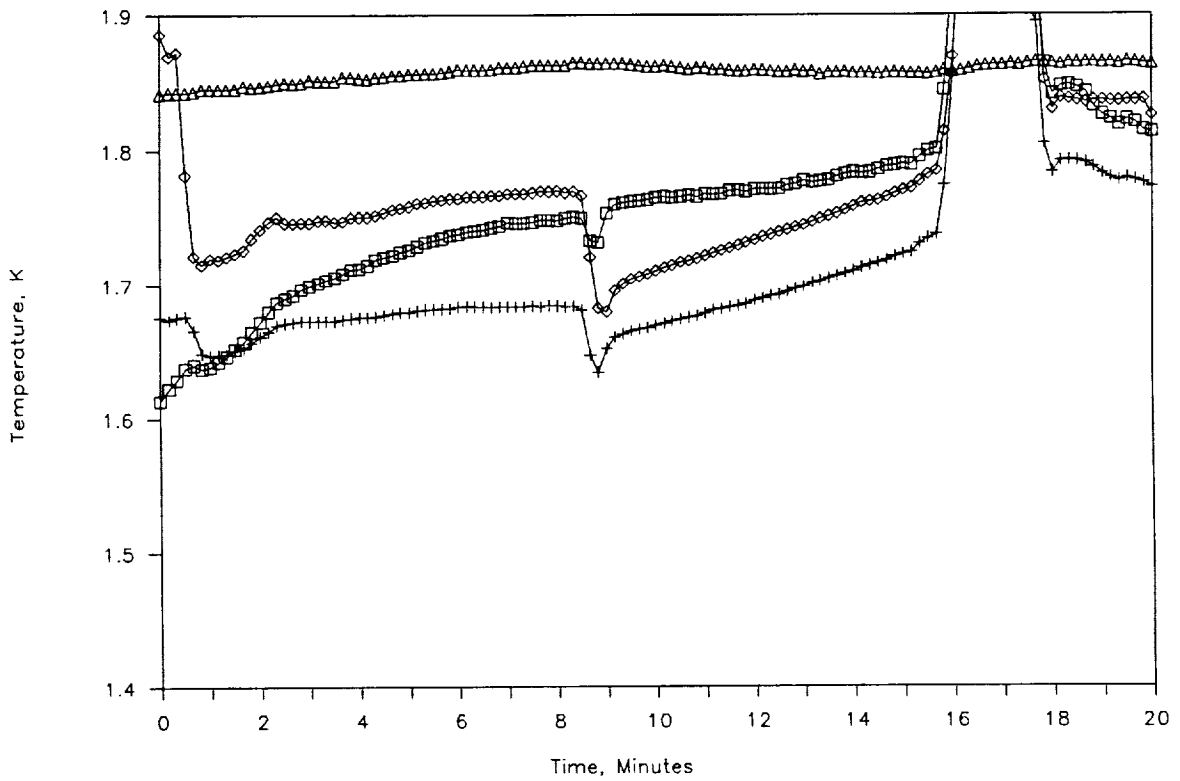


Figure 25. Final three temperatures along path A and the receiver dewar temperature during 1989 run 1. T9 is the  $\square$  symbol, T5 is the + symbol, T6 is the  $\diamond$ , and T8 is the  $\triangle$  symbol.

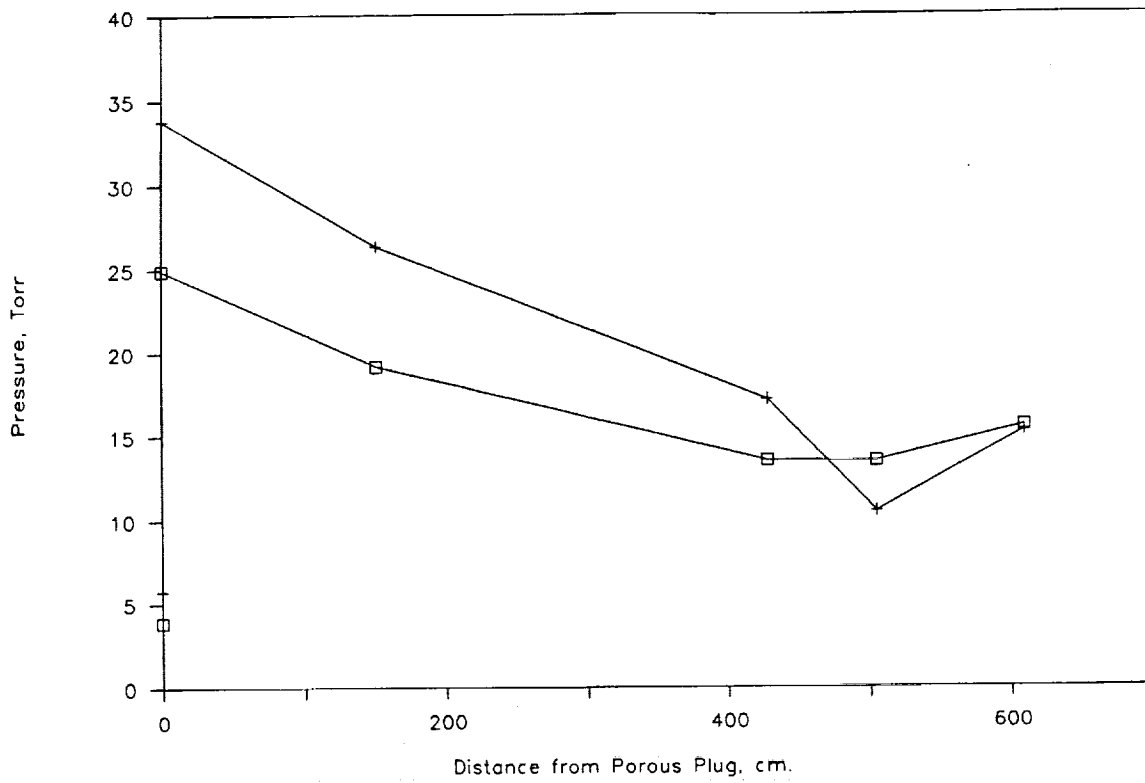


Figure 26. Pressure profile during 1989 run 1 along path A. Data at 8.0 minutes is the □ symbol, and data at 14.0 minutes is the + symbol.

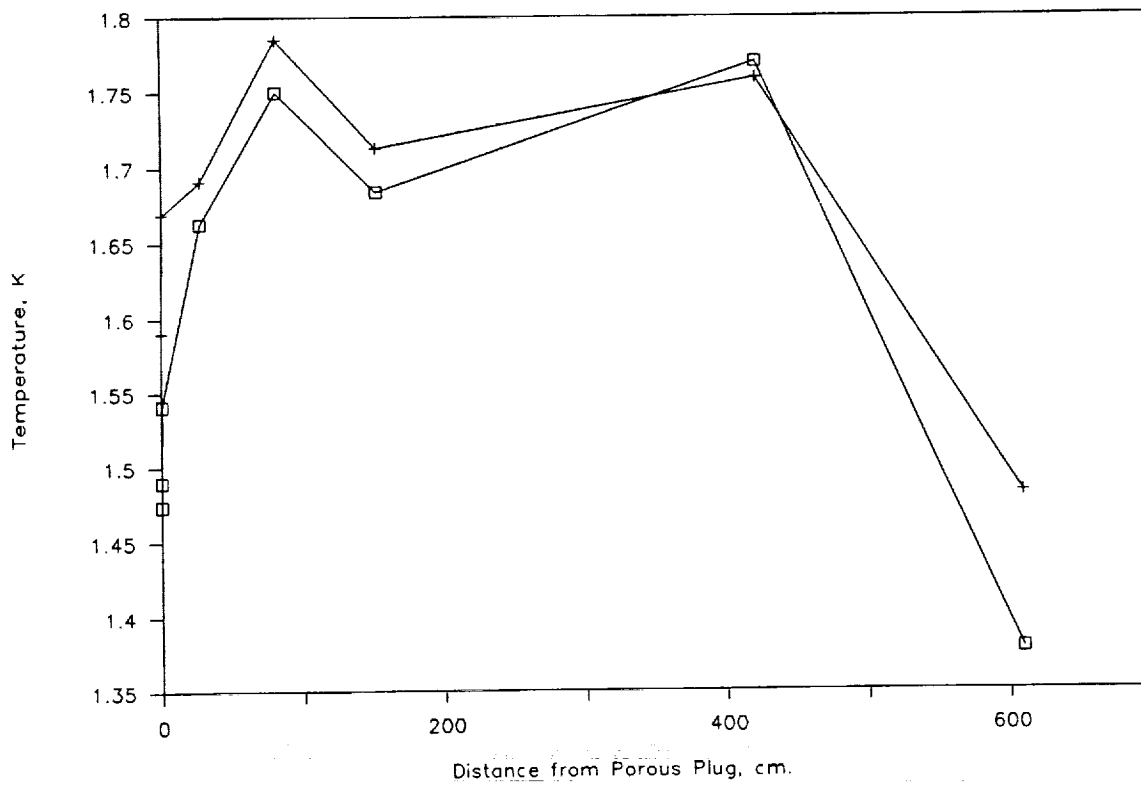


Figure 27. Temperature profile during 1989 run 1 along path A. Data at 8.0 minutes is the □ symbol, and data at 14.0 minutes is the + symbol.

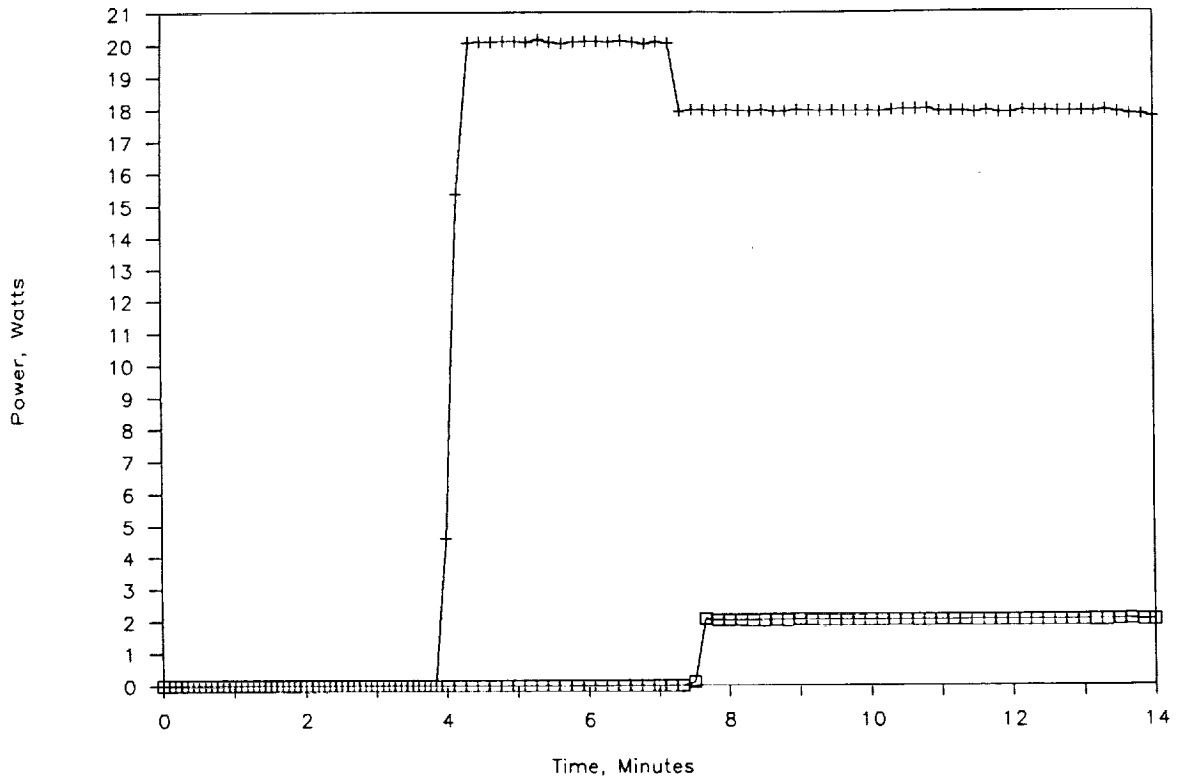


Figure 28. Heater power during 1989 run 2 along path A. The heater power at the porous plug heaters (H2) is the + symbol and heater power at the bayonet heaters (H4) is the □ symbol.

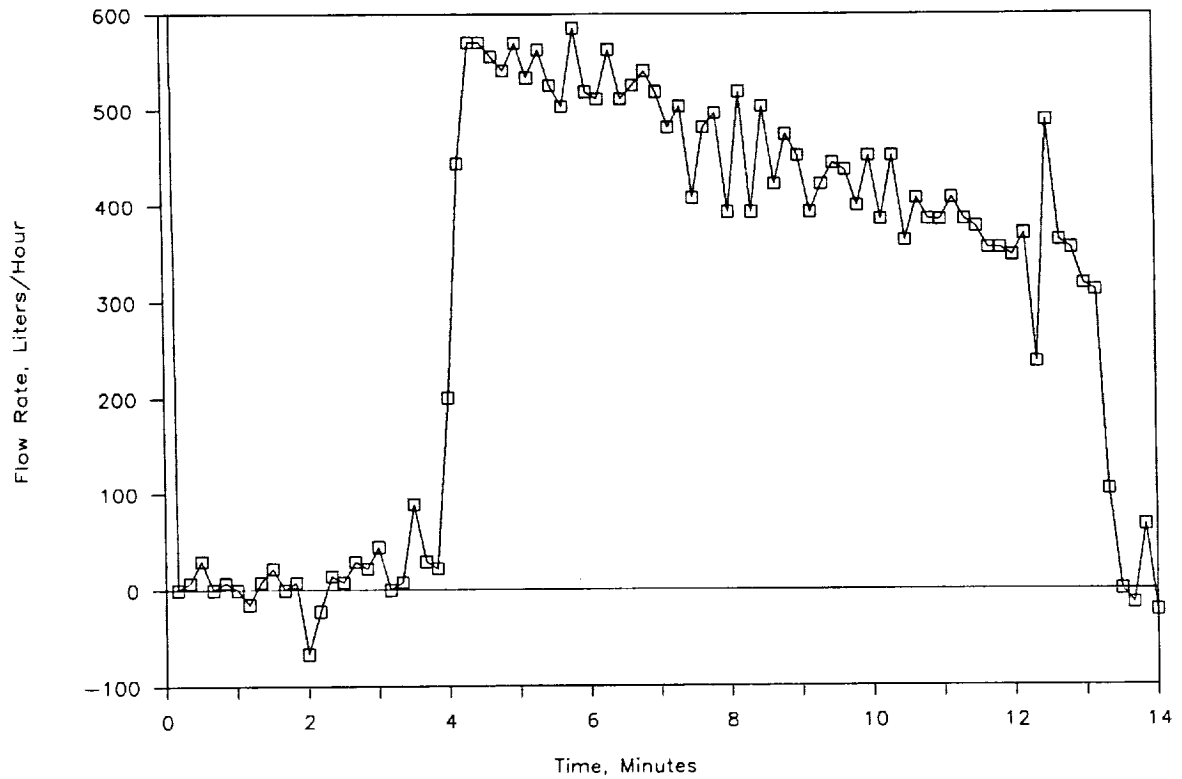


Figure 29. Flow rate out of the small tank during 1989 run 2 along path A.

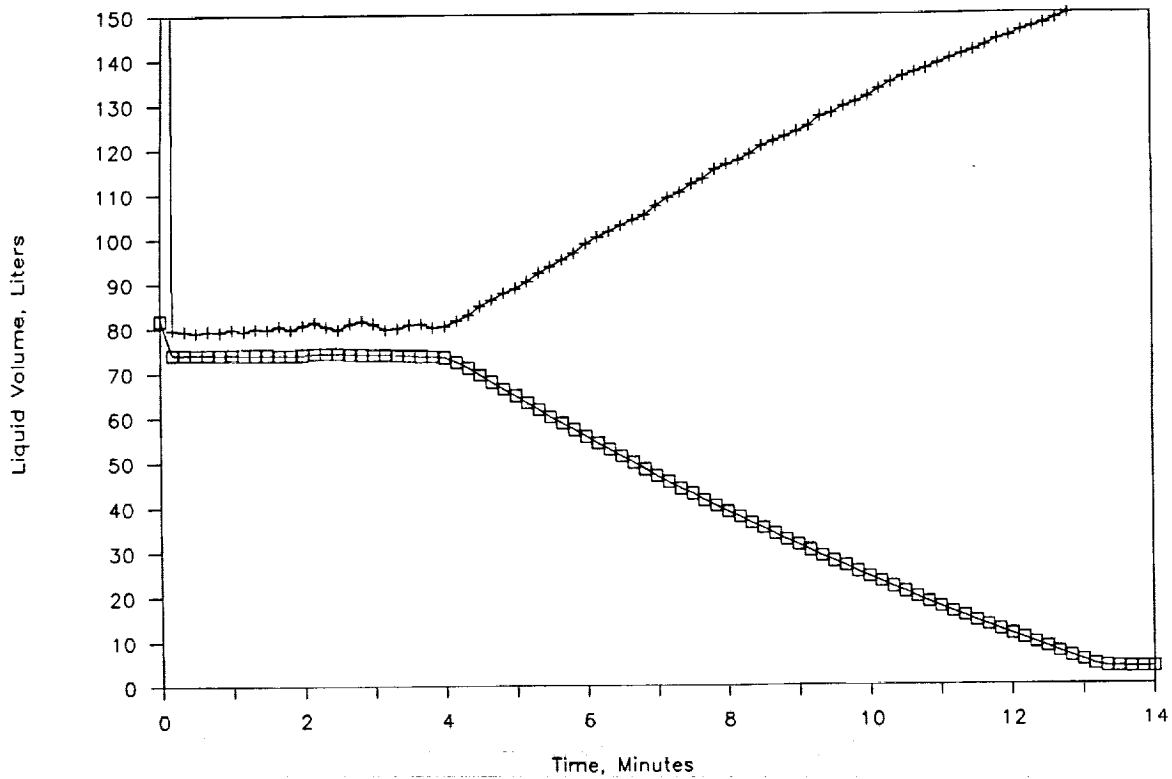


Figure 30. Liquid volume during 1989 run 2 along path A. Liquid volume calculated from LL1 and the small tank geometry is the □ symbol, liquid volume calculated from LL10 and the large tank geometry is the + symbol and the sum of the two volumes is the ◇ symbol.

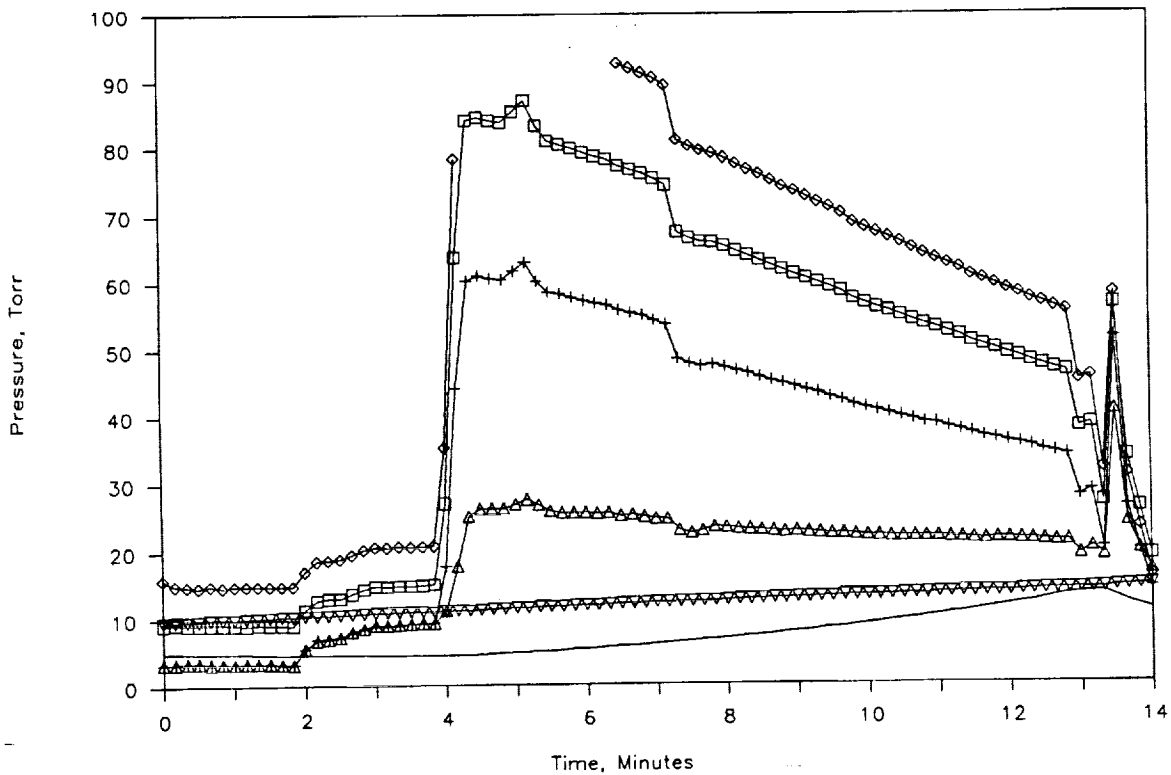


Figure 31. Pressures during 1989 run 2 along path A. The supply dewar is the — symbol, the receiver dewar is the ▽ symbol, CP3 (adjusted to show absolute pressure like the other transducers) is the ◇, CP1 is the □ symbol, CP2 is the + symbol, and CP4 is the △ symbol.

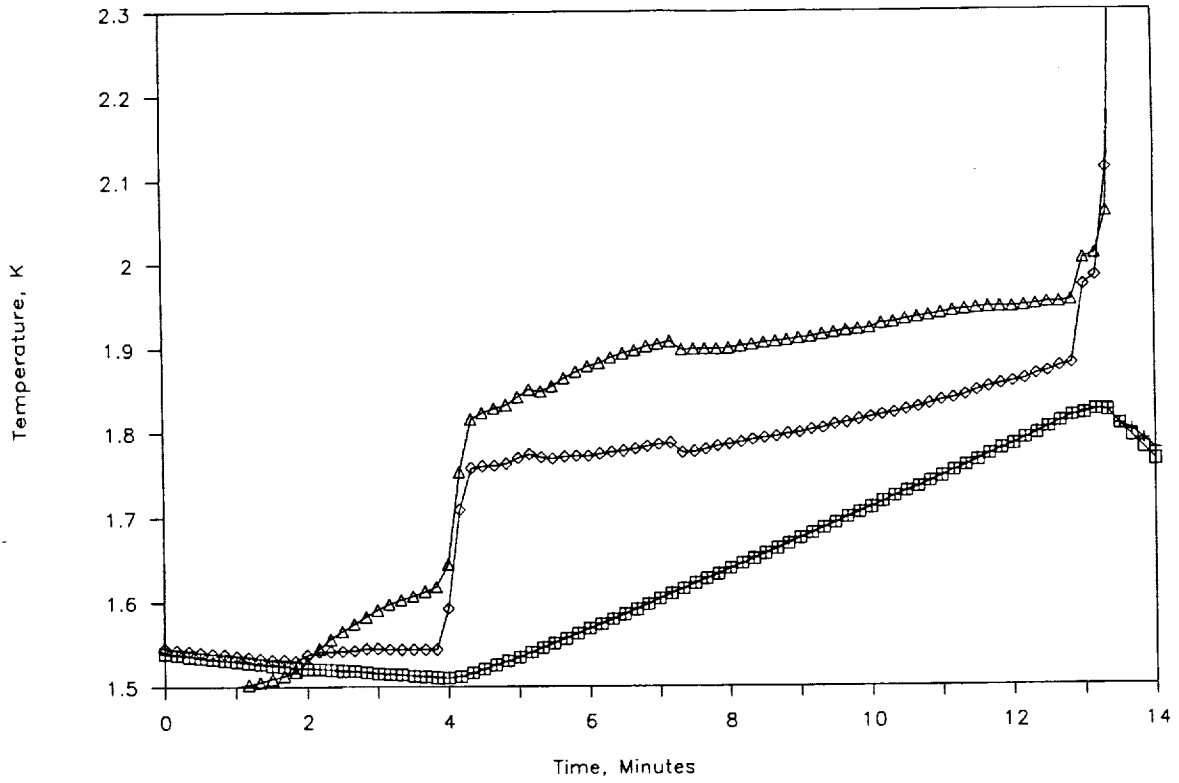


Figure 32. Supply dewar temperature and the first two temperatures along path A during 1989 run 2. T1, the supply dewar, is the  $\square$  symbol, T2 is the  $+$  symbol, T4 is the  $\diamond$ , and T3 is the  $\triangle$  symbol.

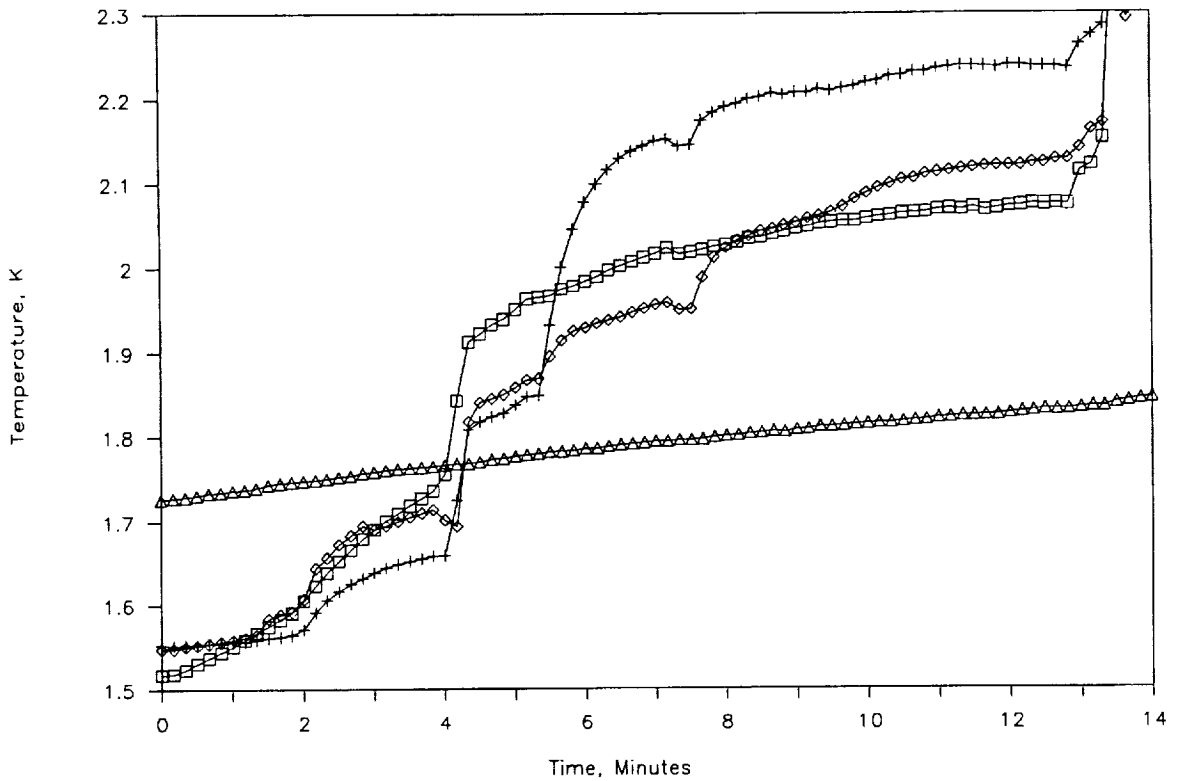


Figure 33. Final three temperatures along path A and the receiver dewar temperature during 1989 run 2. T9 is the  $\square$  symbol, T5 is the  $+$  symbol, T6 is the  $\diamond$ , and T8 is the  $\triangle$  symbol.

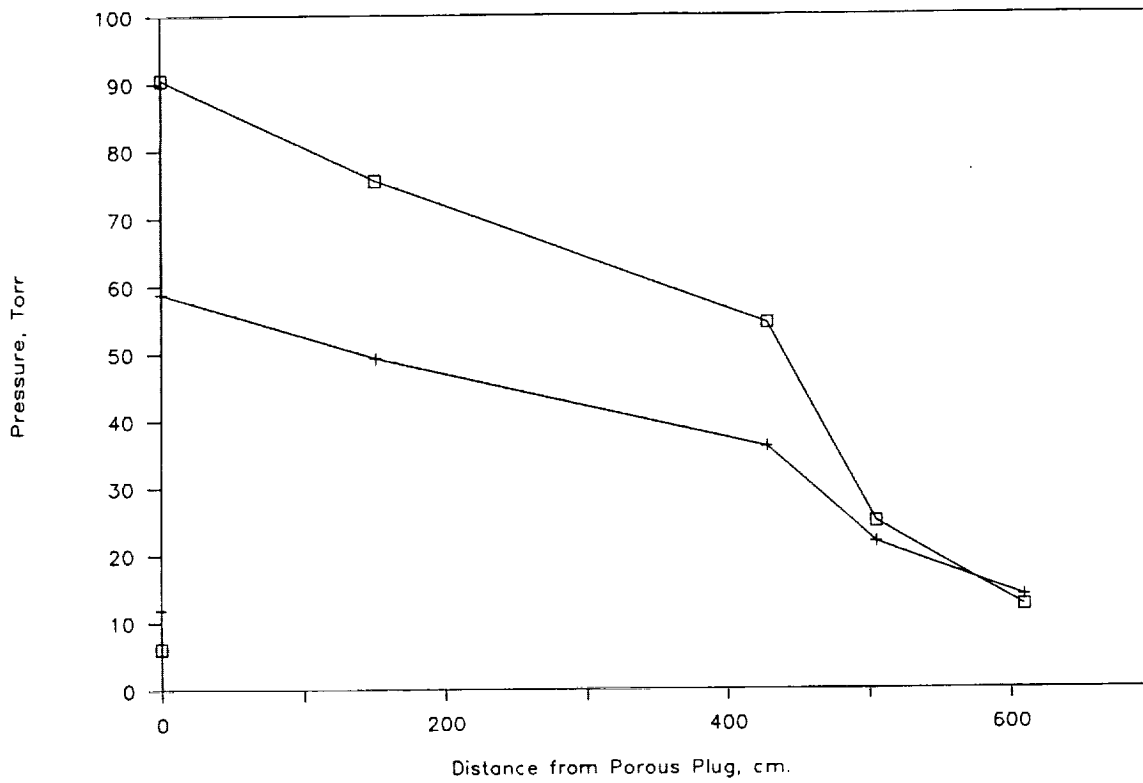


Figure 34. Pressure profile during 1989 run 2 along path A. Data at 7.0 minutes is the □ symbol, and data at 12.0 minutes is the + symbol.

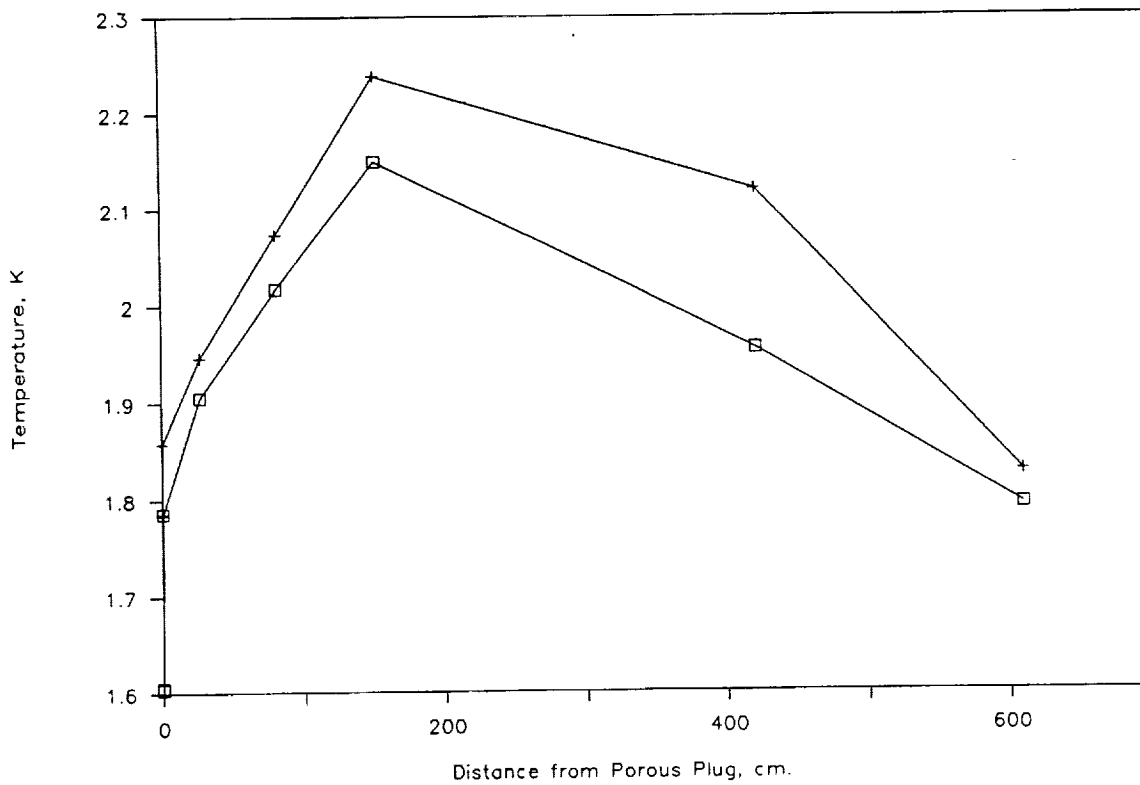


Figure 35. Temperature profile during 1989 run 2 along path A. Data at 8.0 minutes is the □ symbol, and data at 14.0 minutes is the + symbol.

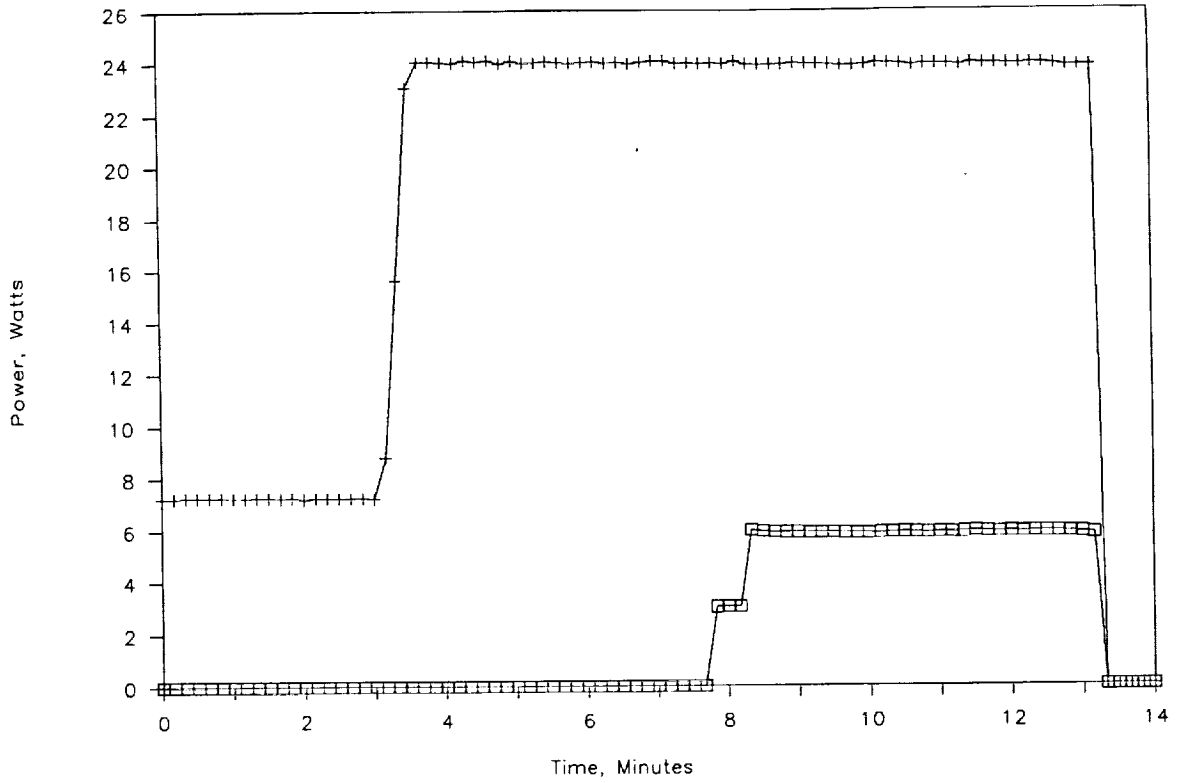


Figure 36. Heater power during 1989 run 3 along path A. The heater power at the porous plug heaters (H2) is the + symbol and heater power at the bayonet heaters (H4) is the □ symbol.

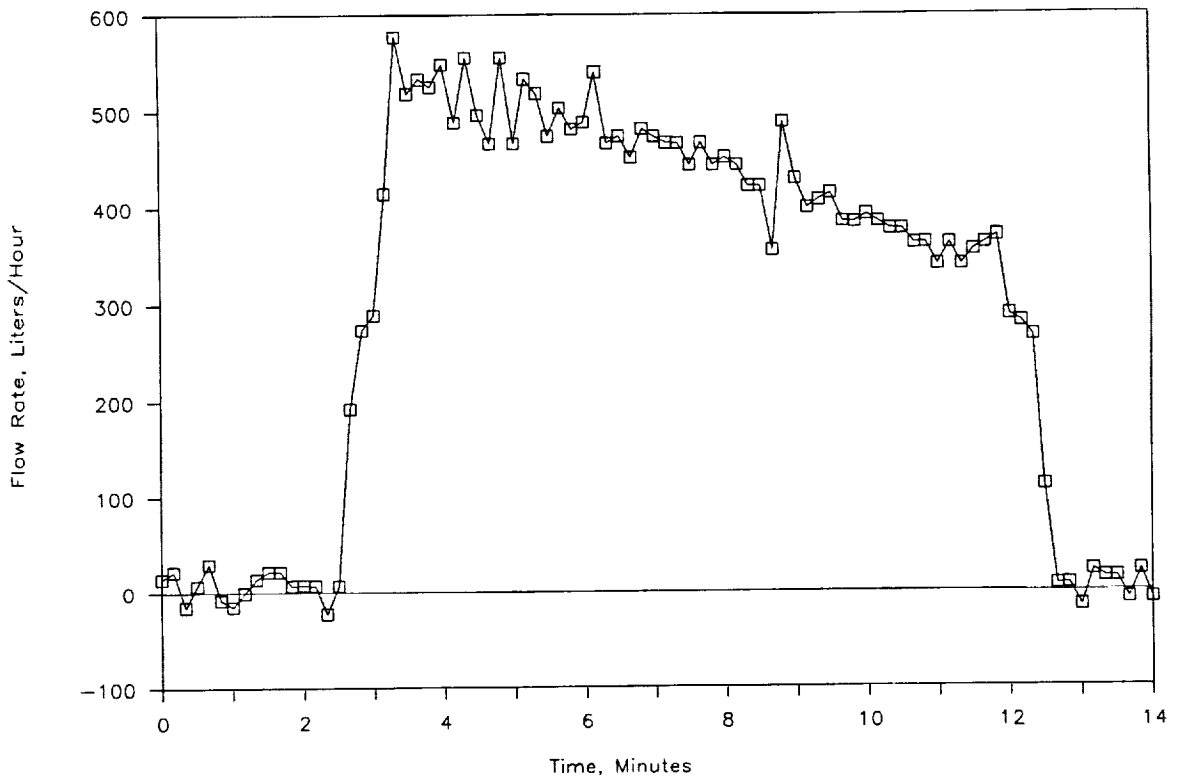


Figure 37. Flow rate out of the small tank during 1989 run 3 along path A.

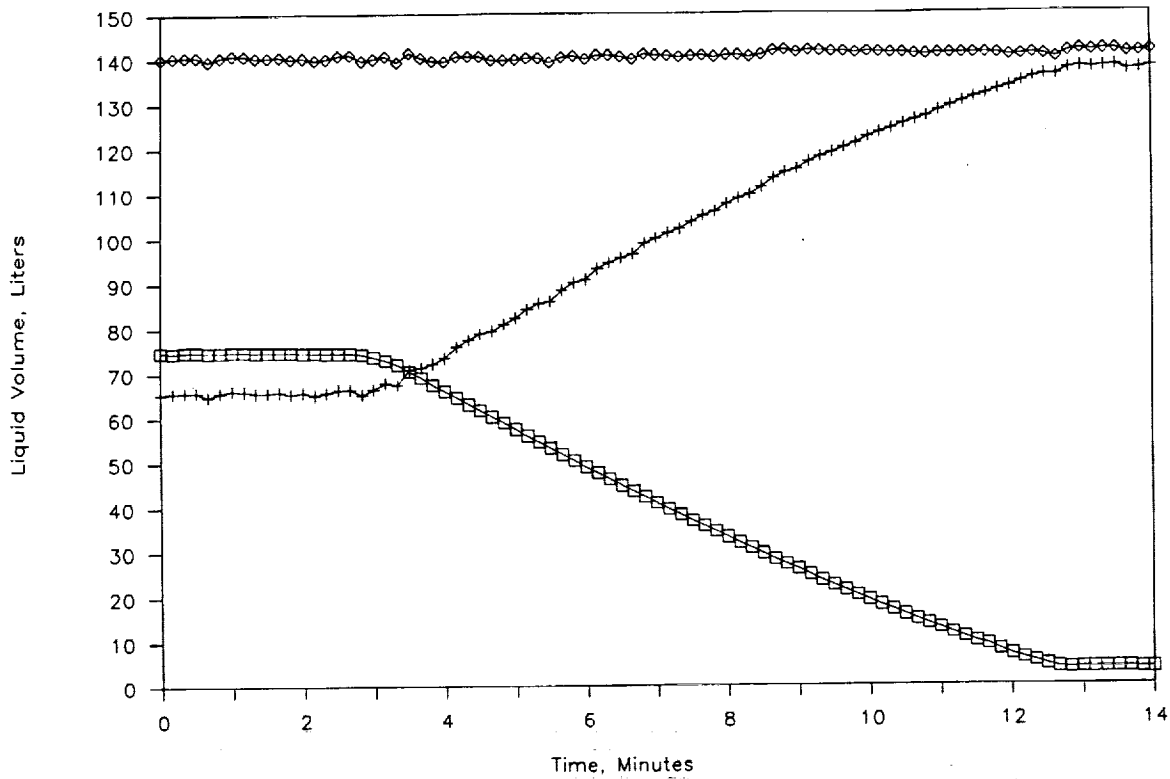


Figure 38. Liquid volume during 1989 run 3 along path A. Liquid volume calculated from LL1 and the small tank geometry is the □ symbol, liquid volume calculated from LL10 and the large tank geometry is the + symbol and the sum of the two volumes is the ◇ symbol.

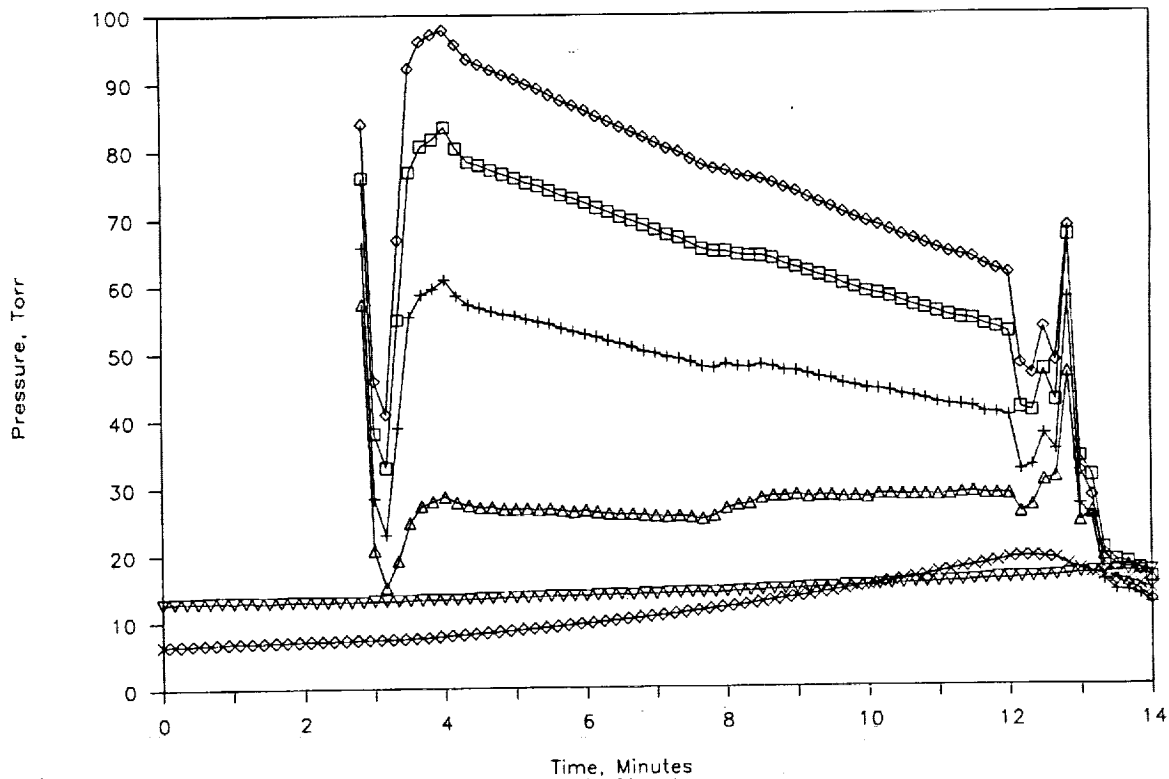


Figure 39. Pressures during 1989 run 3 along path A. The supply dewar is the — symbol, the receiver dewar is the ▽ symbol, CP3 (adjusted to show absolute pressure like the other transducers) is the ◇, CP1 is the □ symbol, CP2 is the + symbol, and CP4 is the △ symbol.



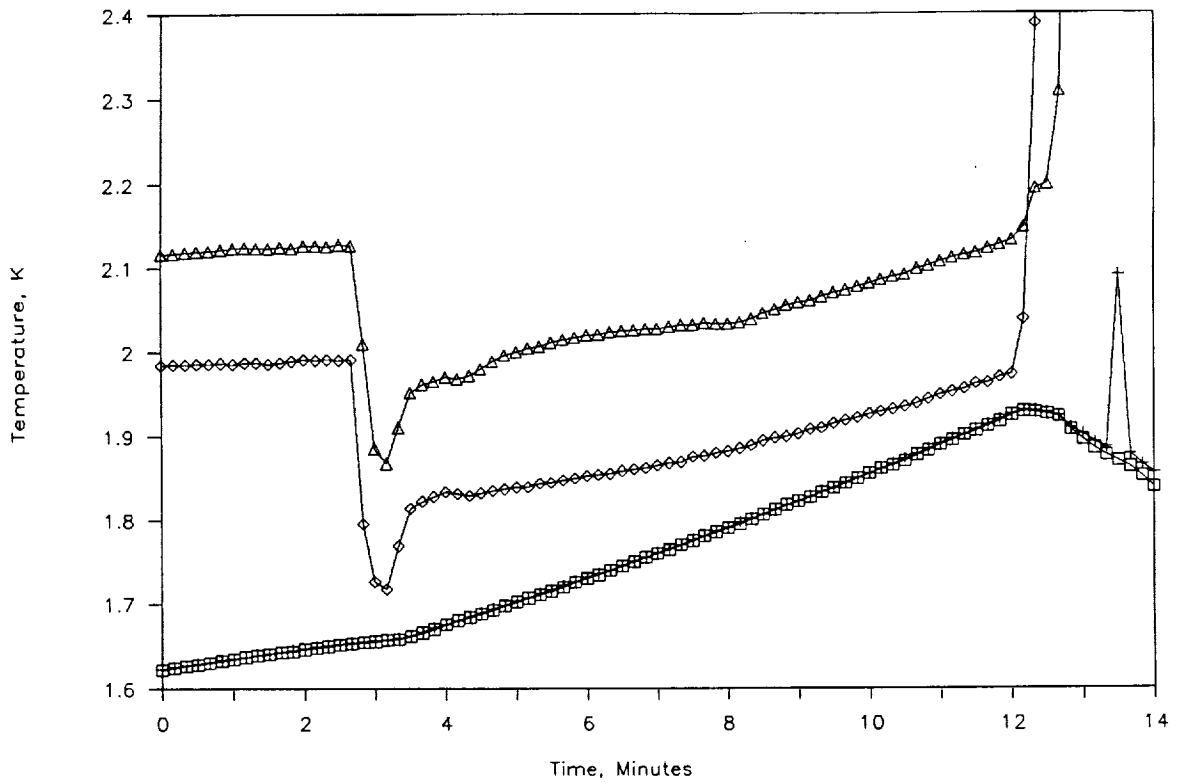


Figure 40. Supply dewar temperature and the first two temperatures along path A during 1989 run 3. T1, the supply dewar, is the  $\square$  symbol, T2 is the  $+$  symbol, T4 is the  $\diamond$ , and T3 is the  $\triangle$  symbol.

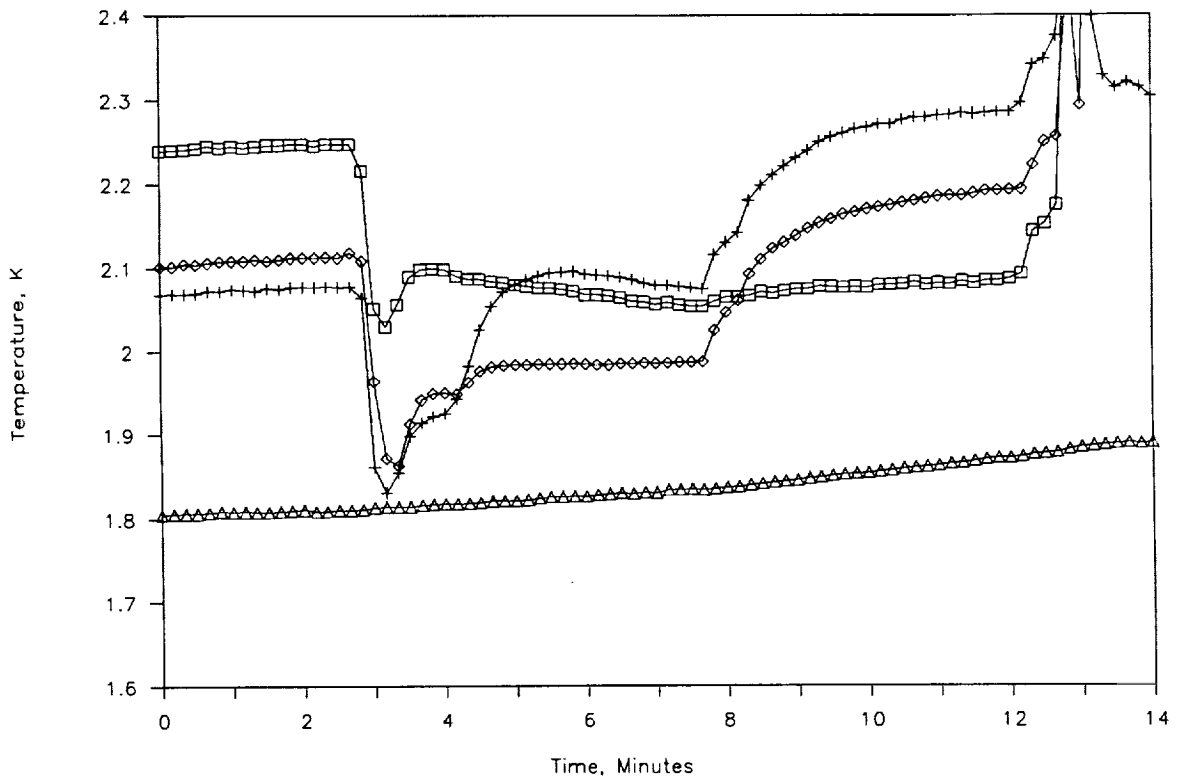


Figure 41. Final three temperatures along path A and the receiver dewar temperature during 1989 run 3. T9 is the  $\square$  symbol, T5 is the  $+$  symbol, T6 is the  $\diamond$ , and T8 is the  $\triangle$  symbol.

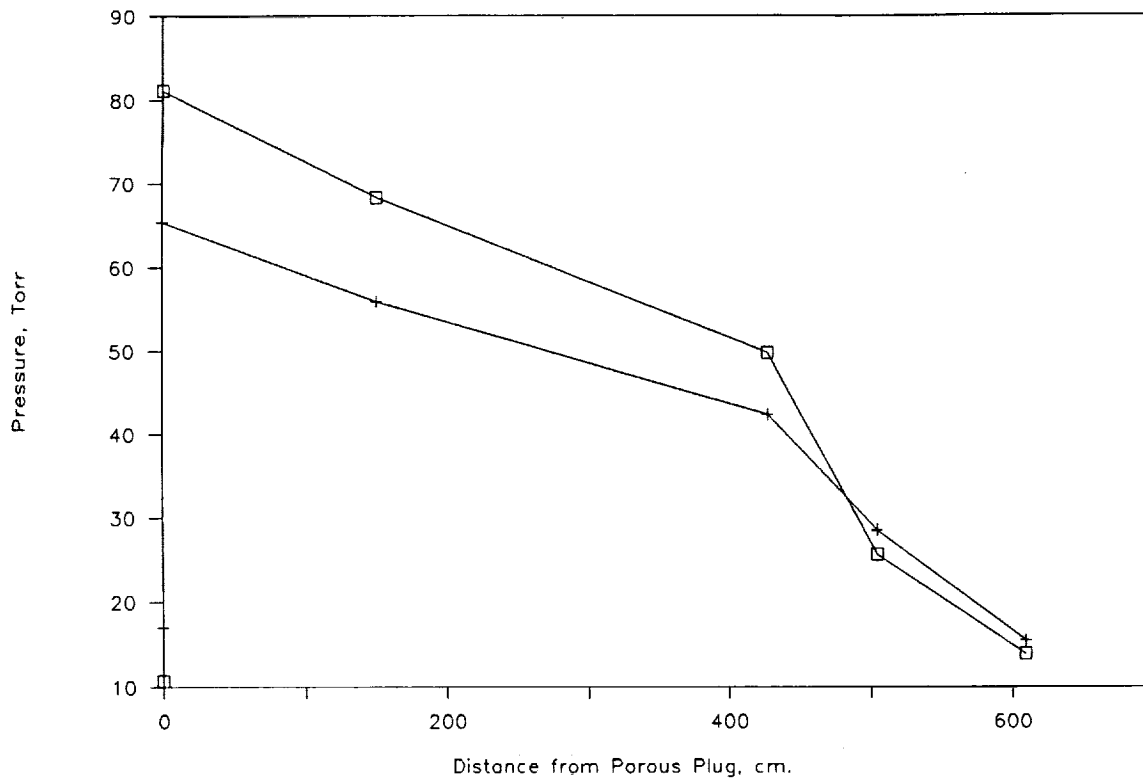


Figure 42. Pressure profile during 1989 run 3 along path A. Data at 7.0 minutes is the □ symbol, and data at 11.0 minutes is the + symbol.

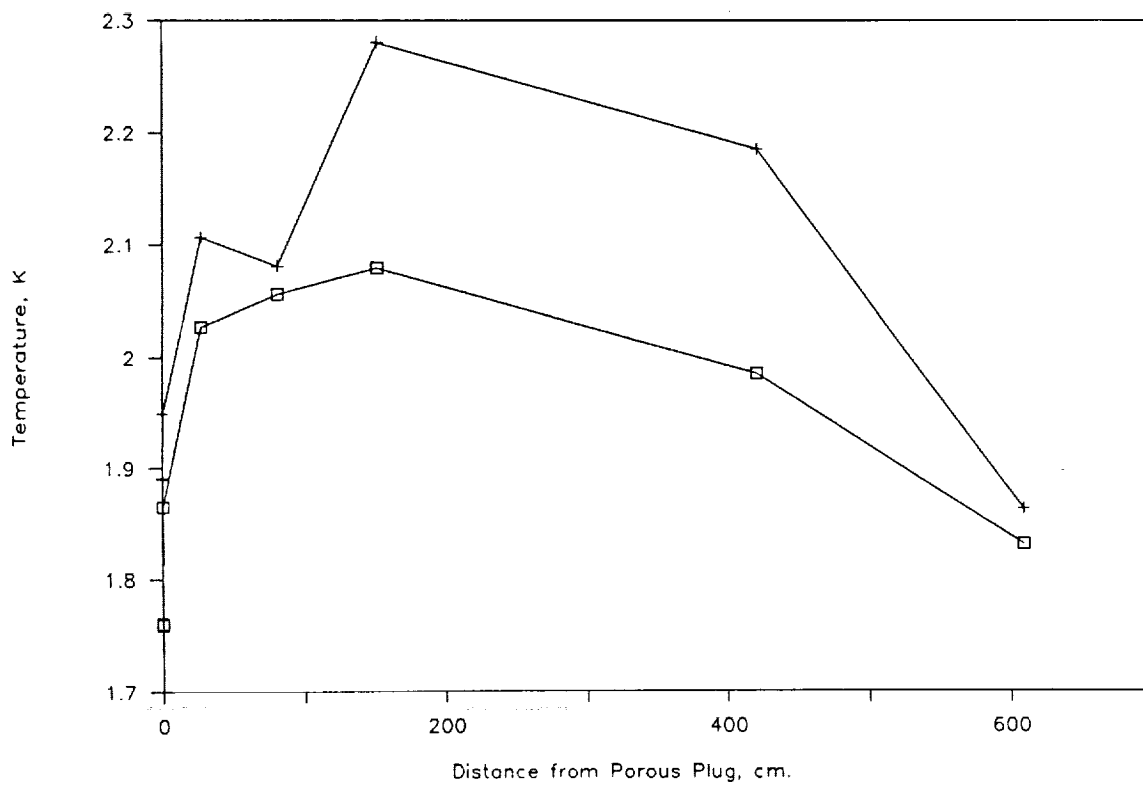


Figure 43. Temperature profile during 1989 run 3 along path A. Data at 7.0 minutes is the □ symbol, and data at 11.0 minutes is the + symbol.

The third transfer was started at the conclusion of the first no-flow test. During the no-flow test, 6.8 W was applied to the porous plug heater. This power was left on during the start of the third transfer. To start the transfer valve, V4 was opened at 2.6 minutes, and 24.0 W of power was applied to the porous plug heater at 3.2 minutes. Five minutes later, 6.0 W of heat was applied to the bayonet heater. The heater power was turned off at 13 minutes and valve V9 opened. During this transfer, only the vent valve for the supply tank (V10) was kept open. The average flow rate over the entire run was 460 liters/hour, with instantaneous flow rates of approximately 550 liters/hour at the beginning of the test run and 350 liters/hour at the end of the test run. Adding 2 W of heat at the bayonet instead of at the porous plug did not have a noticeable effect on the flow rate and had only a slight effect on the transfer line pressures. The bayonet heater did have a very noticeable effect on the temperatures downstream of the bayonet heater. There is no event associated with the sudden rise in temperature of T5 and T6 and 4.2 minutes.

The results of the fourth experimental run are shown in Figures 44 through 51. During the start of the transfer, 12 W was applied to the porous plug heater. This value was chosen as an intermediate point between the 6 W used during the initial run and the 18 W used in the second run. Experimental data was also gathered on the effect of a constriction in the transfer line by partially closing a valve which was in between the supply and receiver dewars. At the end of the experiment, 2 W of power was applied to simulate the heat leak of a bayonet couple.

At 0.5 minutes, 12 W of heater power was applied to the porous plug heater. Valve V4 was opened at 1.5 minutes and the liquid level gauges were not turned on until 1.7 minutes. The latter was a procedural error. At the beginning of the run, valve V1, which is in the middle of the transfer line, was intentionally left open only 1.5 turns. (Note: for this valve four turns is full open.) At 6.5 minutes, V1 was fully opened. Note that the opening of V1 had considerable effect on both the temperature and pressure profiles, but had no effect on the flow rate. The average flow rate before and after V1 was opened was 300 liters/hour. At 13.0 minutes, 2 W of heat was applied to the bayonet heater. Again, while affecting the temperature and pressure profile, it had little effect on the flow rate, which dropped slightly to 280 liters/hour. Heater power was turned off at 15.3 minutes and valve V9 opened at 18.3 minutes. During the transfer of Helium II, the vent valve for both dewars was kept open.

The results of the fifth experimental run are shown in Figures 52 through 59. This was a repeat of the previous experiment with the power supplied to the porous plug heater being raised to 20 W.

To start the fifth transfer valve, V4 was opened at 3.2 minutes and 20 W of heater power was applied to the porous plug heater at 3.6 minutes. Valve V1 was initially positioned as in the fourth run, 1.5 turns open, and was fully opened at 6.4 minutes. The opening of this valve caused a very large change in the pressure profile, a slight change in the temperature profile, and little change in the flow rate. The average flow rate decreased from 450 liters/hour at the beginning of the run to 420 liters/hour at the end of the run. Some of the pressure data had to be taken by hand in the 3.2 to 6.4 minute period which is why some data points are missing. During this transfer, the vent valve for both dewars was kept open. There is no event associated with the sudden rise in temperature of T5 at 5.0 minutes.

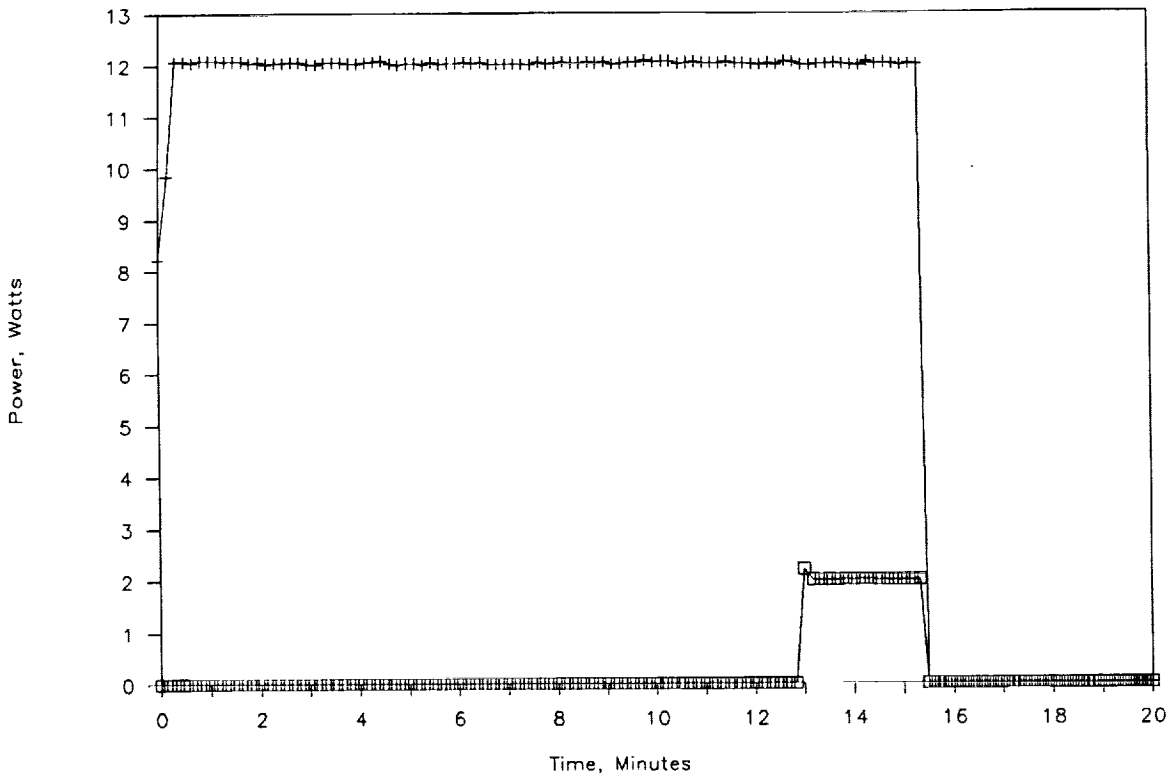


Figure 44. Heater power during 1989 run 4 along path A. The heater power at the porous plug heaters (H2) is the + symbol and heater power at the bayonet heaters (H4) is the □ symbol.

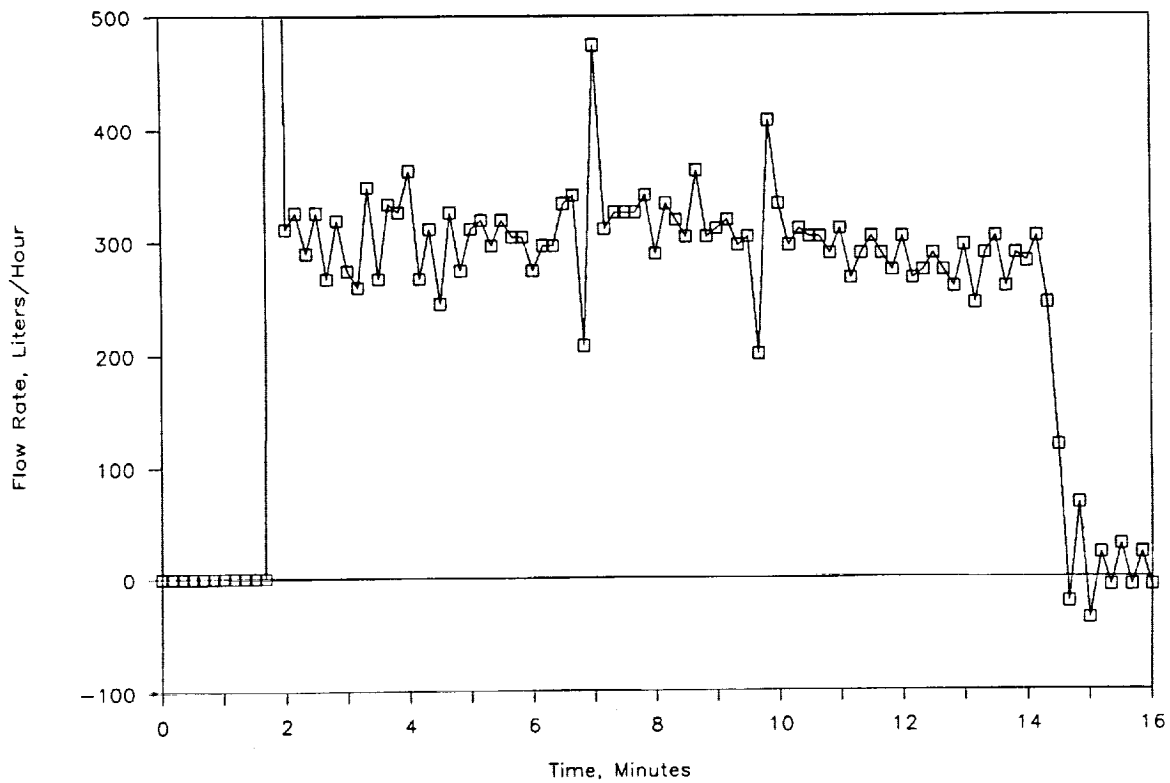


Figure 45. Flow rate out of the small tank during 1989 run 4 along path A.

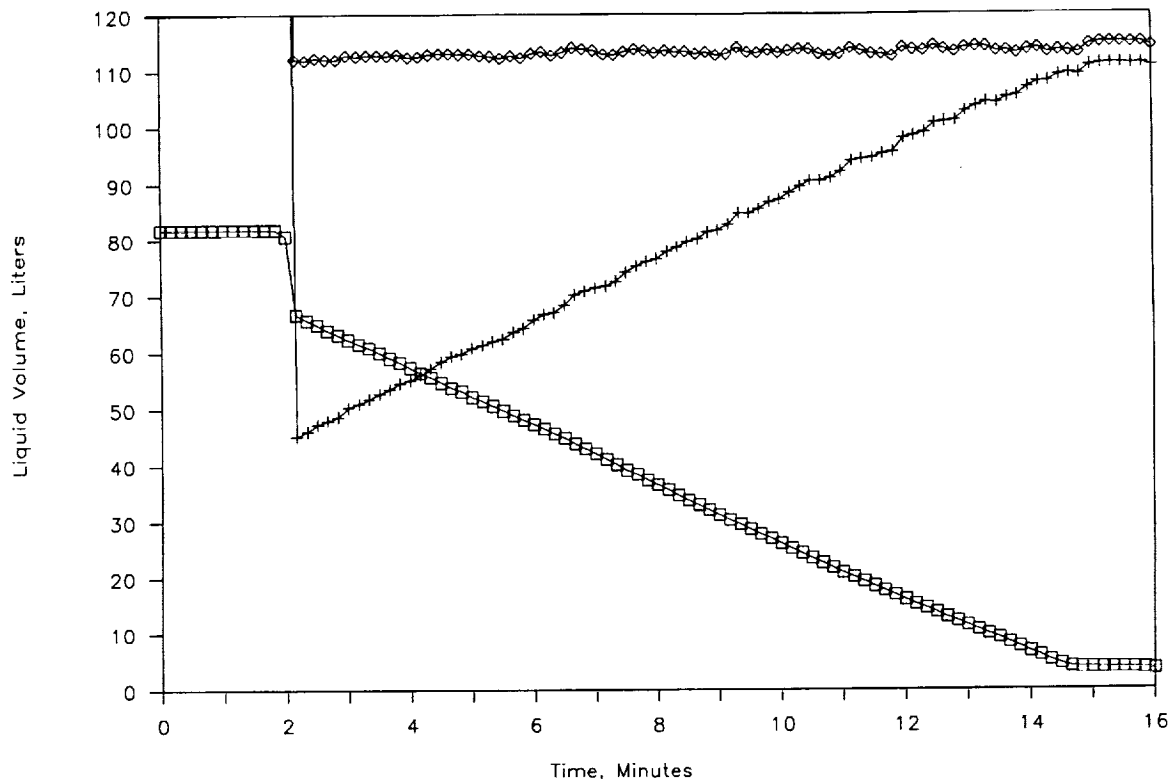


Figure 46. Liquid volume during 1989 run 4 along path A. Liquid volume calculated from LL1 and the small tank geometry is the  $\square$  symbol, liquid volume calculated from LL10 and the large tank geometry is the  $+$  symbol and the sum of the two volumes is the  $\diamond$  symbol.

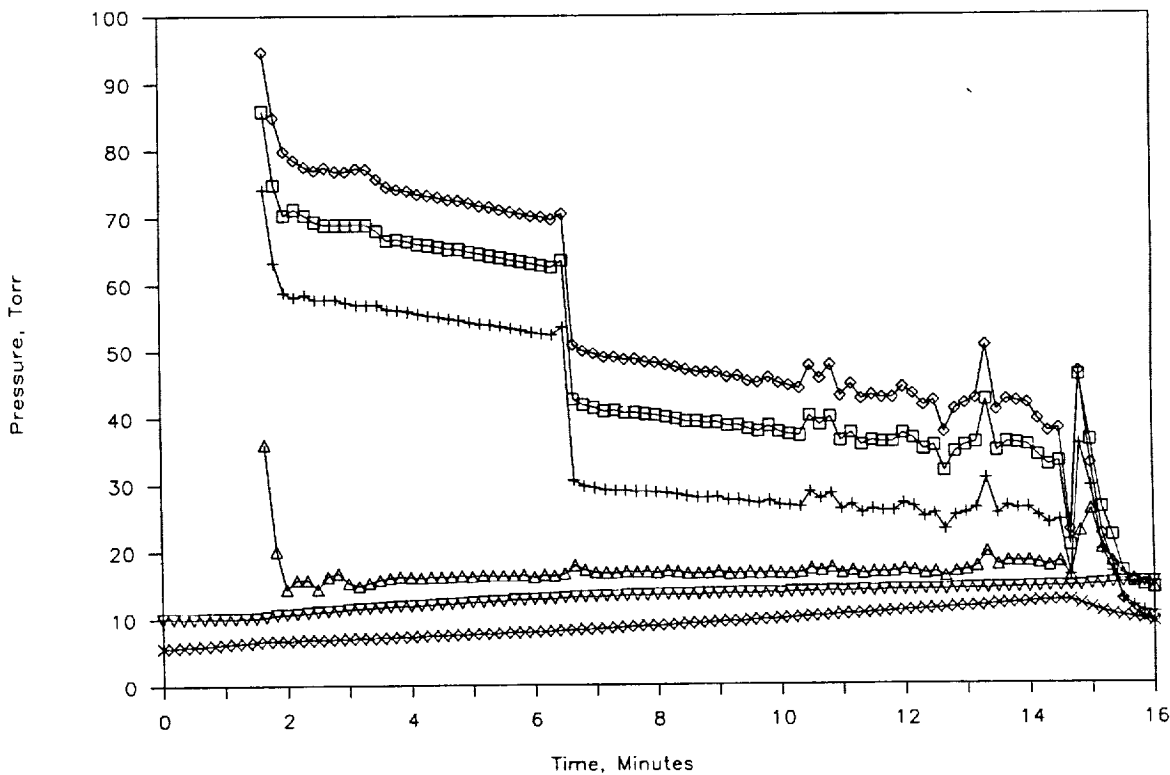


Figure 47. Pressures during 1989 run 4 along path A. The supply dewar is the  $—$  symbol, the receiver dewar is the  $\nabla$  symbol, CP3 (adjusted to show absolute pressure like the other transducers) is the  $\diamond$ , CP1 is the  $\square$  symbol, CP2 is the  $+$  symbol, and CP4 is the  $\triangle$  symbol.

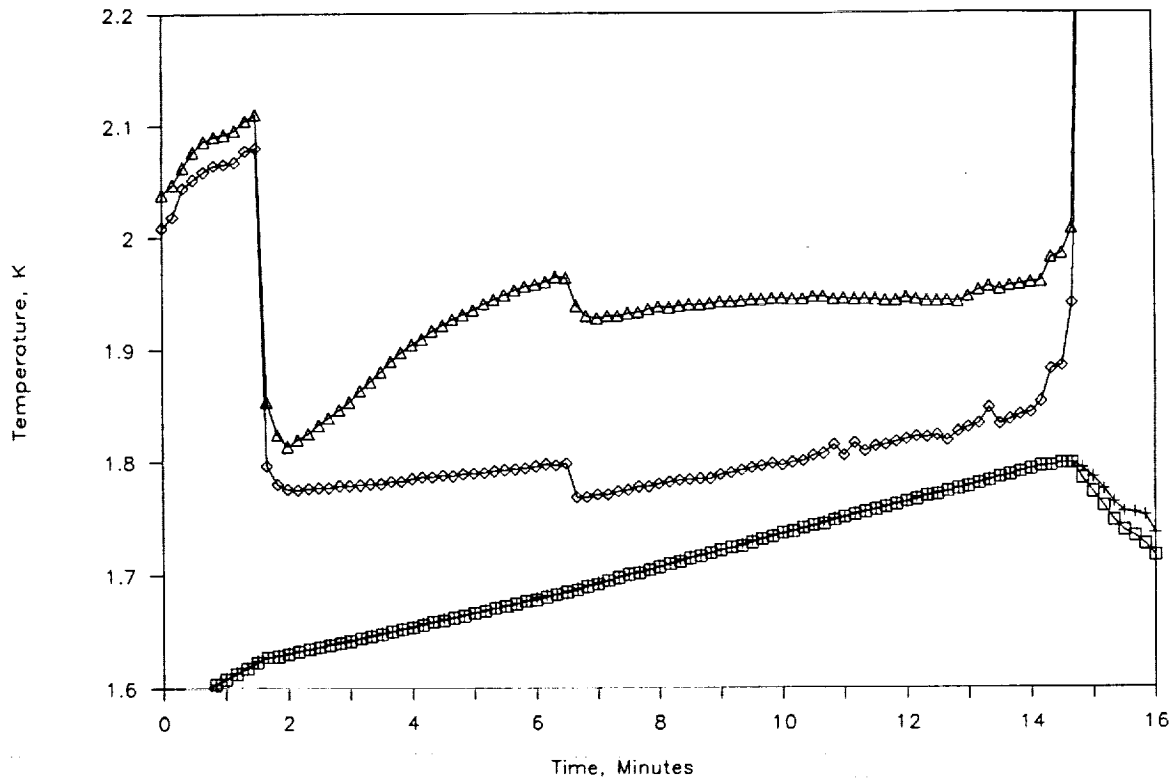


Figure 48. Supply dewar temperature and the first two temperatures along path A during 1989 run 4. T1, the supply dewar, is the  $\square$  symbol, T2 is the  $+$  symbol, T4 is the  $\diamond$ , and T3 is the  $\triangle$  symbol.

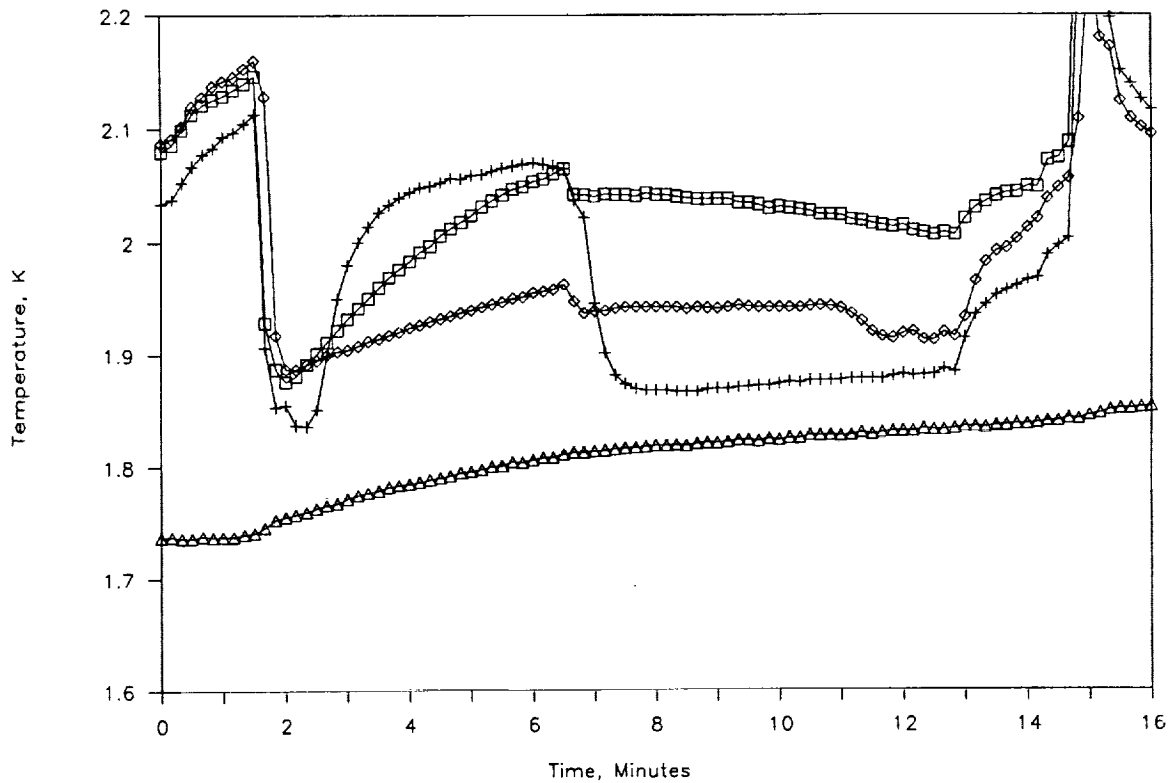


Figure 49. Final three temperatures along path A and the receiver dewar temperature during 1989 run 4. T9 is the  $\square$  symbol, T5 is the  $+$  symbol, T6 is the  $\diamond$ , and T8 is the  $\triangle$  symbol.

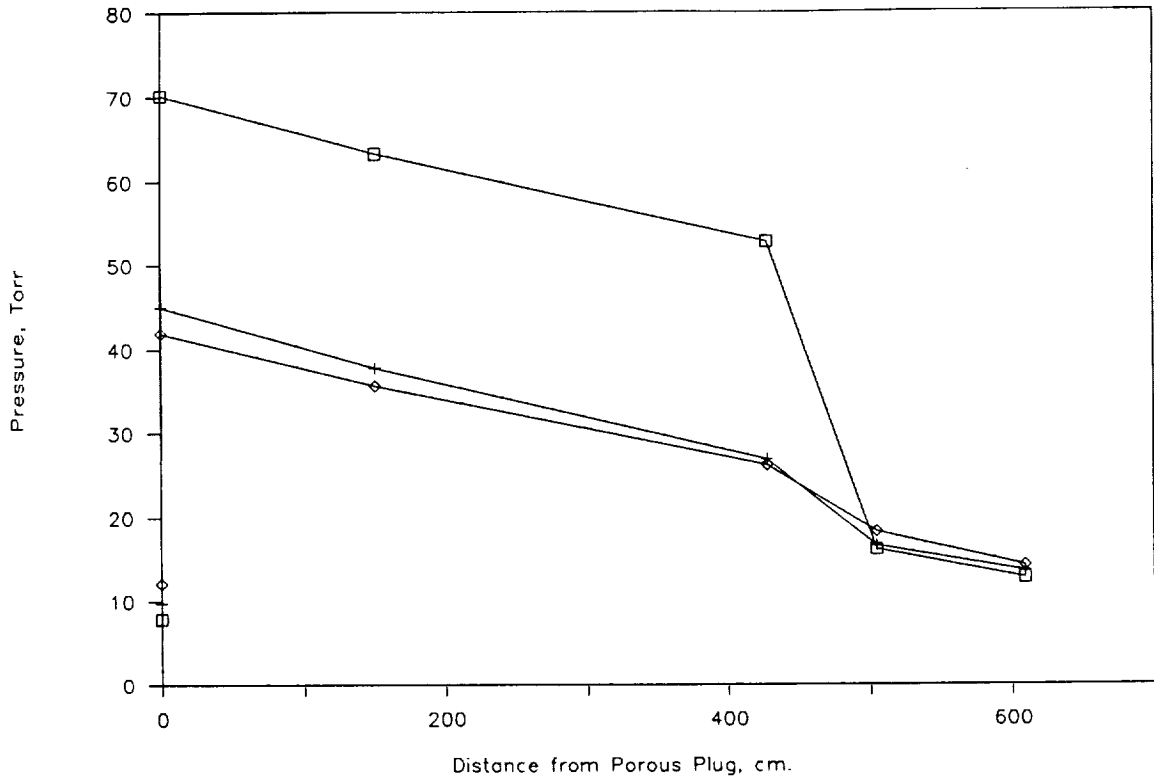


Figure 50. Pressure profile during 1989 run 4 along path A. Data at 6.0 minutes is the □ symbol, data at 10.0 minutes is the + symbol and data at 14.0 minutes is the ◇ symbol.

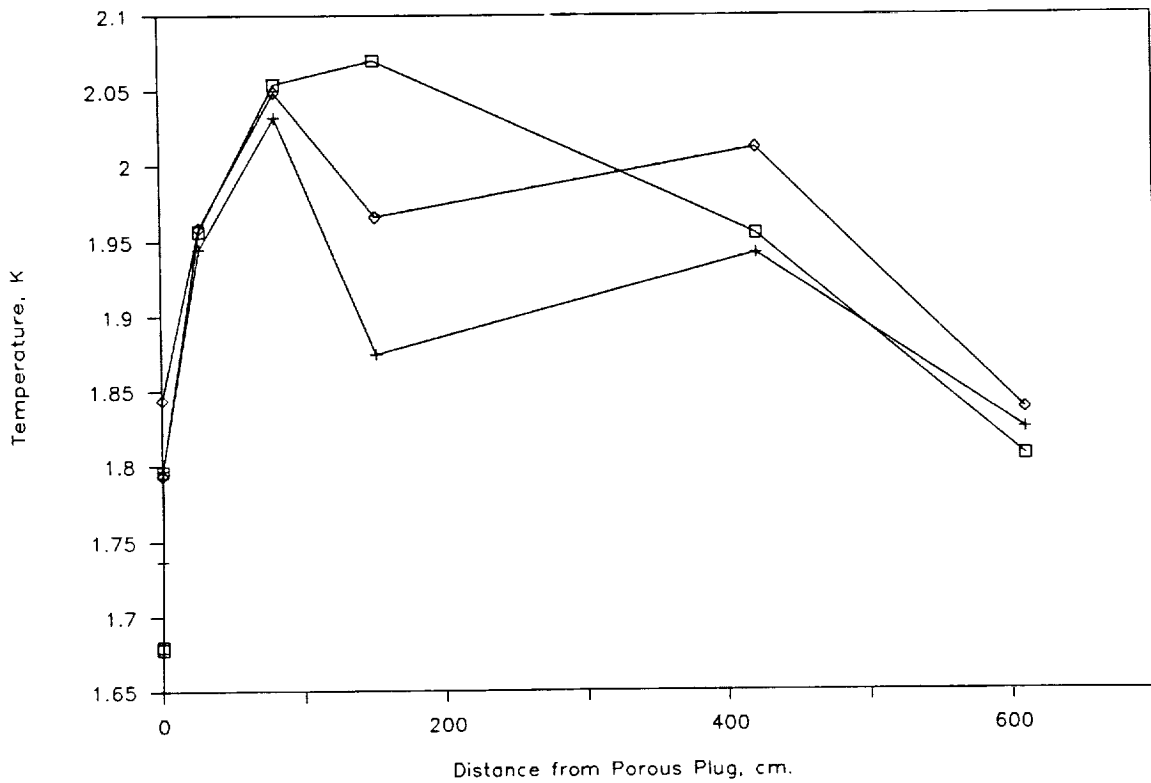


Figure 51. Temperature profile during 1989 run 4 along path A. Data at 6.0 minutes is the □ symbol, data at 10.0 minutes is the + symbol and data at 14.0 minutes is the ◇ symbol.

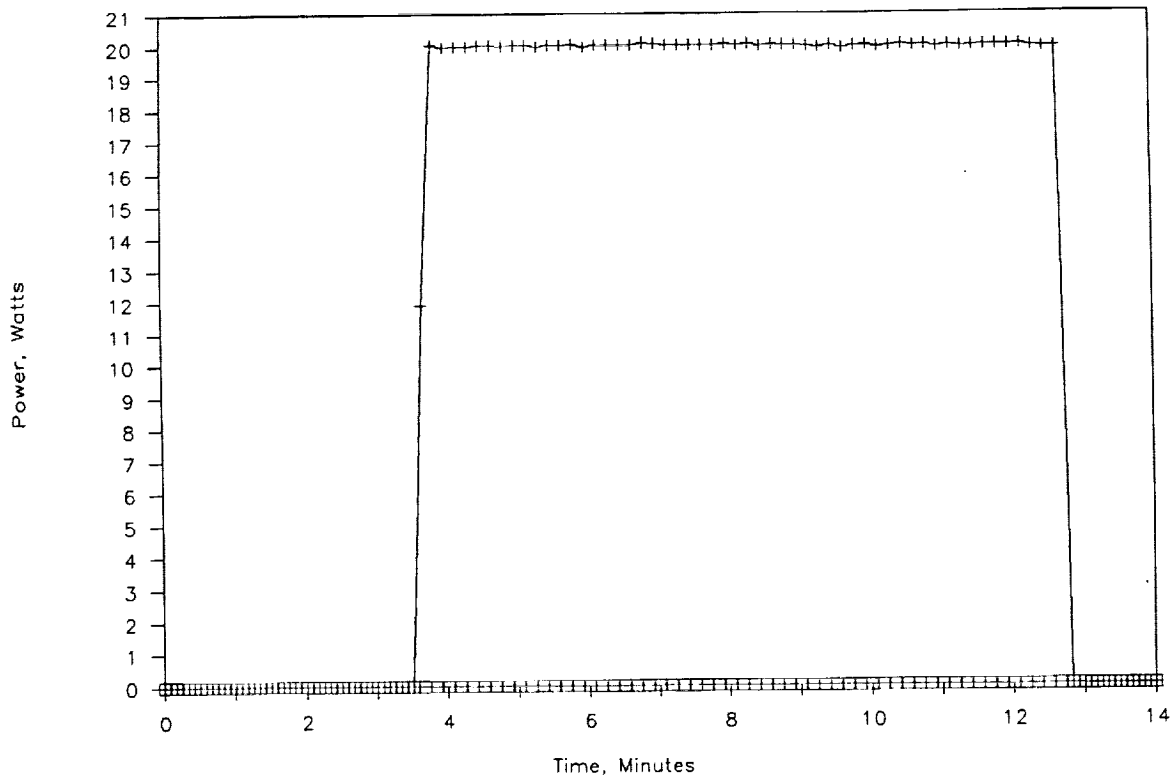


Figure 52. Heater power during 1989 run 5 along path A. The heater power at the porous plug heaters (H2) is the + symbol and heater power at the bayonet heaters (H4) is the □ symbol.

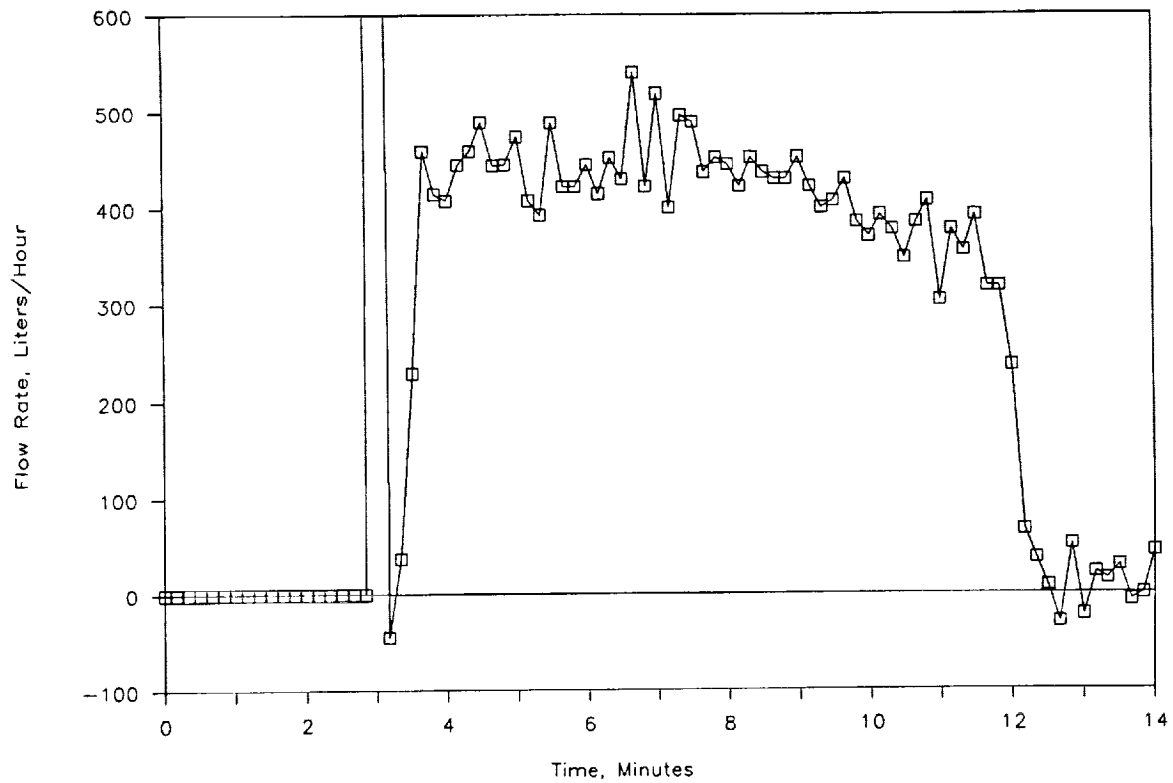


Figure 53. Flow rate out of the small tank during 1989 run 5 along path A.



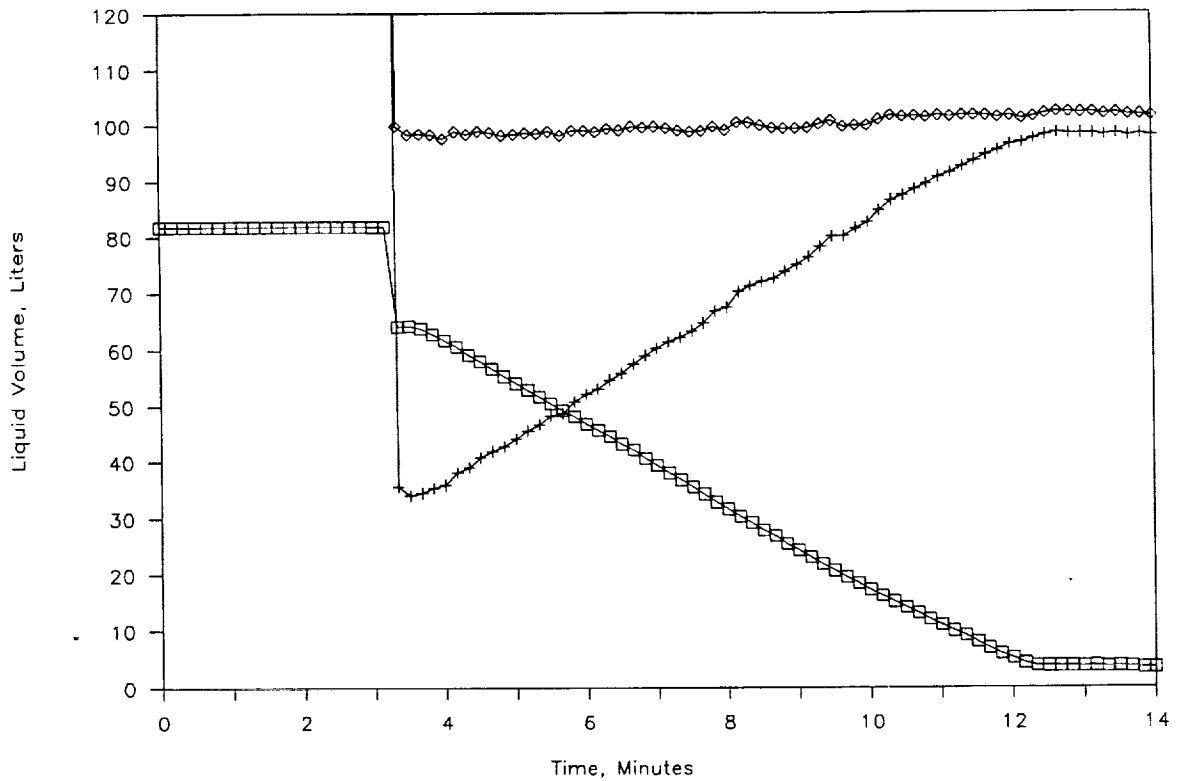


Figure 54. Liquid volume during 1989 run 5 along path A. Liquid volume calculated from LL1 and the small tank geometry is the □ symbol, liquid volume calculated from LL10 and the large tank geometry is the + symbol and the sum of the two volumes is the ◇ symbol.

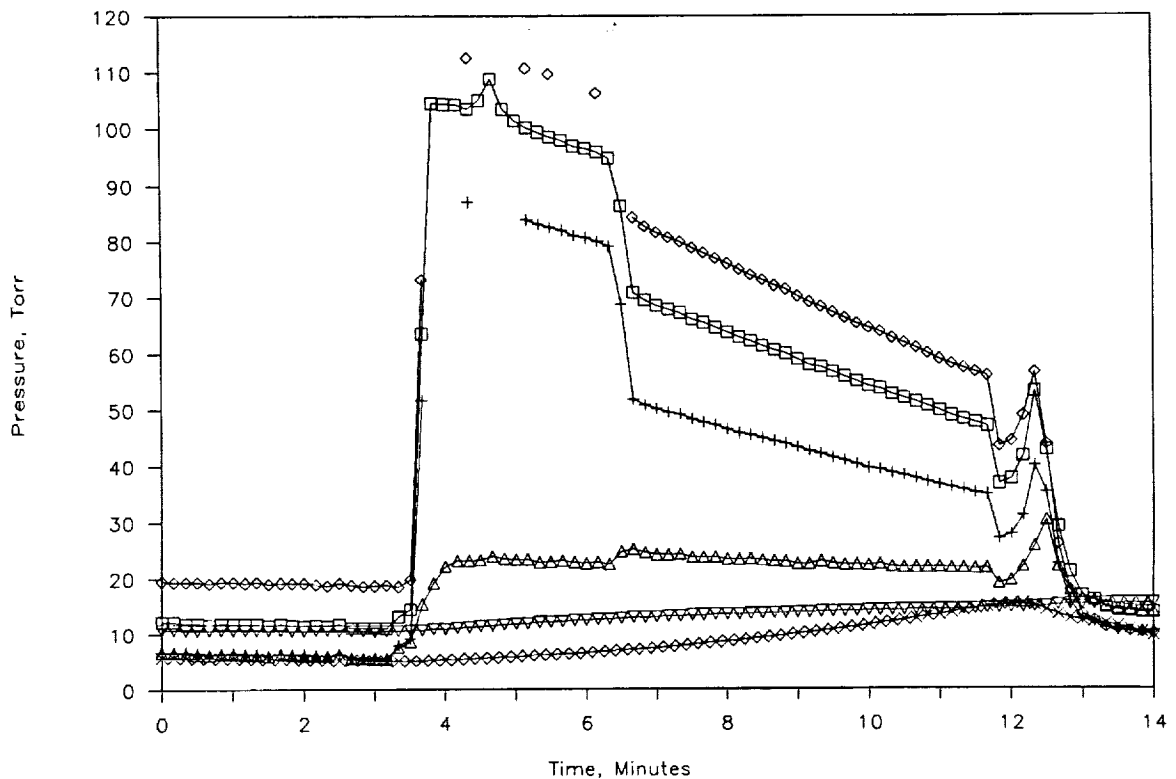


Figure 55. Pressures during 1989 run 5 along path A. The supply dewar is the — symbol, the receiver dewar is the ▽ symbol, CP3 (adjusted to show absolute pressure like the other transducers) is the ◇, CP1 is the □ symbol, CP2 is the + symbol, and CP4 is the △ symbol.

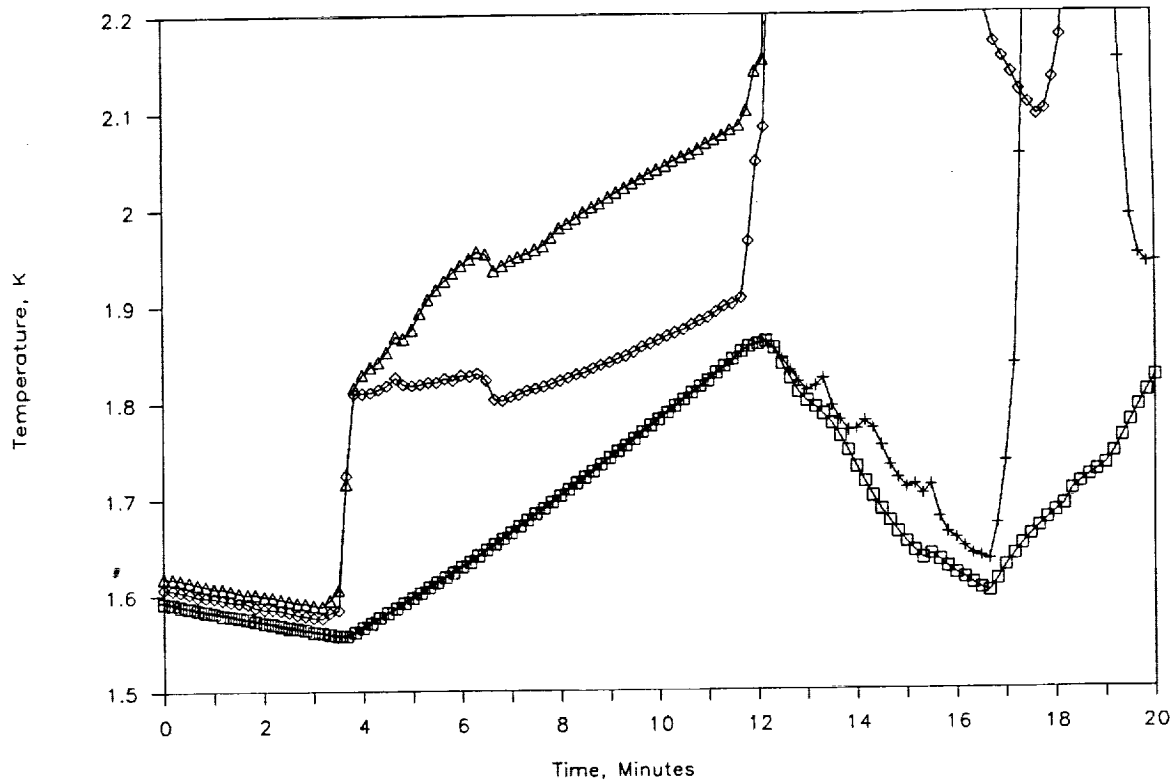


Figure 56. Supply dewar temperature and the first two temperatures along path A during 1989 run 5. T1, the supply dewar, is the  $\square$  symbol, T2 is the + symbol, T4 is the  $\diamond$ , and T3 is the  $\triangle$  symbol.

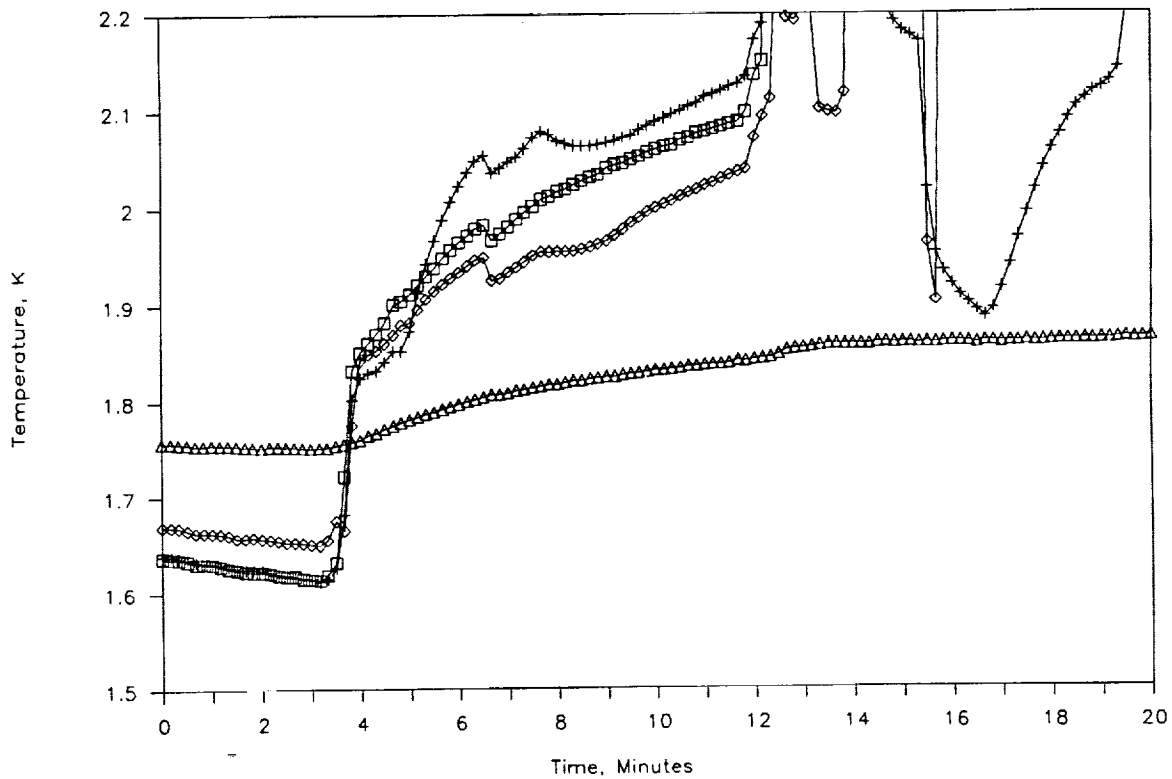


Figure 57. Final three temperatures along path A and the receiver dewar temperature during 1989 run 5. T9 is the  $\square$  symbol, T5 is the + symbol, T6 is the  $\diamond$ , and T8 is the  $\triangle$  symbol.

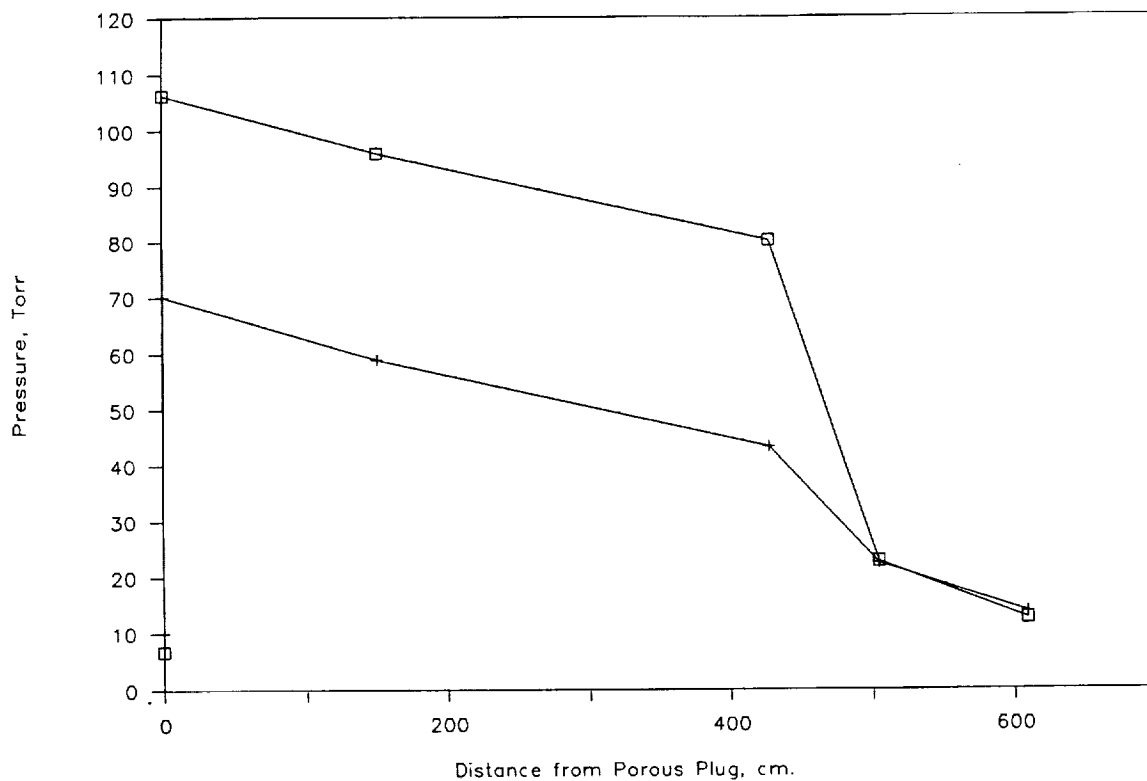


Figure 58. Pressure profile during 1989 run 5 along path A. Data at 6.167 minutes is the □ symbol and data at 9.0 minutes is the + symbol.

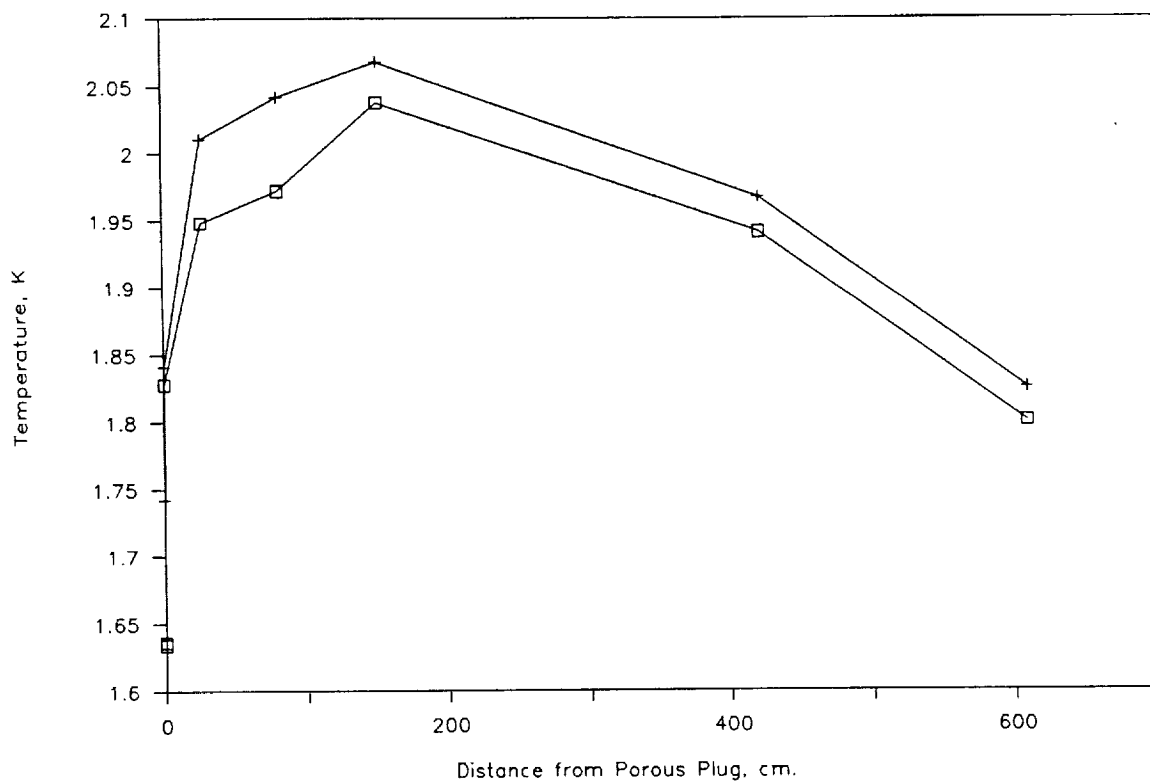


Figure 59. Temperature profile during 1989 run 5 along path A. Data at 6.167 minutes is the □ symbol and data at 9.0 minutes is the + symbol.

### 3.4.2 No-flow Tests

The results from the first no-flow test are shown in Figures 60 through 67. In this experimental run, valve V9 was closed at 3.6 minutes. At 10.8 minutes, 4 W of power was applied to the porous plug heater. A stable temperature and pressure value was reached while this power was being applied. The power was raised to 8 W at 18.3 minutes. The experiment was ended at 22.6 minutes when valve V4 was opened and the third transfer run was begun.

The results of the second no-flow test are shown in Figures 68 through 75. In this no-flow run, 4 W of heater power was supplied to the porous plug heater at 1.7 minutes. Valve V9 was closed at 2.2 minutes. At 6.5 minutes, the heater power was increased to 8 W and increased again to 12 W at 8.5 minutes. Valve V4 was opened at 9.8 minutes ending the no-flow experimental run and beginning transfer run 4.

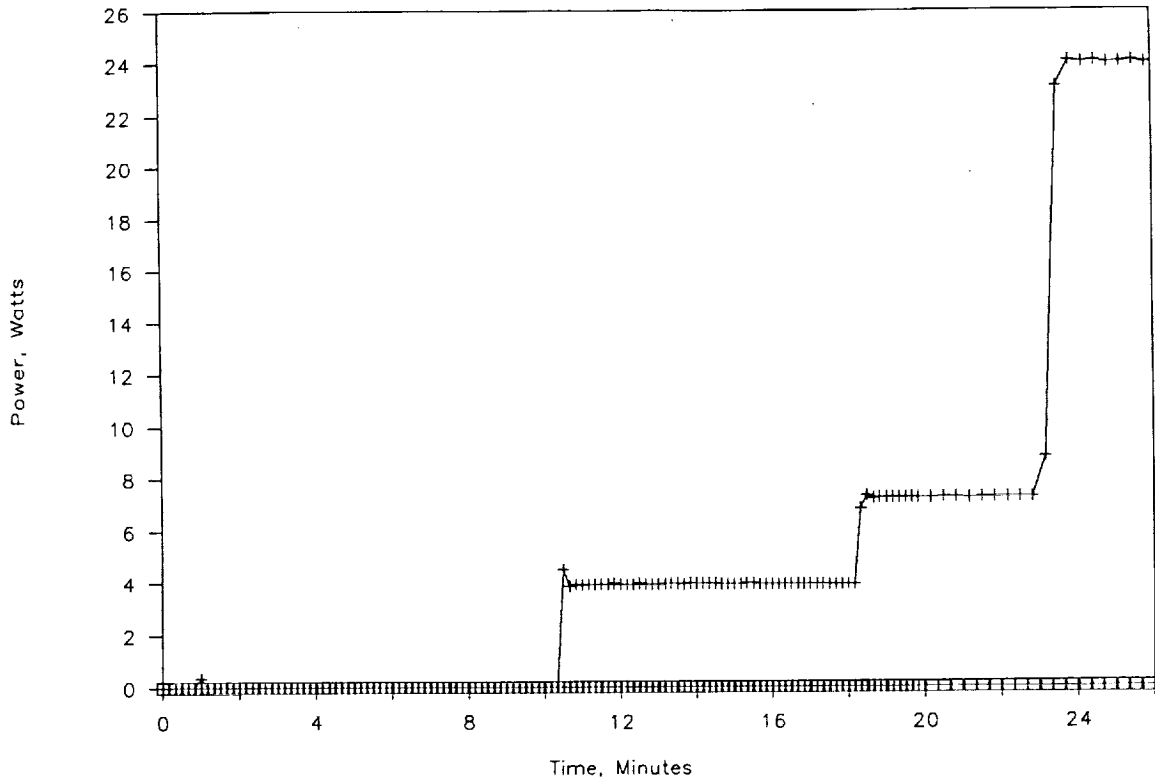


Figure 60. Heater power during 1989 no flow run 1 along path A. The heater power at the porous plug heaters (H2) is the + symbol and heater power at the bayonet heaters (H4) is the □ symbol.

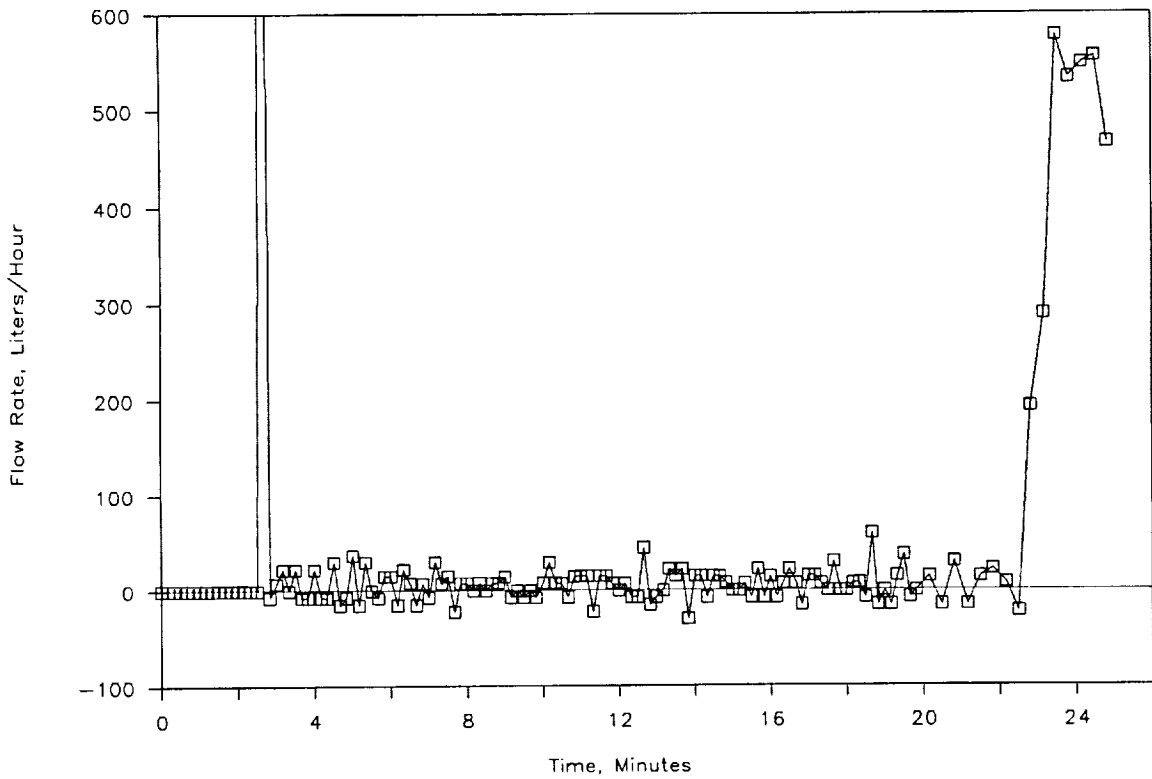


Figure 61. Flow rate out of the small tank during 1989 no flow run 1 along path A.

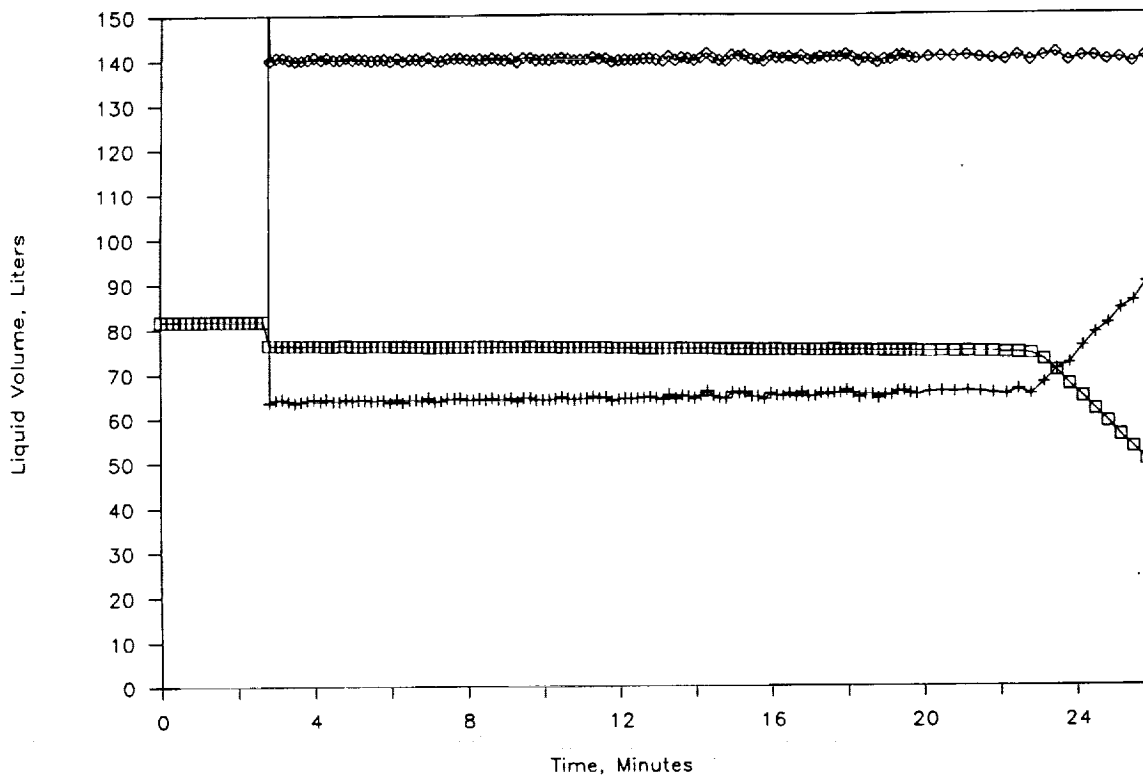


Figure 62. Liquid volume during 1989 no flow run 1 along path A. Liquid volume calculated from LL1 and the small tank geometry is the  $\square$  symbol, liquid volume calculated from LL10 and the large tank geometry is the  $+$  symbol and the sum of the two volumes is the  $\diamond$  symbol.

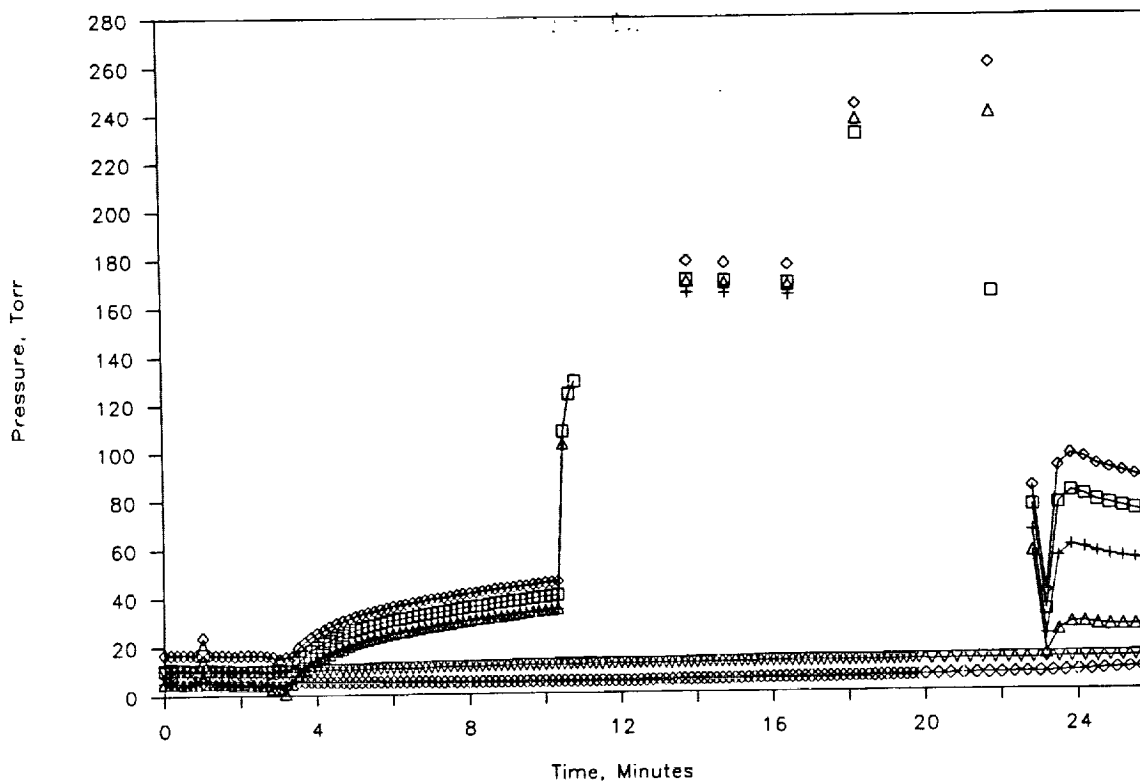


Figure 63. Pressures during 1989 no flow run 1 along path A. The supply dewar is the  $—$  symbol, the receiver dewar is the  $\nabla$  symbol, CP3 (adjusted to show absolute pressure like the other transducers) is the  $\diamond$ , CP1 is the  $\square$  symbol, CP2 is the  $+$  symbol, and CP4 is the  $\triangle$  symbol.

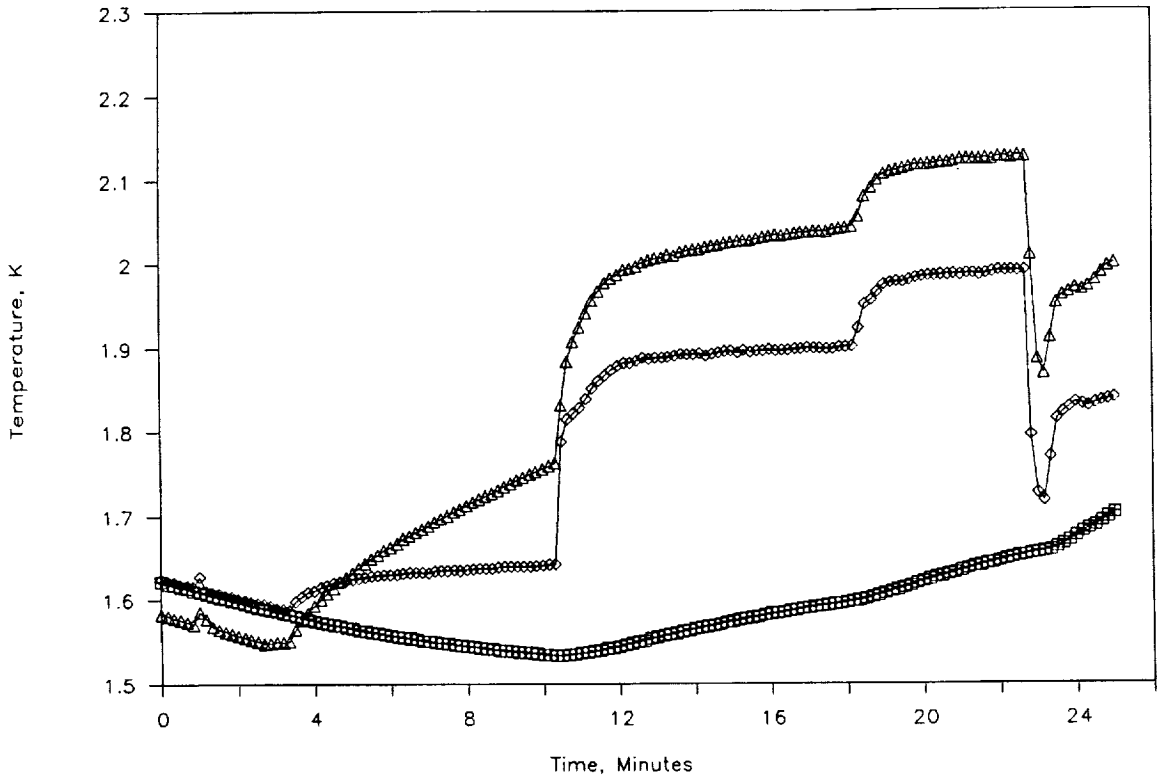


Figure 64. Supply dewar temperature and the first two temperatures along path A during 1989 no flow run 1. T1, the supply dewar, is the  $\square$  symbol, T2 is the + symbol, T4 is the  $\diamond$ , and T3 is the  $\triangle$  symbol.

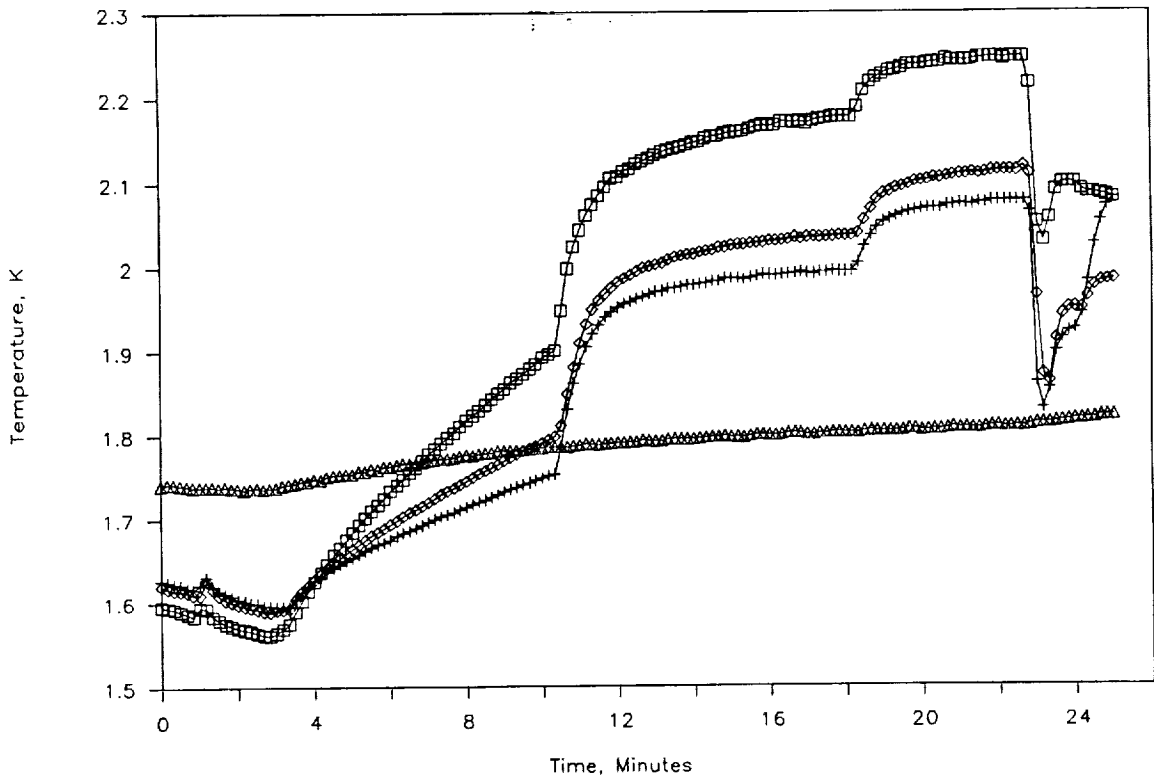


Figure 65. Final three temperatures along path A and the receiver dewar temperature during 1989 no flow run 1. T9 is the  $\square$  symbol, T5 is the + symbol, T6 is the  $\diamond$ , and T8 is the  $\triangle$  symbol.

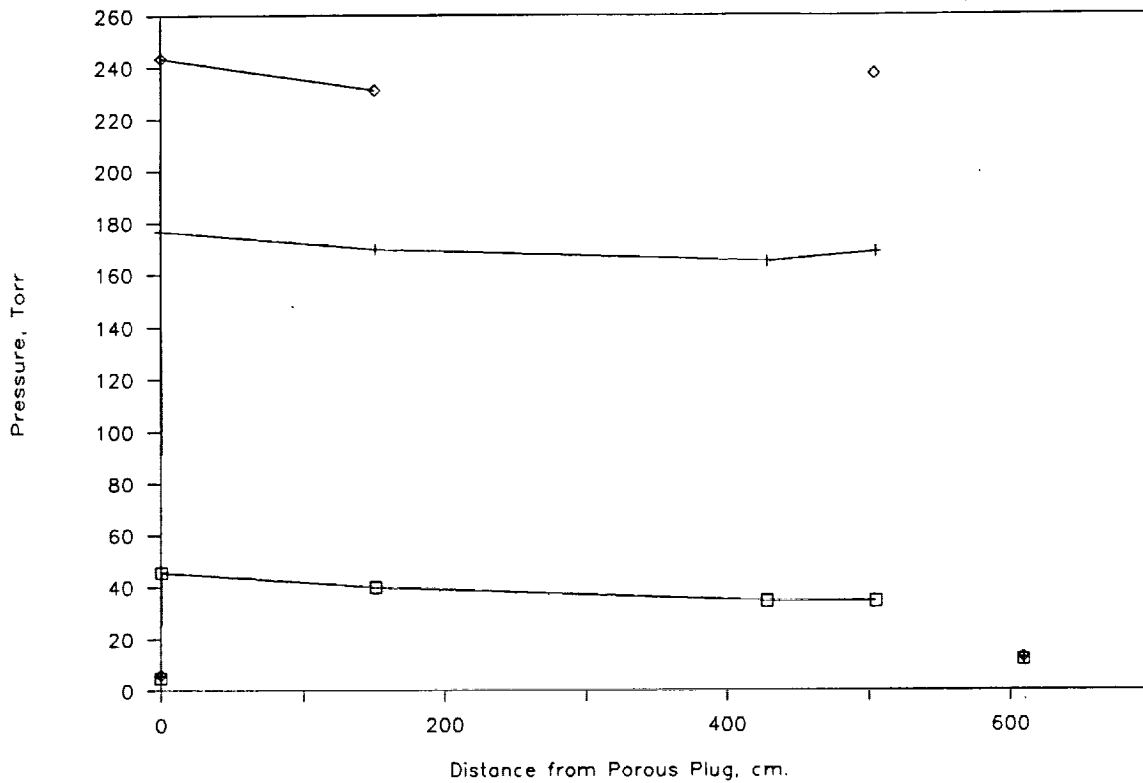


Figure 66. Pressure profile during 1989 no flow run1 along path A. Data at 10.0 minutes is the □ symbol, data at 16.5 minutes is the + symbol and data at 18.33 minutes is the ◇ symbol.

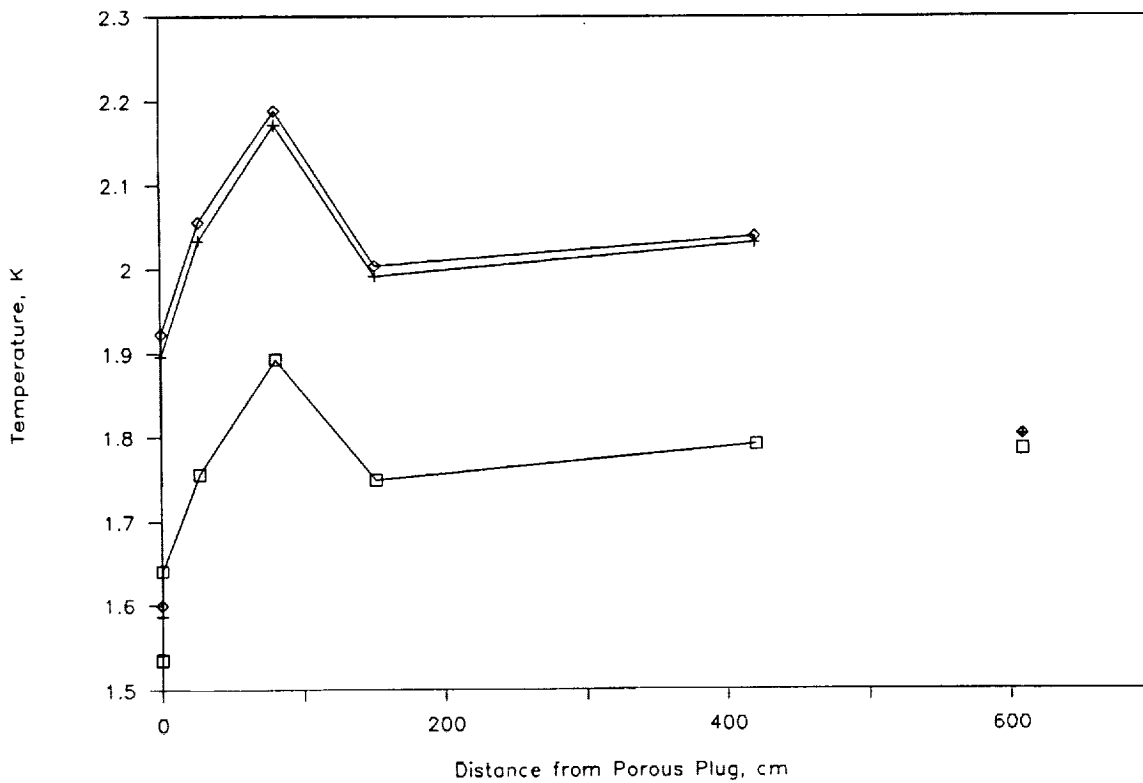


Figure 67. Temperature profile during 1989 no flow run1 along path A. Data at 10.0 minutes is the □ symbol, data at 16.5 minutes is the + symbol and data at 18.33 minutes is the ◇ symbol.



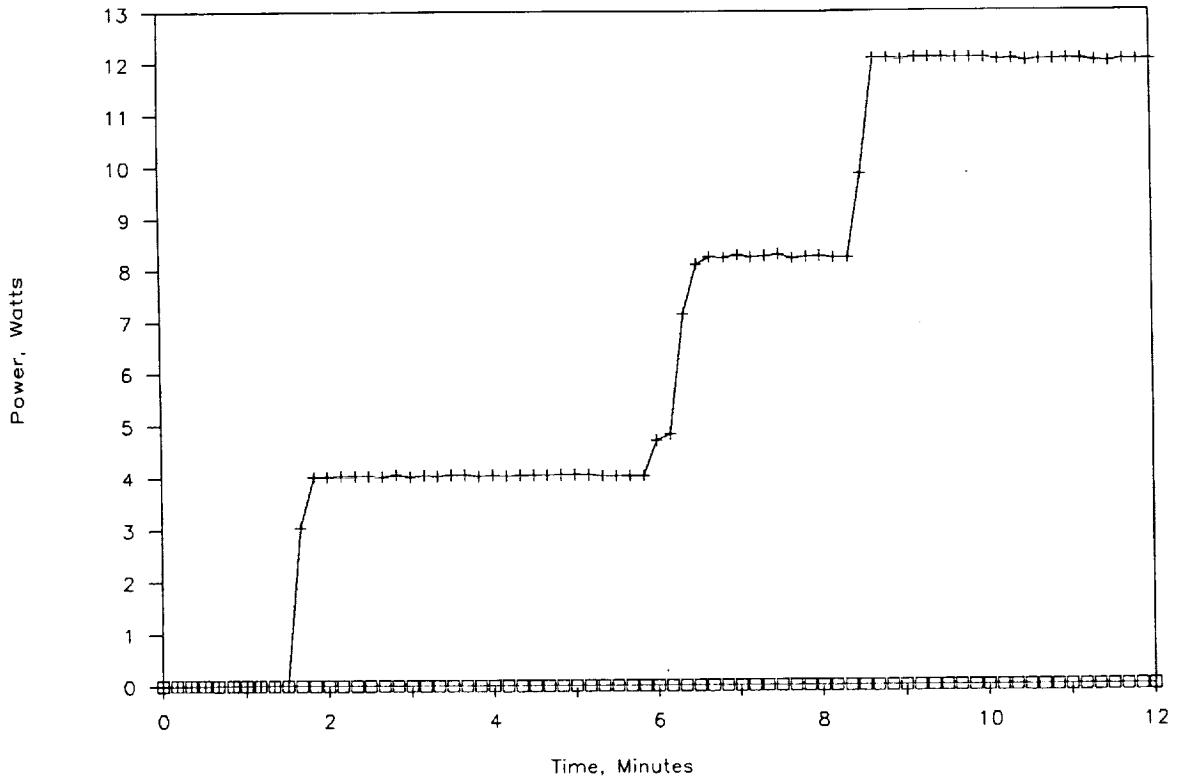


Figure 68. Heater power during 1989 no flow run 2 along path A. The heater power at the porous plug heaters (H2) is the + symbol and heater power at the bayonet heaters (H4) is the □ symbol.

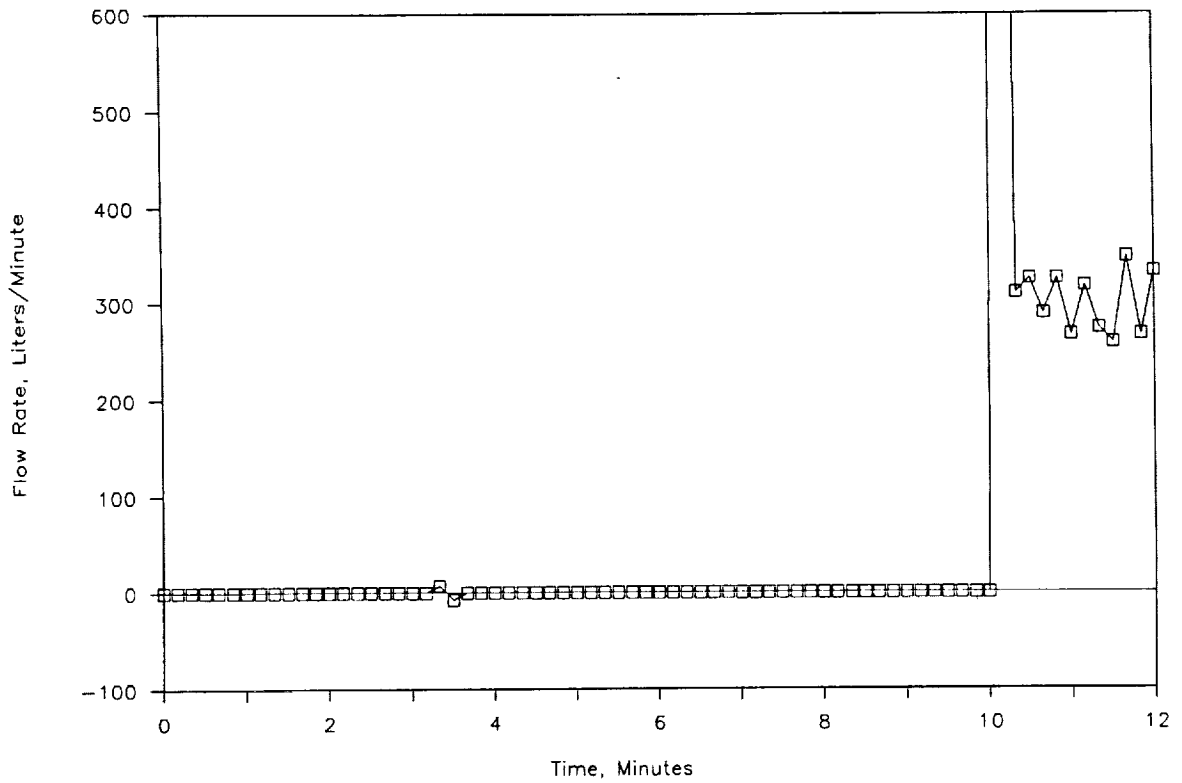


Figure 69. Flow rate out of the small tank during 1989 no flow run 2 along path A.

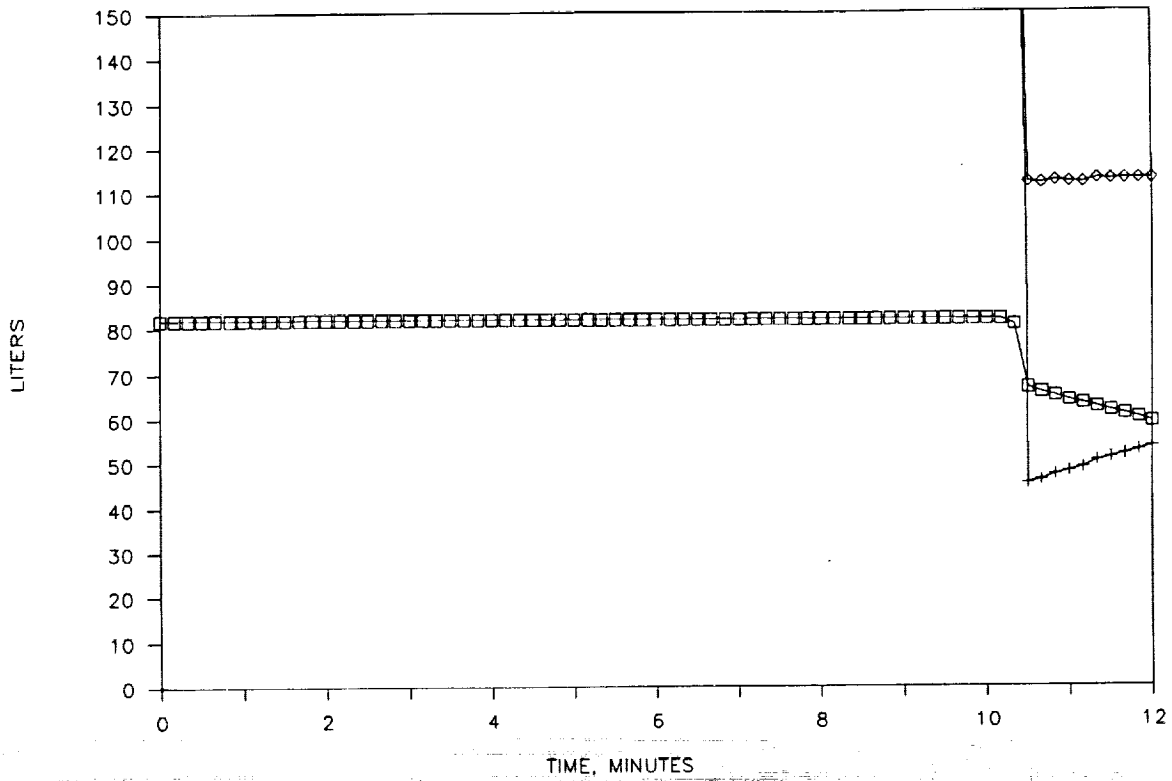


Figure 70. Liquid volume during 1989 no flow run 2 along path A. Liquid volume calculated from LL1 and the small tank geometry is the  $\square$  symbol, liquid volume calculated from LL10 and the large tank geometry is the  $+$  symbol and the sum of the two volumes is the  $\diamond$  symbol.

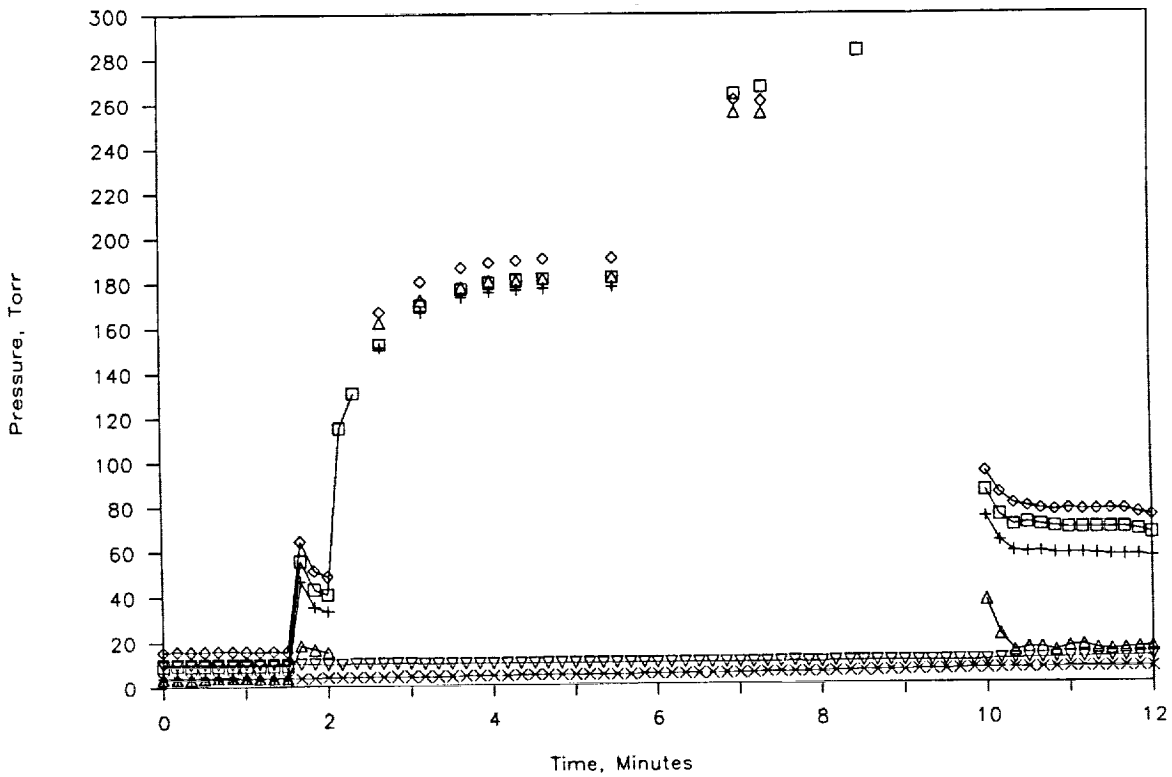


Figure 71. Pressures during 1989 no flow run 2 along path A. The supply dewar is the  $—$  symbol, the receiver dewar is the  $\nabla$  symbol, CP3 (adjusted to show absolute pressure like the other transducers) is the  $\diamond$ , CP1 is the  $\square$  symbol, CP2 is the  $+$  symbol, and CP4 is the  $\triangle$  symbol.

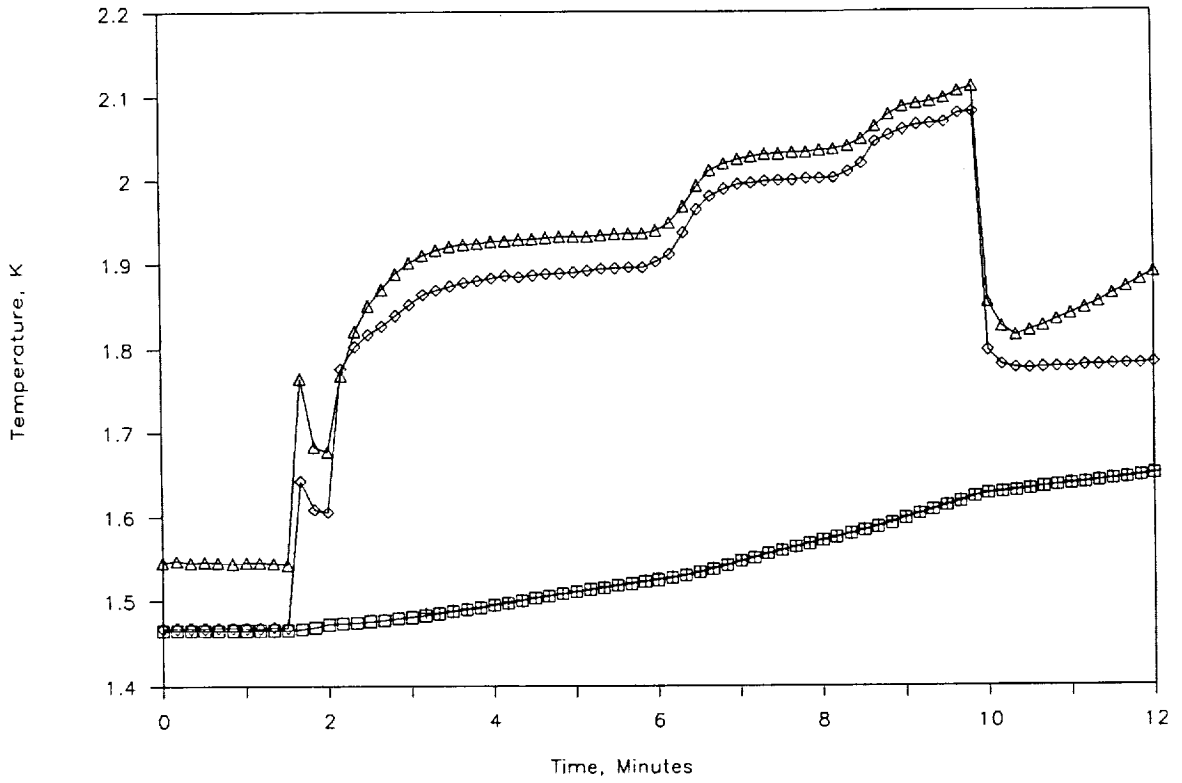


Figure 72. Supply dewar temperature and the first two temperatures along path A during 1989 no flow run 2. T1, the supply dewar, is the  $\square$  symbol, T2 is the + symbol, T4 is the  $\diamond$ , and T3 is the  $\triangle$  symbol.

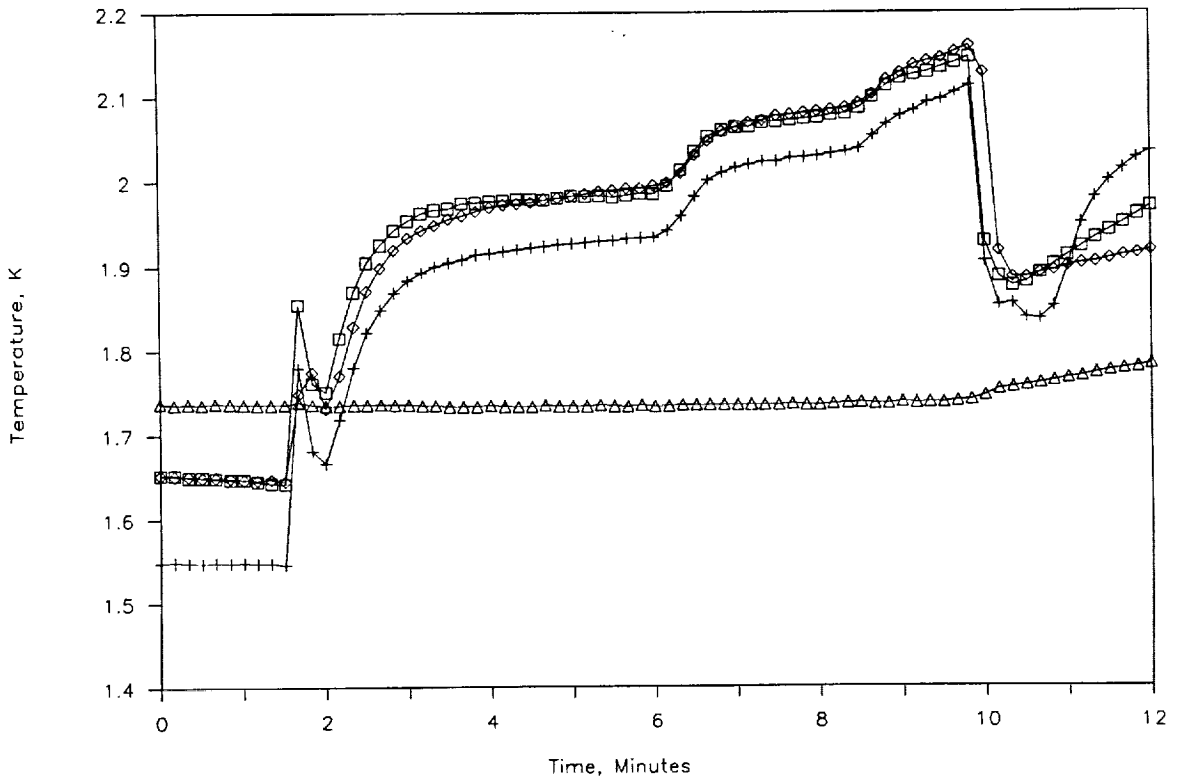


Figure 73. Final three temperatures along path A and the receiver dewar temperature during 1989 no flow run 2. T9 is the  $\square$  symbol, T5 is the + symbol, T6 is the  $\diamond$ , and T8 is the  $\triangle$  symbol.

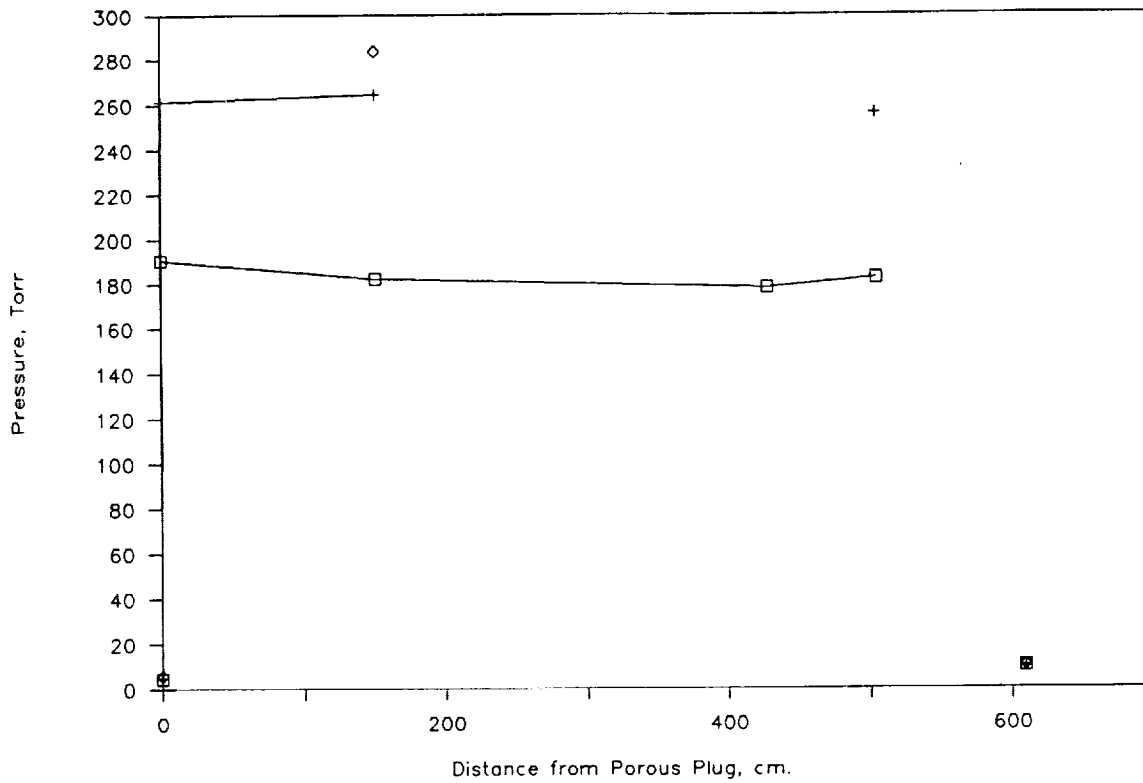


Figure 74. Pressure profile during 1989 no flow run 2 along path A. Data at 5.5 minutes is the □ symbol, data at 7.0 minutes is the + symbol and data at 9.5 minutes is the ◇ symbol.

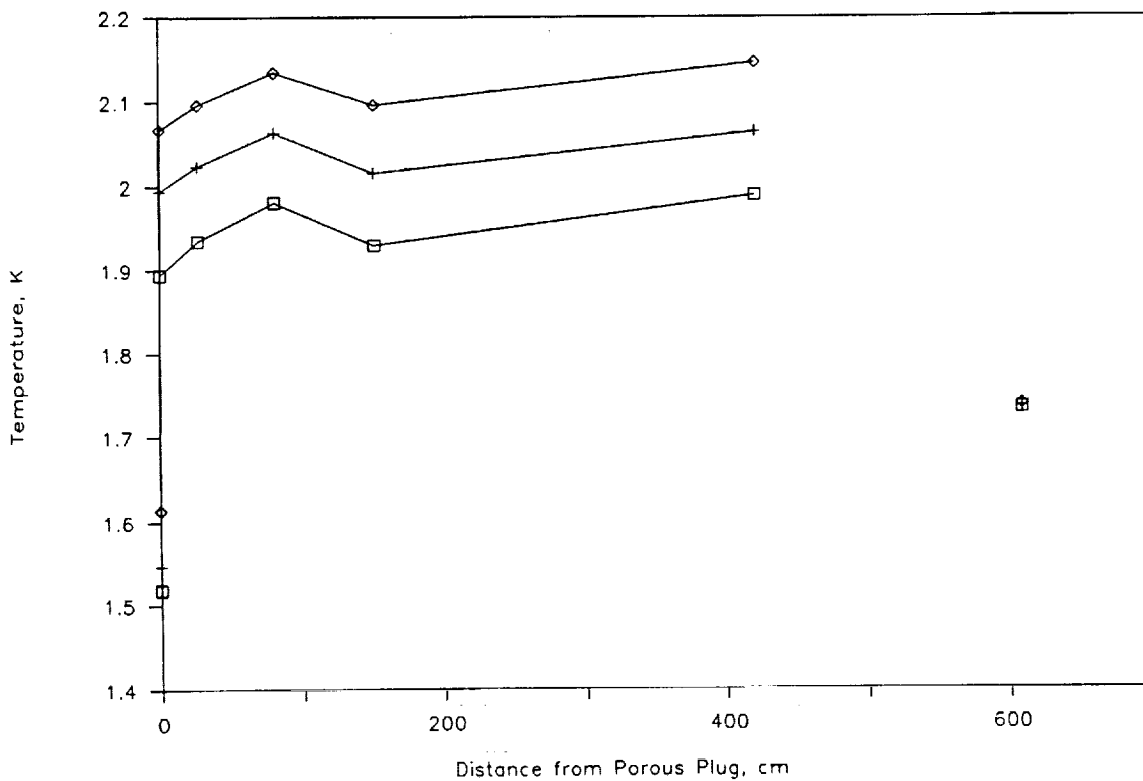


Figure 75. Temperature profile during 1989 no flow run 2 along path A. Data at 5.5 minutes is the □ symbol, data at 7.0 minutes is the + symbol and data at 9.5 minutes is the ◇ symbol.

#### Section 4 COMPARISON TO FLOW MODEL

Our theoretical understanding of Helium II flow through porous plugs and transfer lines has been incorporated in a computer model, Superflow. The current model is running on an IBM PC-AT using the Lotus 1-2-3 software. In the model, the porous plug and transfer line are divided into many one-dimensional finite elements. The number of elements and the length, diameter, and heat input of each element can be easily changed. Mass flow and energy flux are conserved between the elements. The superfluid component flow is driven by the gradient of the Gibbs free energy and dissipated by the Gorter-Mellink interaction with the normal component. The normal component flow is driven by the pressure gradient and is dissipated by viscous friction. The friction factor is calculated from the Reynolds number.

Since the model is one-dimensional, it does not account for the pressure drop due to the turning of the fluid as it goes through bends and valves or through corrugated tubing. This is accounted for by using the concept of equivalent length; that is, geometries which cause the fluid to turn are modeled by making the flow path longer. However, the amount by which the flow is increased for a given geometry can only be determined by empirical data.

Other parameters which must be determined empirically are the tortuosity of the plug and the pore size. The tortuosity is the ratio of the average flow path length to the thickness of the plug. A tortuosity greater than one affects the flow by increasing the flow path length and decreasing flow area due to conservation of plug volume. The tortuosity used in the model, 2.6, was chosen to match the observed temperature rise across the plug in the 1986 experiments. The pore size was chosen to be 0.2 micron based, in part, on bubble tests of the porous plug which determined that the largest pores at the surface were 0.5 micron. The 0.2 micron value which was used appeared reasonable based on the SEM photographs of the porous plug material and resulted in pressures and flow rates which were closer to the experimental values.

The equivalent length for the corrugated tubing and valves was chosen to match the observed flow rate and transfer line pressure profile. It was found that an equivalent length of 10 for the corrugated tubing caused the pressure drop calculated by the model to be closer to the experiment data and is consistent with the equivalent length for corrugated tubing reported in the literature.<sup>11</sup>

The equivalent length of the two valves was then increased from the initial estimates (which were based on water valve data) in order to match the pressure data as close as possible from one data point. This adjustment of the model equivalent lengths is shown in Figure 76. The same model was then run for two other data points.

Figures 76 through 78 show the observed and calculated pressure profiles from the supply dewar to the receiving dewar for the three different cases. Only the boundary conditions of supply and receiver dewar temperature and heater power were changed. Note that the pressure profiles and flow rates agree with the measured data within 10 percent.

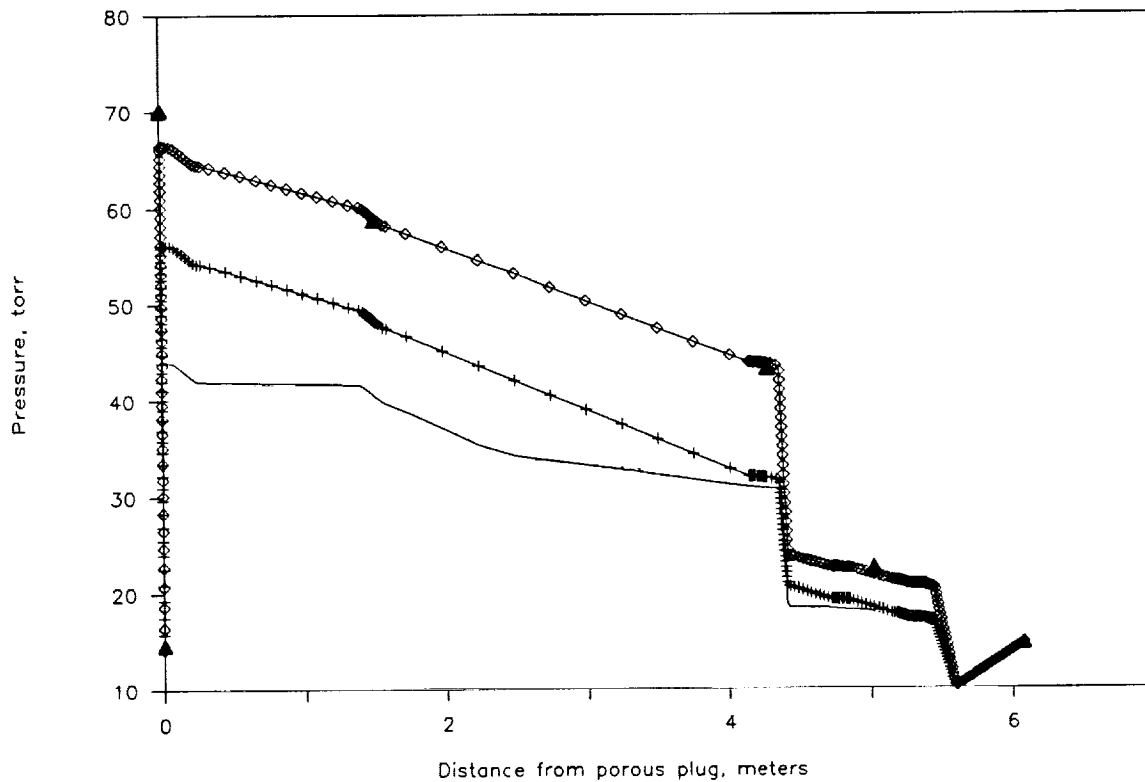


Figure 76. Experiment and computer generated pressure profiles for 1989 run 5, 9.0 minutes, along path A. The power input at this point was 20 watts at the porous plug only and the measured flow rate was 430 liters/hour. The experiment data is the ▲ symbol. The original computer model is the — symbol and had a flow rate of 462 liters/hour. The computer model with ten times the equivalent length for the corrugated line is the + symbol and had a flow rate of 431 liters/hour. The final model is the ◇ symbol and had a flow rate of 406 liters/hour. In the final model, the equivalent length of the corrugated line is ten times that of the smooth line in the original model and the equivalent length of the two valves was adjusted to match the experiment pressure profile.

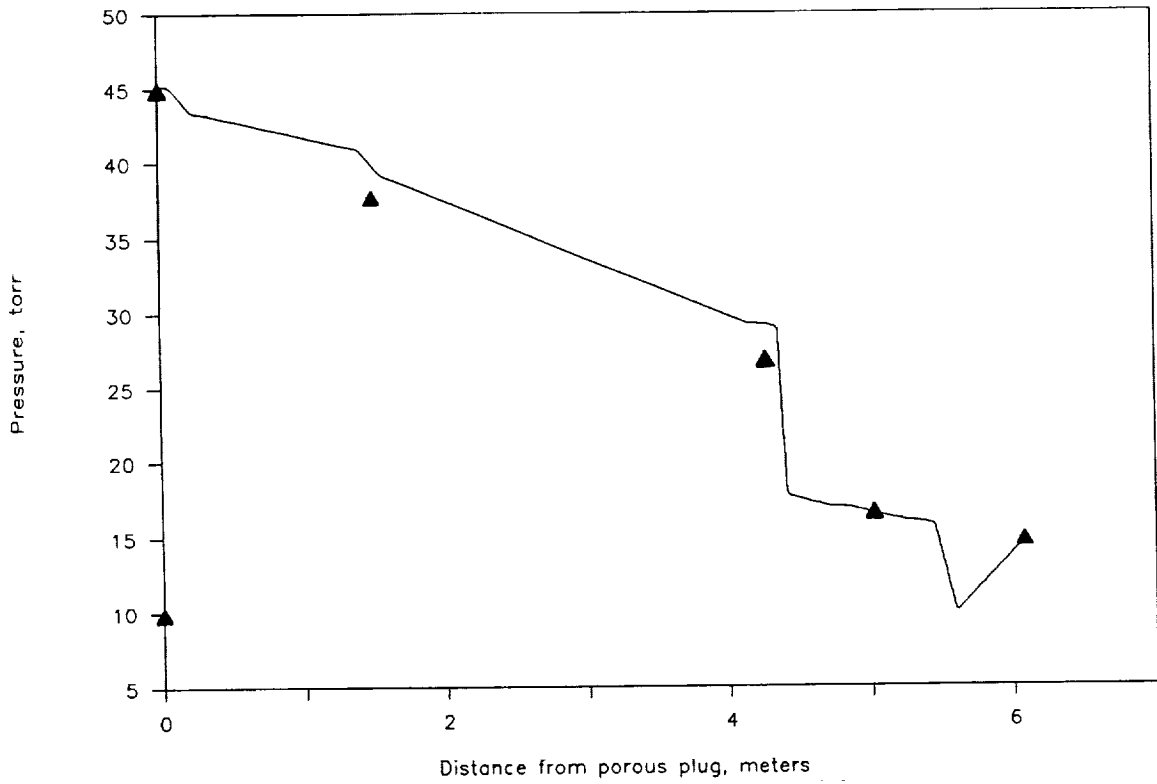


Figure 77. Experiment and computer model generated pressure profiles for 1989 run 4, 10.0 minutes, along path A. The power input at this point was 12 watts at the porous plug only and the measured flow rate was 313 liters per hour. The experiment data is the ▲ symbol. The computer model is the same as the final model in figure 76, is the — symbol and had a flow rate of 298 liters/hour.

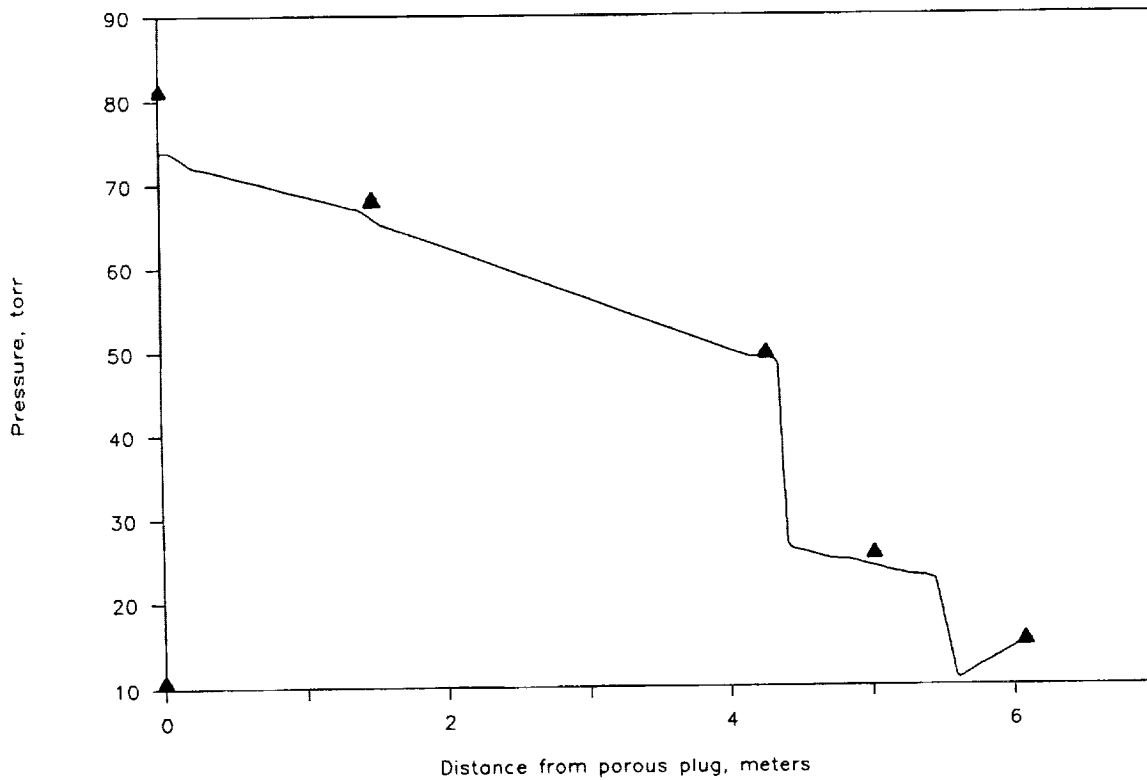


Figure 78. Experiment and computer model generated pressure profiles for 1989 run 3, 7.0 minutes, along path A. The power input at this point was 24 watts at the porous plug only and the measured flow rate was 469 liters perhour. The experiment data is the ▲ symbol. The computer model is the same as the final computer model in figure 76, is the — symbol and had a flow rate of 436 liters/hour.



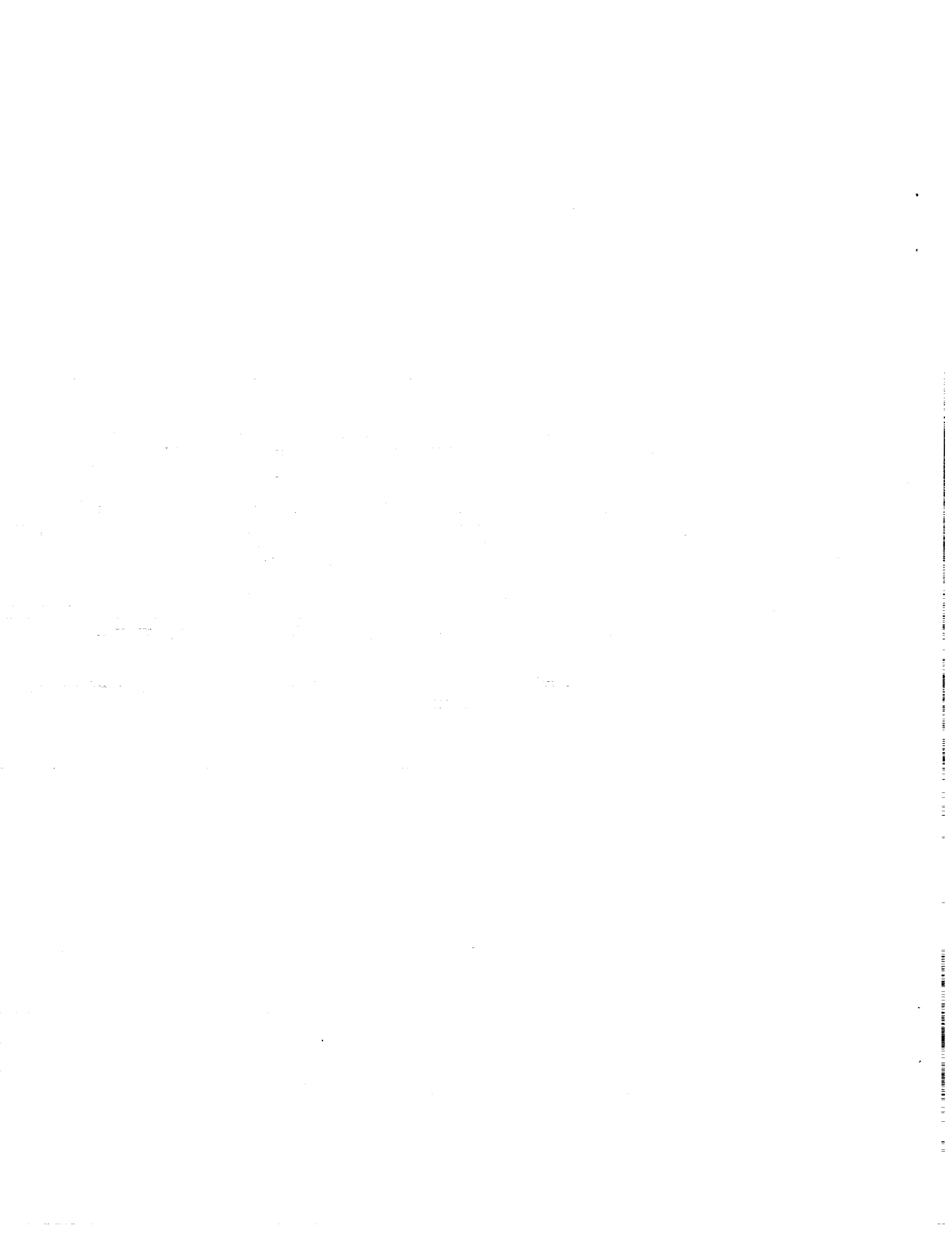
Section 5  
OVERALL STUDY CONCLUSIONS

1. Thermomechanical pumps can rapidly transfer large quantities of Helium II from one dewar to another through a long transfer line with significant flow restrictions and heat input. We achieved flow rates of 550 liters/hour through a transfer line that was 6.1 meters long and contained two valves.
2. Thermomechanical pumps are an efficient and reliable means for transferring Helium II.
3. Thermomechanical pumps can be used to cool and fill an initially warm tank. We cooled and filled a dewar tank that was initially at 60 K using only a thermomechanical pump.
4. A necessary condition for liquid to break through a porous plug is that the pressure on the downstream side of the plug be equal to or greater than the supply side.
5. Thermomechanical pumps can be used to fill the receiving dewar completely full of Helium II.
6. Thermomechanical pumps appear to be "positive displacement" pumps. That is, up to some limit, downstream restrictions do not affect flow rate. The limit is probably the maximum pressure that can be generated by the pump.
7. The thermomechanical pumps used in these tests can produce pressures of at least 280 torr and possibly much higher.
8. There is significant heat flow from the warmer "downstream" side of the porous plug to the cooler "upstream" side during no-flow conditions and probably during the flow conditions.
9. The flow rate through thermomechanical pumps appears to be a function of supply dewar temperature and heat input near the porous plug and unit area, and very little else. This is consistent with the established theory of thermomechanical pumps.
10. Addition of heat to the transfer line far downstream of the porous plug and at high flow rates has very little effect on the flow rate.
11. The pressure drop through corrugated bellows tubing appears to be approximately 10 times higher than through smooth tubing. This is consistent with the results reported by other experimenters.
12. The temperature profile in many of the flow runs is very unexpected and interesting in that the flow temperature continues to rise after the heater. We believe this to be a real phenomenon, not due to instrumentation error, since it is much larger than what we believe to be our estimated temperature error and it occurred in the 1986 and 1989 runs.

13. The Ball model, Superflow version 2.0, accurately predicts the flow rate and pressure profile for the various cases tested once the proper plug characteristics and component equivalent length are used in it.

## REFERENCES

1. C. M. Lyneis, M. S. McAshan, H. A. Schwettman, "Applications of the Fountain Effect in Superfluid Helium," Department of Physics, Stanford University, September 1968, NTIS AD678719.
2. W. F. Brooks, "Helium Transfer for the Space Station Era," Cryogenics 26:61 (1986).
3. A. J. Mord, et. al., "Concepts for On-orbit Replenishment of Liquid Helium for SIRTF," Cryogenics 26:68 (1986).
4. P. Kittel, "Liquid Helium Pumps for In-orbit Transfer," Cryogenics 27:81 (1987).
5. V. Arp, "Comparison of Centrifugal and Fountain Effect Pumps," Cryogenics 26:103 (1986).
6. H. A. Snyder, "Dewar to Dewar Transfer Model for Superfluid Helium Transfer," Space Cryogenics Workshop, University of Wisconsin at Madison, 21-23 June 1987.
7. L. A. Hermanson, A. J. Mord, H. A. Snyder, "Modeling of Superfluid Helium Transfer," Cryogenics 26:107 (1986).
8. E.T. Hammel, Jr. and W.E. Keller, Physical Review 124, 1641 (1961).
9. F. London, Superfluids, Dover Publications, New York, (1954).
10. National Bureau of Standards, "The Thermodynamic Properties of Helium II from 0 K to the Lambda Transitions," NBS Technical Note 1029
11. P.L. Walstrom, et. al., "Turbulent Flow Pressure Drop in Various Helium II System Components," Cryogenics 28:101 (1988).





# Report Documentation Page

1. Report No. NASA CR-177541		2. Government Accession No.		3. Recipient's Catalog No.	
4. Title and Subtitle BASG Thermomechanical Pump Helium II Transfer Tests			5. Report Date March 1990		
			6. Performing Organization Code		
7. Author(s) G. L Mills, D. A. Newell, and A. R. Urbach			8. Performing Organization Report No. A-90127		
			10. Work Unit No. 188-78-44		
9. Performing Organization Name and Address Ball Aerospace Systems P. O. Box 1062 Boulder, CO 80306			11. Contract or Grant No. NAS2-11979		
			13. Type of Report and Period Covered Contractor Report		
12. Sponsoring Agency Name and Address National Aeronautics and Space Administration Washington, DC 20546-0001			14. Sponsoring Agency Code		
			15. Supplementary Notes Point of Contact: Walter F. Brooks, Ames Research Center, MS 244-10, Moffett Field, CA 94035-1000 (415) 604-6547 or FTS 464-6547		
16. Abstract <p>The purpose of the effort described in this report was to perform experiments and calculations related to using a thermomechanical pump in the space-based resupply of the Space Infrared Telescope Facility (SIRTF) with Helium II. The need for this effort was identified in the original SIRTF Instrument Changeout and Cryogen Replacement (STICCR) study.</p> <p>Thermomechanical (fountain effect) pumps have long been suggested as a means for pumping large quantities of Helium II. The unique properties of Helium II have made it useful for cooling space instruments. Several space science missions, including SIRTF, are now being planned which would benefit greatly from on-orbit resupply of Helium II.</p> <p>We performed a series of experiments to demonstrate that large volumes of Helium II can be transferred with a thermomechanical pump at high flow rates and at high efficiency from one dewar to another through valves and lines that are similar to the plumbing arrangement that would be necessary to accomplish such a transfer on-orbit. In addition, temperature, pressure, and flow rate data taken during the tests were used to verify and refine a computer model we have developed.</p> <p style="text-align: center;">WHICA WAS</p>					
17. Key Words (Suggested by Author(s)) Space infrared telescope facility Liquid helium transfer Zero-G Cryogenics			18. Distribution Statement Unclassified-Unlimited  Subject Category - 18		
19. Security Classif. (of this report) Unclassified		20. Security Classif. (of this page) Unclassified		21. No. of Pages 76	22. Price A05

